Investigating the Molecular Building Blocks of Loose and Tight Cattle Hide

A thesis presented in partial fulfilment of the requirements for the degree of

Masters of Science

In

Biochemistry

At Massey University, Manawatu, New Zealand.

Catherine Ann Maidment

2019

Abstract

Looseness is a defect found in 7 % of leather made from cattle hides. It affects the quality of leather, resulting in the leather being downgraded or potentially being discarded altogether. The similarity in appearance between loose leather and wrinkly skin led to the hypothesis that they may share the same causative agent(s). While little to no research has been done to elucidate the molecular basis of loose leather, there are many reports detailing the characteristics and causes of wrinkly skin, especially in ageing humans. Studies have shown that changes in three molecular components of skin are correlated with the appearance of wrinkles; collagen, elastin and glycosaminoglycan's (GAGs).

Cattle hides that produce loose leather were identified by processing half of the selected hides to leather and using the SATRA break scale. Only four hides were suitable for this study with two being loose and two being tight. Although this small sample size limited the statistical significance of the results, it did, however, enable a vast number of analyses on the molecular components of the hides to be carried out. Microscopic techniques were utilised to investigate the localisation and structure of a range of molecular components in loose and tight hides and a series of biochemical assays were used to assess the carbohydrate components, particularly the GAGs. Quantitation of amino acids in the whole hide and different layers of the hide; grain, grain to corium junction and corium provided insight into the total collagen found in loose and tight hides and proteomic analysis using in-gel mass spectrometry (in-gel LC-MS/MS) enabled quantitation of all soluble proteins found in loose and tight hides as well as the extent of collagen glycosylation.

Overall loose hides appear to have a decrease in fibrillar collagen, this paired with changes in total crosslinks and glycosylation of collagen potentially result in changes to the structure and organisation of the collagen network. This causes easier extraction of non-collagenous components during leather processing and thus results in loose leather.

This study uses a variety of techniques to link differences in the molecular components of hide to the defect looseness. This greater understanding of how the molecular components of raw hide can affect the quality of leather will be of use in developing methods to identify faults in the hide before it is processed to leather and developing methods to produce high quality leather.

Acknowledgements

At the end of any journey there are acknowledgements to make and as this journey has been longer and rockier than I think any of us could have imagined at the beginning I want to take special care to thank everyone who helped me jump, crawl and hobble my way to the finish line. I apologise in advance if I have missed anyone out.

Firstly, to my supervisor Associate Professor Gillian Norris thank you very much for your guidance, support and patience throughout this long journey. To my co-supervisors Dr. Meekyung Ahn and Dr. Mark Patchett thank you very much for your guidance and knowledge during the experimental stages. We will always puzzle over why those western blots remained elusive. I wish you all the best with your future endeavours.

Thank you to everyone who shared their extensive knowledge with me including: Nikki Murray, Emma Crawford, Trevor Loo, Dr. Rafea Naffa and Dr. Torsten Kleffmann.

I would also like to thank all my friends and family for their continued support and love throughout this long process. There are not many people who would listen to me moan about experiments not working for almost 5 years like you have and not tell me to shut up.

Finally, I would like to thank Tasman Tannery, Whanganui for providing the hides used for this project and LASRA/MBI for funding this project.

List of Abbreviations

1D SDS PAGE...One dimensional sodium dodecyl sulfate polyacrylamide gel electrophoresis

2D..... Two-dimensional

3D..... Three-dimensional

ACP..... Aldol condensation products

AGE.....Advance glycation end products

APS .....Ammonium persulfate

AQC 6-Aminoquinolyl-N-hydroxysuccinimidyl

BAW .....Butanol: Acetic acid: H_2O

BS.....Blocking solution

BSA..... Bovine serum albumin

CaO .....Lime

CAPS.....N-cyclhexyl-3-aminopropane sulfonic acid

CHAPS detergent..... 3-[(3-cholamidopropyl)dimethylammonio]-1-propanesulfonate

CV%..... Correlation coefficient

CPC ..... Cetylpyridinium chloride

Des .....Desmosine

DHLNL .....Dihydroxylysinonorleucine

DMMB .....1,9-dimethylmethylene blue

DTT.....DL-Dithiothreitol

ECM..... Extracellular matrix

FACIT .....Fibril-associated collagens with interrupted triple helices

GAGs.....Glycosaminoglycans

HA.....Hyaluronic acid

HAS2 ..... Hyaluronic acid synthase 2

HCD ..... Higher energy C-trap dissociation

HCl ..... Hydrochloric acid

HHL ..... Histinohydroxylysinorleucine

HHMD ..... Histinohydroxymerodesmosine

HLNL ..... Hydroxylysinonorleucine

HPLC ..... High pressure liquid chromatography

HyLys ..... Hydroxylysine

In-gel LC-MS/MS ..... In-gel liquid chromatography mass spectrometry with fragmentation

LASRA ..... Leather and Shoe Research Association

LCMS ..... Liquid chromatography mass spectrometry

MgO ..... Magnesium oxide

MS ..... Mass spectrometry

NaCl ..... Sodium chloride

$NaHCO_3$ ..... Sodium bicarbonate

NMR ..... Nucleotide magnetic resonance

OSP ..... Official sampling position

PBS ..... Phosphate buffered saline

PTM ..... Post translational modifications

RGD ..... Tripeptide Arg-Gly-Asp

RPHPLC ..... Reverse phase high pressure liquid chromatography

SDS ..... Sodium dodecyl sulfate

SLRP ..... Small-leucine rich proteoglycans

TCA ..... Trichloroacetic acid

TCMTB 2-Thiocyanatomethylthiobenzothiazole

TEMED ..... N, N, N’N’-tetramethylenediamine

TGFβ ..... Transforming growth factor β

TPPS.....5,10,15,20-tetraphenyl-21H,23H-porphine tetra-sulfonate

TLC ..... Thin layer chromatography

UV ..... Ultraviolet

Table of Contents

Index of Figures

Index of Tables

1. Introduction and Literature Review

1.1 Skin, leather and the defect called looseness

Skin

Skin constitutes the largest organ of the body in mammals. It has many important functions including protecting the animal from physical damage and dehydration, forming an immunological barrier against harmful environmental agents and regulating temperature [1, 2]. Skin consists of three layers: the epidermis, dermis and hypodermis all of which have unique roles in maintaining skin health and functionality [1]. The extracellular matrix (ECM) is the non-cellular component of tissue. It is tissue specific and provides the physical scaffolding for cellular components initiating the crucial biochemical and biomechanical cues necessary for tissue morphogenesis, differentiation and homeostasis [3, 4]. The ECM of skin is composed of many different molecular components including water, proteins, proteoglycans, glycosaminoglycans (GAGs), complex carbohydrates and lipids [3, 4]. Collagen is the dominant protein found in skin making up 75 % of its dry weight [5]. Skin defects generally arise because of changes in its molecular components that may be genetic in origin or result from environmental factors. Age also affects the structure and composition of the molecular components of skin often resulting in a changed appearance. Understanding the cause of these defects can help to reduce and control them.

Leather

The leather industry is New Zealand's seventh largest industry [6]. Leather is a durable and flexible material that is made by tanning degradable animal skins or hides, that are generally by-products of the agricultural industry, to produce a material that is stable, and no longer subject to bacterial degradation. [7]. The product is classed as high value and is used to make

clothing, footwear and furniture [7, 8]. Whilst leather can be made from the skin or hide of any animal, in New Zealand the common species used are cow (bovine), sheep (ovine) goat (caprine) and deer (cervine) [6]. Skins of larger animals such as cattle hides are typically referred to as hides. Figure 1.1 illustrates the key stages in leather processing.

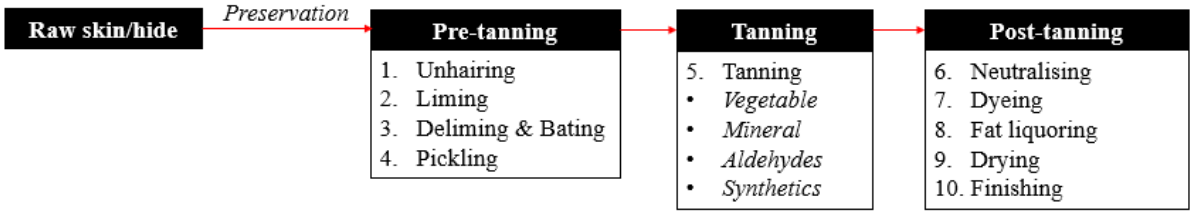

Figure 1.1 Key processing stages in leather making [7, 8].

Raw skins and hides are removed from the carcass by either hand flaying or mechanical pulling [7, 8]. As the distance between the abattoir and tannery can be long, preservation to prevent putrefaction of the starting material becomes an important consideration. As the raw skins/hides contain about 70 % water the potential for bacterial activity is high [7]. This is typically combatted by dehydrating the skins/hides with salt in combination with the application of biocides to minimise microbial growth and hence reduce the degradative effect of proteolytic enzymes [7, 8].

Pre-tanning

Initial steps in processing include trimming off unwanted edges and removing any remaining meat tissue and fat (fleshing) from the skin/hide [7]. The skin/hide is then soaked in water containing detergents to remove unwanted material such as blood, dung or salt from the preservation stage. This also aids the uniform movement of reagents through the skin/hide during tanning [7]. The hair is usually removed by the addition of alkali and reducing agents which break down the cystine (disulfide linkages) in the keratin, the major protein in hair,

allowing penetration by other chemicals or enzymes and weakening it so it can be removed by scraping. [6, 7]. Liming uses chemicals similar to those found in depilation. It uses a combination of chemical and physical action to affect the protein in skin/hide particularly collagen. It causes hydrolysis of amide groups, modification of guanide groups, hydrolysis of keto-imide links in protein chains, swelling and removal of unwanted material such as globular proteins and other interfibrillary substances [6, 7]. Deliming and bating tend to happen simultaneously. During deliming the skin/hide structure is further opened up and the pH is adjusted using acid salts such as ammonium chloride or ammonium sulphate [6, 7]. Bating uses the action of enzymes to further remove unwanted material from the skin/hide. Pickling is a preservation step that adjusts the pH to 3-3.5 using a solution of salt and sulphuric acid [6, 7].

Tanning

Tanning imparts a variety of properties to the final product including stability, flexibility and aesthetic qualities [7]. There are many different types of tanning agents, and the one used depends on the properties required in the finished leather. Vegetable tannins are typically prepared from extracts of bark and wood of trees. They produce a relatively dense, firm or solid leather that is typically used for soles of shoes, upholstery and bags [6, 8]. The main mineral tannin is chromium sulfate. It produces a soft or resilient leather that is mainly used for shoe uppers, gloving and clothing [6, 8]. Aldehyde tannins include formaldehyde, glutaraldehyde or oxazolidine. They produce a soft leather that is typically used to make washable gloves and clothing [6, 8]. Synthetic tanning materials can also be used as a replacement for vegetable tanning materials. The type of leather produced varies though it is typically similar to those found in vegetable tannins and is frequently used for specialty leathers [6, 8].

Post-tanning

After tanning the pH of the leather is neutralised using sodium formate before dyeing to change the colour of the hide to match its end application. Many commercial dyes are available, and their mode of use varies depending on the type. Fat liquoring involves the addition of lipids to the dyed skin/hide to lubricate the tanned fibres enabling them to move over each other, thus producing soft, supple leather [6-8]. The final steps in the process involve the removal of water, enhancement of fullness (filling), restoration and repair of appearance (buffing), adjustment of moisture content to 14-25 % (conditioning and toggling) and surface coating to provide protection, decoration and durability [7, 8].

Looseness

Defects in leather affect its quality and consequently its market value. Defects in the hide may be a result of its environment, *e.g*. scarring and insect infestation; the preparation of hides and skins for tanning *e.g.* flay-cuts and gouges, putrefaction and heat damage; or during tanning processing due to poor tanning practices [8]. It is also possible that defects can be caused by a change in the molecular components of skins/hides caused by poor nutrition, stress, disease or genetic factors.

Cattle hide is one of the biggest exports in New Zealand, reaching a total of NZD $475 million annually [9]. Looseness is one such defect that impacts the export market as it is found in approximately 7% of New Zealand hides [9] reducing the value of the affected hide by 5 – 10 %, even after trimming [10]. Looseness is characterized by the wrinkly appearance of finished leather when it is subjected to certain forces as seen in Figure 1.2B [11].

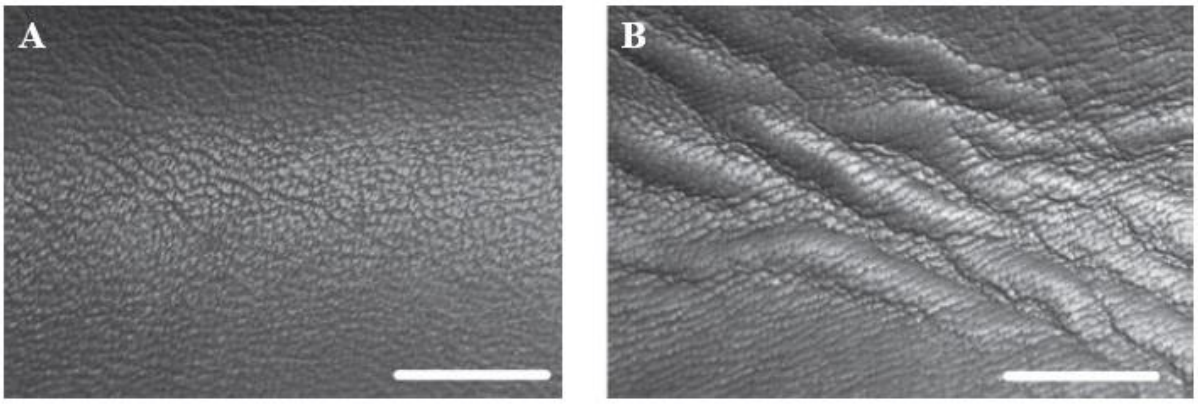

Figure 1.2 Images of (A) tight and (B) loose leather. Scale bar 2 mm. Taken from Wells, Holmes and Haverkamp [10] with permission of the publisher.

The cause of looseness has only recently been investigated, with most of the studies focusing on the structural changes of collagen fibres between loose and tight leather. Wood [12] used microscopy to show that loose leathers have more space between the collagen fibre bundles compared to tight leathers. Microscopy studies by Wells *et al.* [10] also showed a larger separation between the fibre bundles in loose leather, as well as a region below the grain, which contained cavities where the fibres were not so densely packed. Liu *et al.* [13] found there was a difference in the grain to corium junction with microscopy showing that loose leathers have a gap between the two layers that is absent in tight leathers. A difference in the grain structure of loose leathers could also contribute to the formation of this gap as in loose leathers the grain layer appears sheet like and is less tightly packed.

Looseness is known to be exacerbated during different processing stages through bad tanning practices (Figure 1.3) [7, 12, 14]. However, in some batches of finished leather that have been processed the same way there are hides that show looseness and those that do not. Thus, it is probable that looseness is sometimes a defect of the raw material that is only detected after processing. Age, nutrition, breed, gender, and time of year have all been suggested as contributors to looseness [9, 15, 16]. One study suggested that underfed and older animals have

a greater tendency to produce loose leather [14], indicating that the raw material used to produce leather is likely to have an impact on whether the leather is loose or tight.

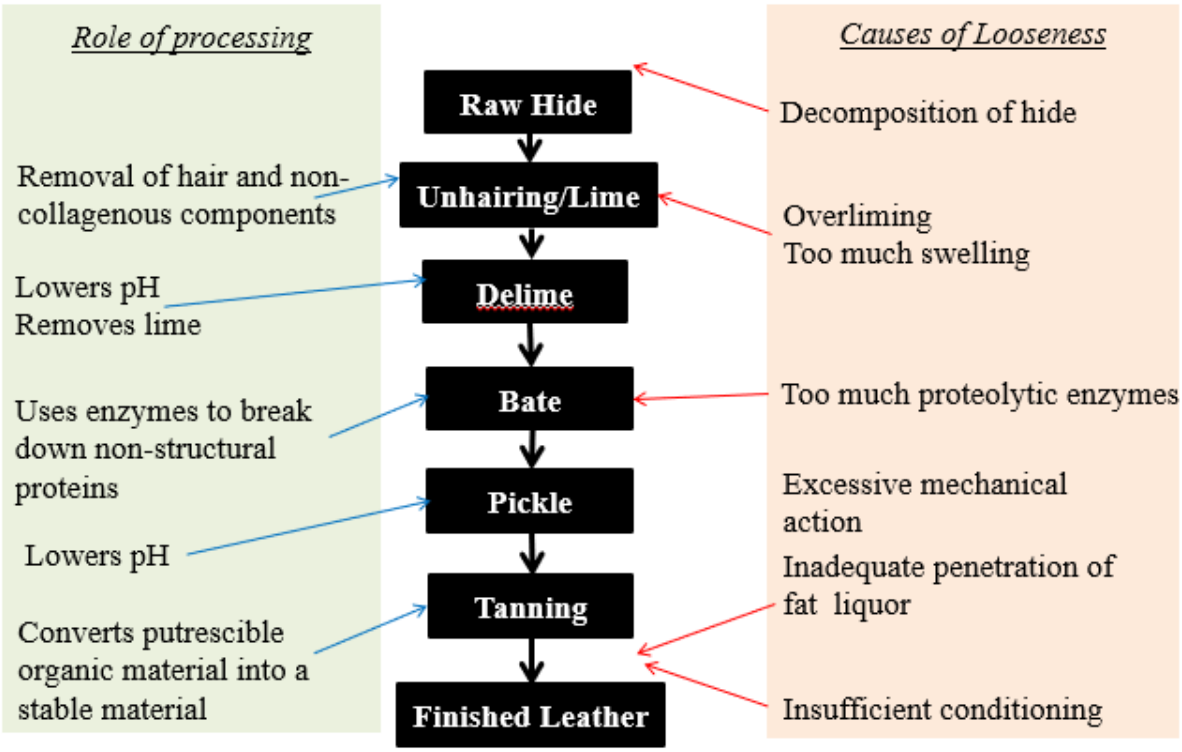

Figure 1.3 Flow diagram showing the different stages of leather processing that can have an influence on looseness [7, 12, 14].

To date there have been no reports investigating the molecular basis of looseness in the raw hide possibly because of the difficulty in detecting looseness in the raw material. However, methods are currently being developed to determine looseness at earlier stages of processing. One of these is nuclear magnetic resonance (NMR) transverse relaxation analysis [17] and the other is ultrasound [18]. An understanding of the molecular basis of looseness in the raw hide will aid in developing methods for early detection of the problem, thus minimising losses to the industry. As there are many different macromolecules that make up hide, previous research looking into the cause of wrinkles of other animals such as humans with ageing and Shar-Pei dogs was used as a starting point to develop this project.

1.2 Structure

Skin/hide is composed of three layers: the epidermis, dermis and hypodermis (Figure 1.4).

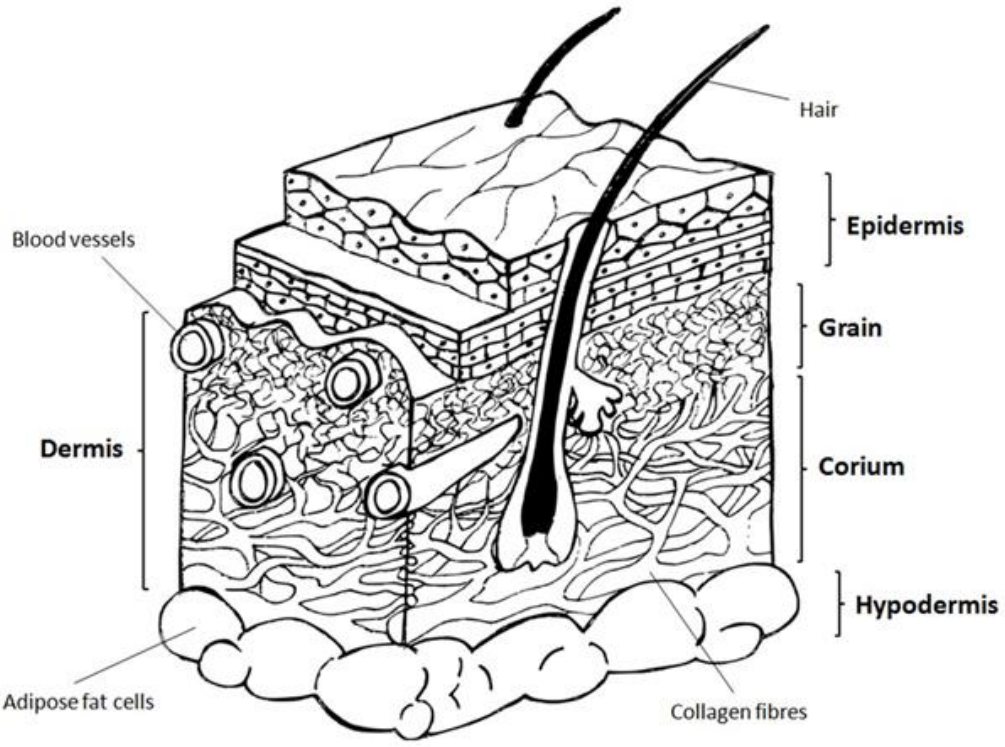

Figure 1.4 Diagram of skin/hide illustrating the three different layers**.**

Epidermis

The epidermis is the outer layer of the skin/hide. It regulates water loss from the body and prevents entry of harmful materials such as microorganisms [1]. The epidermis consists of keratinocytes, melanocytes, dendritic cells, natural moisturizing factors and epidermal lipids [1, 19, 20]. The epidermis also contains the hair, wool, nails, scales, horns and hooves of the animal which are removed early on in leather processing unless specialised leather is being produced [7, 8].

Dermis

The dermis is the largest layer of the skin/hide and is made up of two zones: the grain and the corium [1, 7]. The grain consists of hair shaft and roots, sebaceous glands, erector pili muscles and arteries and veins [7]. The collagen fibres are relatively thin and randomly orientated to

form a meshwork [21, 22]. This layer makes up the surface of the leather and hence its visual appeal needs to be high. The corium in contrast consists of loosely interwoven, large, wavy, randomly orientated, tightly packaged collagen bundles. The fibre bundles in the corium are the largest, measuring approximately 0.1 mm in diameter [1, 7, 21]. The bundles divide and recombine with other fibres resulting in a material that is both strong and flexible. It was initially thought that the main function of the dermis was to provide a structural foundation. However, a significant number of diseases correlate to mutations in proteins found in the dermis, suggesting it has other underlying functions [1, 23]. In leather it is this layer that contributes the most to strength.

Hypodermis

The hypodermis layer has a membrane like 'character' and contains layers of fat cells that serve to connect skin/hide loosely with the underlying muscles and bones. It contains about 50 % of the body's fat, serving as an energy store and padding for the dermis [1]. During leather processing this layer is mostly removed by a machine called a flesher [7].

The structure of skin/hide is well established resulting in a large array of literature. Its structure is often assessed using histological experiments to identify the large number of macromolecules that comprise the different layers.

1.3 Molecular Components of skin and hide

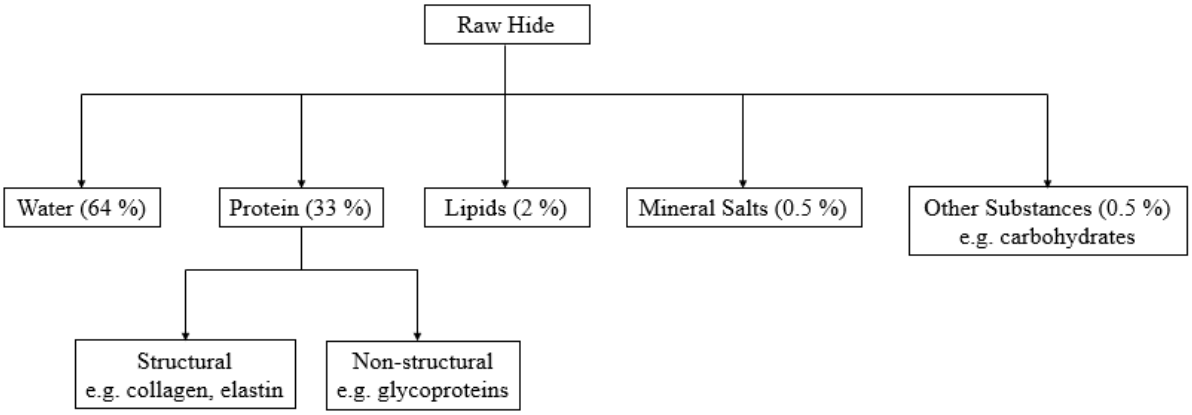

Figure 1.5 Diagram illustrating the molecular composition of hide. Based on figure from Sharphouse [8].

Skin/hides are comprised of many different macromolecules (Figure 1.5). The three main groups are; proteins, carbohydrates and lipids. The molecules in skin/hide have been extensively studied using a variety of different techniques and are frequently linked to skin diseases and defects. Changes that lead to wrinkles in skin/hide were of particular interest to this research because of the similarities to the defect looseness. Wrinkles are defined as the creases and folds that develop in skin. They form as part of the intrinsic ageing process and may be acerbated by environmental factors such as ultraviolet (UV) radiation, called extrinsic factors [24]. Excessive wrinkles in skin can also result from genetic disorders such as gerodermia osteodysplastica and cutis laxa [25]. Some species such as Shar-Pei dogs and naked mole rats have wrinkly skin at birth. In the case of the naked mole rat this provides an evolutionary advantage as it helps the animal move through burrows [26], whilst the trait of wrinkles in Shar-Pei dogs has been selectively bred for by humans [27]. Figure 1.6 illustrates how the molecular components collagen, elastin and GAGs are thought to change in aged skin contributing towards wrinkle formation [28], which will be discussed in depth in later sections. Understanding how the molecular composition changes in wrinkly skin/hide compared to tight

skin/hide will increase our knowledge of the possible cause(s) of wrinkles and provide the basis for an investigation into the molecular cause of looseness in leather.

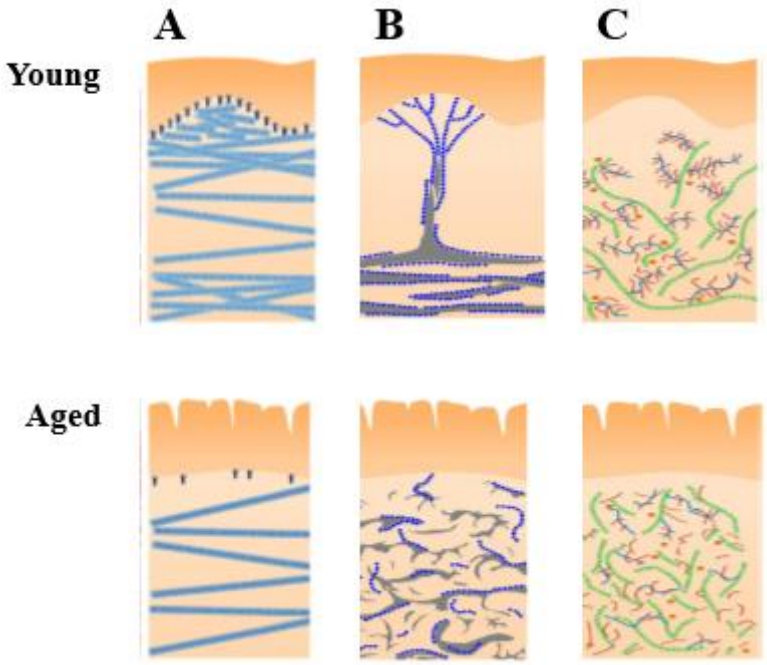

Figure 1.6 Schematic diagram of (A) collagen, (B) elastin and (C) GAGs in young and aged skin samples showing the affect age has on the structure and concentration of these compounds. Taken from Naylor, Watson and Sherratt [24] with permission of the publisher.

1.4 Proteins

Proteins are the most abundant macromolecule found in skin/hide with collagen accounting for approximately 75 % of its total dry weight [5]. Proteins provide the structural scaffold that makes up skin/hide and either support or are directly responsible for all its biological functions. The four main groups of proteins found in skin/hide are collagen, elastin, proteoglycans and glycoproteins. Conventional methods for detection and quantitation of proteins focus on the analysis of single molecules, some of which are mentioned below. Advances in proteomic tools such as mass spectrometry (MS) has enabled the large scale identification and quantitation of expressed proteins, isoforms and post translational modifications (PTMs) [29]. This enables experiments to be designed to investigate how skin/hide is affected by factors such as age, external or internal stress and disease [30-32].

1.4.1 Collagen

Collagen is the predominant protein in skin/hide. It has important physiological properties including maintaining structure, cell adhesion, migration, dynamic interplay between cells, regulation of tissue remodelling during growth, differentiation, morphogenesis and wound healing [33, 34]. Twenty-eight different types of collagen have been identified and characterised [33-35] although only nine of them have been identified in skin/hide (Table 1.1). Of these, collagen types I and III are the predominant collagens found in skin/hide. They are fibrous and help resist tension. Collagen type I is mainly found in the corium while type III forms the fine fibrils that are mainly found in the grain [36]. Others include type IV which forms a non-fibrillar meshwork and is associated with the basement membrane [37], type V which regulates fibril formation in cell movement and differentiation [38], type VI which forms beaded filament-forming collagen networks that together with decorin regulate fibril assembly [39], type VII an anchoring fibril that forms links between collagen VI to maintain dermal-epidermal junction integrity [40], and types XII, XIV and XVI which are non-fibrillar, fibril-associated collagens with interrupted triple helices (FACITs), that are associated with the surface of collagen fibrils and fibres and interact with other ECM components [41, 42].

Structure

The amino acid composition of collagen is unique. It contains all of the standard amino acids apart from tryptophan which hinders the formation of the triple helix [43]. It also contains two unique amino acids hydroxyproline and hydroxylysine, which help stabilize the tropocollagen and fibrillar structure [34, 44, 45]. Hydroxylysine is especially important for stabilizing the structure of collagen fibrils through the formation of covalent crosslinks. The amino acid sequence contains multiple three amino acid repeats of glycine-X-Y where 30 % of the time X is proline and 30 % of the time Y is hydroxyproline [7, 46].

Table 1.1 Types of collagen found in skin/hide [34-37, 39-42, 47-49].

Classification	Collagen type	Role
Fibrillar collagen	I	Large fibril diameter Approximately 90 % in skin
	III	Small fibril diameter High in grain layer Approximately 10 % in skin
	V	Regulatory fibril forming collagen Found in association with collagen I
Basement membrane collagens	IV	Forms thin sheets (40-50 nm) Interlaced networks Aids in molecular filtration
	VII	Creates anchoring filaments Found in dermal-epidermal junction
Bead filament collagen	VI	Bead filaments with short triple helical regions Maintains tissue integrity Regulates fibril assembly with decorin
FACIT collagens	XII	Interact directly with fibrillar collagen molecules
	XIV	
	XVI	

Biosynthesis

Most collagens are synthesised using a similar biochemical pathway (Figure 1.7). After the mRNA has been transcribed, the procollagen undergoes multiple steps of PTMs including hydroxylation of specific proline and lysine residues and glycosylation of selected hydroxylysyl residues [34, 35]. Three-left handed α helices are folded into a right-handed triple helix. The individual chains can either be the same or different [34, 35]. Tropocollagen is formed after the procollagen is transported out of the fibroblasts into the ECM and the pro-peptides are cleaved by specific proteinases [34, 35]. Tropocollagen self-assembles into fibrils with a diameter of approximately 20-100 nm, forming a staggered array that is responsible for the d-banding with a periodicity of 67 nm [46, 50, 51]. Enzymes such as lysyl oxidase are responsible for the formation of covalent crosslinks with other collagenous and non-

collagenous molecules, which help maintain the collagen's structure and confer mechanical strength [35, 44]. Collagen fibrils then assemble into fibres and fibre bundles with the aid of other collagenous and non-collagenous proteins.

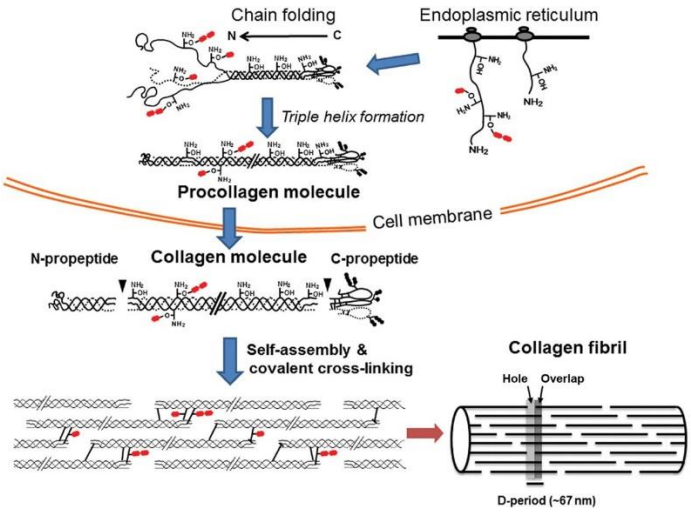

Figure 1.7 Schematic diagram of the different stages of fibrillar collagen biosynthesis**.** Procollagen is formed within the cells through a series of complex reactions. The molecule is then transported into the extracellular space where it assembles into collagen fibres and is stabilised by the formation of covalent crosslinks. Taken from Yamauchi and Sricholpech [52] with permission of the publisher.

Collagen crosslinks

Collagen crosslinks are formed when the collagen is classified as tropocollagen [35, 53]. There are two types of crosslinks; enzymatic and non-enzymatic. Enzymatic crosslinks depend on the amount of hydroxylysine and lysine in the collagen molecules and their location in the helical and telopeptide domains [54, 55]. They are formed by lysyl oxidase which modifies specific lysine residues. These then form Schiff base intermolecular crosslinks between both non-helical and helical domains of adjacent molecules [56, 57]. Non-enzymatic crosslinks are typically called advanced glycation end products (AGEs), and are the result of glucose spontaneously binding to specific lysine and arginine residues through the Maillard reaction.

This reaction is influenced by age and disorders such as diabetes and results in collagen fibres with decreased mechanical strength [54, 58].

Enzymatic crosslinks

Enzymatic crosslinks are characterised by the chemical pathways that produce them. There are two pathways that cause enzymatic crosslinks; one based on allysine (a lysine-derived aldehyde) and the other on hydroxy-allysine (a hydroxylysine-derived aldehyde) [54, 59]. The allysine pathway is the most prominent in skin/hide [59]. The crosslinks so formed are further characterised by their structure and properties. The lysine or hydroxylysine-derived aldehyde reacts with corresponding aldehydes on adjacent polypeptide chains to form aldol condensation products (ACP) or with unmodified lysine and hydroxylation residues to form bifunctional crosslinks [54]. Hydroxylysinonorleucine (HLNL) and dihydroxylysinonorleuncine (DHLNL) are examples of reducible, bifunctional crosslinks that are found in skin/hide (Figure 1.8). HLNL is formed by an allysine reacting with hydroxylysine [60] while DHLNL is formed by hydroxyallysine reacting with hydroxylysine [60]. The reducible crosslinks react with other amino acids to form mature crosslinks. Two mature cross links that have been identified in skin/hide are histidinohydroxylysinonorleucine (HHL) a trivalent crosslink and histidinohydroxymerodesmosine (HHMD), a tetravalent crosslink (Figure 1.8) [57, 61]. Both contain histidine [59]. HHL is formed as the skin /hide matures and occurs when HLNL reacts with histidine [59, 60]. There is still some controversy over whether HHMD is a collagen crosslink or an artefact arising from the experimental conditions used to isolate crosslinks from tissue [59]. Some studies suggest HHMD is produced by the reaction of HHL with DHLNL or by the reaction of hydrdroxylysine with allysine-aldol and histidine [59, 60].

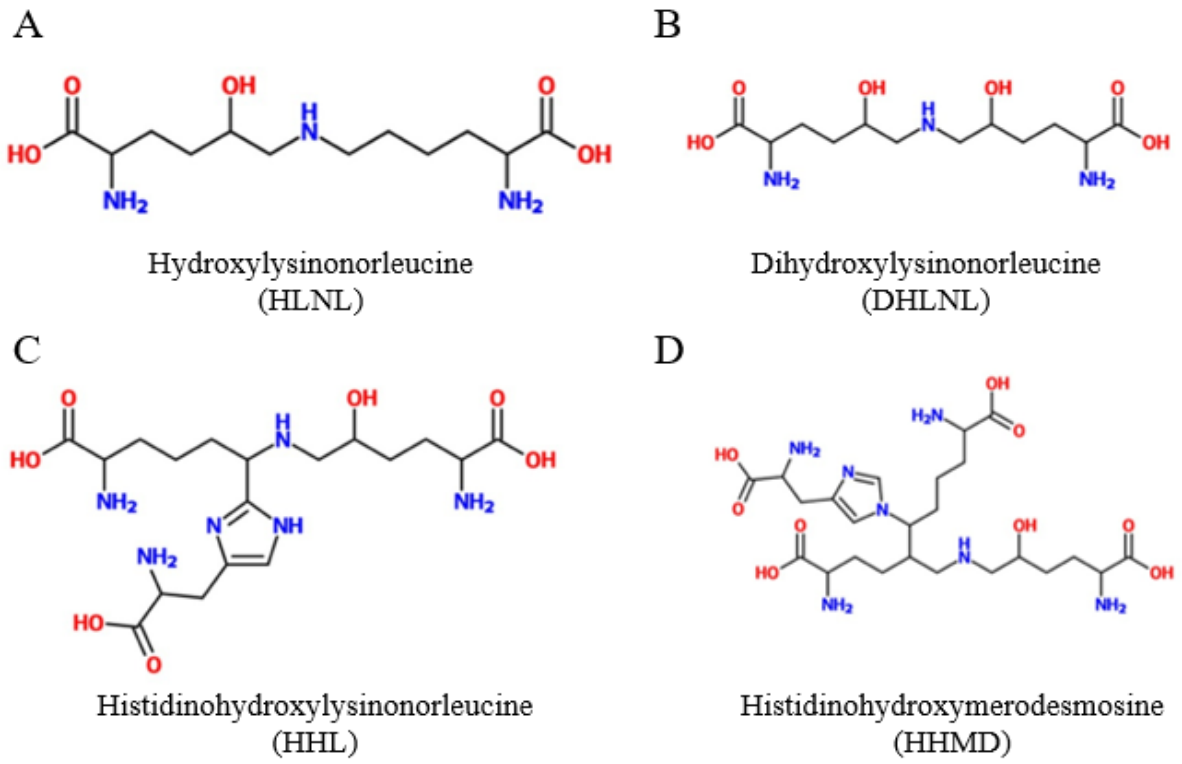

Figure 1.8 Structure of key collagen crosslinks found in skin/hide: (A) HLNL, (B) DHLNL, (C) HHL and (D) HHMD. Taken from Naffa *et al.* [57, 61] with permission of the publisher.

Non-enzymatic crosslinks

Non-enzymatic crosslinks are formed due to glycation of collagen. Less is known about the synthesis of non-enzymatic crosslinks. However, they are thought to be formed by Maillard reactions. Lysine or hydroxylysine amino acids form a Schiff base in the presence of a reducing reagent and the product is then rearranged into more stable Amadori products [54]. Two examples of lysine-arginine crosslinks are pentosidine, a fluorescent product formed from ribose and glucosepane a non-fluorescent product formed from glucose [35]. Non-enzymatic crosslinks have been linked to age and diabetes and result in alterations in the physiochemical properties of collagen including conformation, ligand binding, enzymatic crosslinking and interactions between collagen and other macromolecules [35, 54].

Techniques used to study differences in collagen structure, concentration and composition in wrinkly and tight skin/hide

The structure of collagen has mainly been studied using histological techniques which look at the organisation and orientation of collagen, but do not give quantitative data. Over time many different techniques have been used; for example, Lavker *et al.* [62] used a combination of light microscopy, transmission electron microscopy and scanning electron microscopy to discover that in aged skin, the collagen fibres form aggregates of loosely woven primarily straight fibres that pack less tightly compared to those of young skin. They also showed an increased density of collagen which probably reflects the decrease in spaces between individual fibres. These three techniques were used to examine the organization, fine structure and geometry of the collagen fibres in the skin. Other studies have used techniques such as *in vivo* ultrasonic imaging to show that in aged skin there is a relative increase in thin collagen bundles as opposed to large ones [63]. Another used confocal laser scanning microscopy and optical coherence tomography to show that aged skin has a thinner epidermis and a flatter dermo-epidermal junction [64]. The use of multiple techniques each with their own advantages and disadvantages has produced an overview of the physical characteristics of wrinkly skin. However, the difficulty of analysing only wrinkly skin has caused some debate as to whether wrinkly skin is different or if it is just aged skin that is different [28].

The concentration of collagen is typically estimated using hydroxyproline, as hydroxyproline is an amino acid specific to collagen. Two techniques can be used; colorimetric assays with dyes specific to hydroxyproline or high-pressure liquid chromatography (HPLC). Whilst colorimetric assays are typically quicker, the HPLC technique is shown to be more sensitive, specific and accurate [65]. Experiments using these techniques typically suggest that collagen

concentration decreases with age [28, 66] (Figure 1.6A) although other reports have provided evidence that the collagen concentration does not vary significantly [67].

The composition of collagen has also been shown to vary with age. Many results indicate that the ratio of type III to type I collagen increases with age [68]. There has also been some debate about the amount and distribution of collagens IV and VI [24]. The different types of collagens and their effects on aged skin have been investigated using a variety of techniques including immunohistochemistry, western blotting and MS. Whilst immunohistochemistry and western blotting enables the researcher to study only one protein at a time, MS enables multiple proteins to be studied at once and is more sensitive [69, 70].

The crosslink profile of collagen in skin/hide changes as the animal matures, possibly resulting in the formation of wrinkles. Immature (reducible, bifunctional) crosslinks like HLNL and DHLNL have been found to decrease with age whilst mature (trivalent and tetravalent) crosslinks like HHL and HHMD have been shown to increase [53, 71]. Non-enzymatic crosslinks also increase with age and cause changes to the properties of collagen that can result in stiffness and wrinkle formation [54, 56]. Collagen crosslinks can be reduced by sodium borohydride into a stable form which enables them to be detected and isolated [72]. Multiple different methods have been used to detect and isolate crosslinks including ion-exchange and HPLC and single ion-exchange columns [71]. A recent technique has been developed which isolates the crosslinks using a CF-11 column, and separates and detects all of the known collagen crosslinks using MS [57, 61].

Collagen in Leather

Leather processing is known to affect the natural collagen network, for example, the fibre structure opens up during liming which enables tanning chemicals to better penetrate the skin/hide [6, 7, 73]. The variations in crosslinking observed for different species impart different physical properties to the skins/hides, and can affect the degree of fibre order and the amount it opens up during processing [61]. During leather processing most of the covalent crosslinks are removed in the liming and bating stages then are replaced during the pre-tanning and tanning stages [73]. It is thought that crosslinks provide stability to the network structure, that is compromised by their removal, destabilising the network so that the fibrils become more aligned [73]. Some collagens, such as collagen IV which is found in the epidermis and extends into the hair follicles, can be damaged during the processing affecting the appearance of the final product [7]. The collagen structure of skin/hide affects the structure of leather; thus, it is not surprising that skin/hide defects affecting collagen such as those that cause wrinkles will inevitably affect the final leather product.

1.4.2 Elastin

Elastin is the protein that contributes to elasticity of skin/hide. It also regulates activity of transforming growth factors β (TGFβs) through its association with fibrillin microfibrils, and is involved in cell adhesion, migration, survival and differentiation as well as acting as a chemotactic agent [74]. Elastin is typically located in the grain layer, although it can also be found close to the hypodermis [7]. It is an insoluble non-glycosylated protein with a molecular weight of approximately 60 kDa [74]. The elastic fibres are composed of both amorphous and microfibrillar components, with the amorphous component making up approximately 90 % of the mature elastic fibre [74-76]. Elastin microfibres consist mainly of the glycoprotein fibrillin but also include other proteins such as fibulins and proteoglycans such as biglycan [74].

Elastin has a similar amino acid composition to collagen although it has more hydrophobic amino acids, less hydroxyproline [74, 76] and no hydroxylysine [59, 74]. The hydrophobic regions are rich in valine, proline and glycine. Glycine appears in approximately one third of the sequence similar to what is seen in collagen, however unlike collagen its distribution is not uniform [76]. The hydrophobic domains are thought to form a loose and very mobile structure of stacked β-sheets with β-turns that are responsible for the resilience of the protein [74, 76]. Elastin interacts with water which aids the three dimensional (3D) organization of elastin fibres as well as the degree of hydration and elasticity [74].

Elastin is initially synthesised as tropoelastin with a characteristic primary structure of alternating hydrophobic and crosslinking domains. After secretion, the individual tropoelastin molecules are specifically aligned on a scaffold of fibrillin-rich microfibrils, and stabilized by the formation of the intermolecular crosslinks desmosine and isodesmosine (Figure 1.9) [51, 75, 76]. While other crosslinks are present in elastin, desmosine and isodesmosine are unique to it [59, 74]. They are formed from the linking of a single lysine side chain to three allysines [59]. The exact biosynthetic pathway of elastin crosslink formation is, however, not clear despite the initial condensation products, dihydrodesmosines having been identified [59].

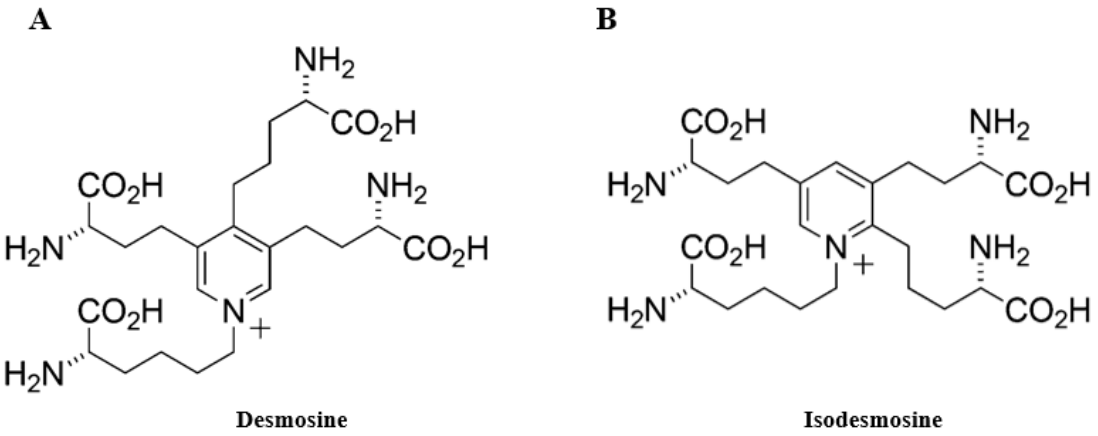

Figure 1.9 Structure of elastin cross links in skin/hide (A) desmosine and (B) isodesmosine. Taken from Murakami *et al.* **[77] with permission of the publisher.**

Techniques used to study elastin in wrinkly and tight skin/hide

Histological studies using stains such as orcein, resorcin and fuchsin can be used to look at the structure and location of elastin in skin/hide [78-81]. However, these methods do not provide quantitative data. Typically, two different methods are available for the quantitative study of elastin; gravimetric analysis of elastin after its isolation and determination of its concentration using biomarkers such as desmosine and isodesmosine crosslinks [61, 82, 83]. Gravimetric analyses such as colorimetric assays, have the requirement of extraction and weighing which necessarily limits their accuracy. Colorimetric assays also have limited specificity as they depend on the dye used and how it binds to the substrate molecule [61, 83]. The concentration of desmosine and isodesmosine can be detected using a variety of techniques such as electrophoresis, radioimmunoassay, enzyme immunoassay, thin layer chromatography (TLC), and HPLC/MS [61]. HPLC/MS determines the concentration of desmosine and isodesmosine simultaneously with high accuracy while other techniques such as TLC and electrophoresis are less accurate and more prone to interference by other sample components [61].

Studies using a combination of these techniques showed that changes in elastin structure and concentration are common to wrinkled skin resulting from ageing and from the genetic disorder cutis laxa. The majority of elastin is synthesised and produced before or just after birth and due to its long half-life, its concentration in the skin/hide is actually thought to increase with age [28, 84]. Over time, however, the elastic fibres are thought to become linked through glucose-mediated crosslinking, and to be damaged by calcium and lipid accumulation as well as the time-dependent modification of aspartic acid residues [28, 84]. This affects their ability to stretch and recoil, (Figure 1.6B) [24] and contributes to the formation of wrinkles. The genetic disorder cutis laxa is thought to be due to a mutation in the gene that encodes elastin. This results in less elastin content in the elastic fibres suggesting that the mutant tropoelastin protein

alters the architecture of the elastic fibres [75, 76]. The elastin in patients with cutis laxa contains fewer crosslinks resulting in reduced elastic recoil and the wrinkly skin characteristic of this condition [75, 76].

Elastin in Leather

Elastin is typically removed during the bating step of leather processing [7, 85], enabling the grain to relax and flatten which increases the area of the final product [7, 79, 85]. Elastin remaining in the skin/hide during later stages of leather processing can lead to the elastin fibres forming crosslinks with the tanning agents, resulting in rigid leather with little elasticity [85].

1.5 Carbohydrates

Carbohydrates in skin/hide are split into two categories:

- GAGs – long unbranched polysaccharides that have repeating disaccharide units and are found on proteoglycans.
- Glycans – glucose or lactose molecules that are covalently attached to hydroxylysine.

1.5.1 GAGs

GAGs are negatively charged, unbranched polysaccharides with molecular weights of 10 – 100 kDa [86]. They are made up of repeating disaccharides containing an aminoglycan and uronic acid [86, 87]. The saccharides can be sulfated at any of the available positions. The hydroxyls at the 2, 4 and 6 positions are those most commonly sulfated with disaccharides often being sulfated in groups which is thought to impart biological function [88]. GAGs interact with water and help hydrate the skin/hide, they also create a fluid that fills the space between the collagen and elastin fibres giving them turgidity [24, 86]. Other roles attributed to GAGs include cell adhesion, growth, differentiation and signalling as well as anticoagulation [86, 87].

Five different types of GAGs are typically found in the skin/hide; dermatan sulfate, chondroitin sulfate, heparin/heparin sulfate, keratan sulfate and hyaluronic acid (Table 1.2).

Table 1.2 Classification of GAGs found in skin/hide [86, 89-97].

Type	Structure	Function
Dermatan sulfate	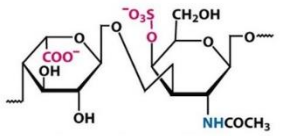	Major GAG found in skin When associated with decorin, it is directly involved in collagen fibril formation
Chondroitin sulfate	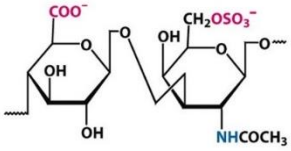	Collagen fibrillogenesis Facilitates collagen crosslinking
Heparin/heparin sulfate	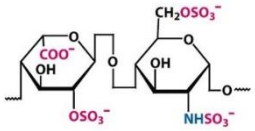	An *in vivo* study reported that heparin inhibits collagen fibrillogenesis by hindering lysyl oxidase activity
Keratan sulfate	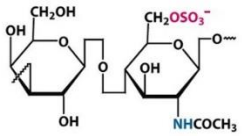	Covalently linked to lumican and associated with fibrillar collagen
Hyaluronic acid	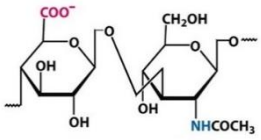	Maintains normal hydration of skin Distributes salts and nutrients Enhances enzymatic resistance and mechanical properties of collagen Associated with collagen fibrils and elastin fibres involved in structure and organisation

Dermatan sulfate

Dermatan sulfate is the major GAG found in skin/hide. It has a molecular weight of 15-40 kDa and is composed of repeats of *L*-iduronic acid and 2-acetyl-galactosamine [98]. It is sulfated at the carbon 4 and 6 of the hexosamine and carbon 2 of the *L*-iduronic acid which results in a highly charged, highly acidic proteoglycan [98, 99]. Through its interaction with proteins it stabilises the ECM, regulates enzyme activity, and interacts with signalling molecules, cofactors and/or co-receptors for growth factors, cytokines and chemokines [98]. Experiments

have shown that when dermatan sulfate is associated with decorin it is directly involved in collagen fibrillogenesis [91, 93].

Chondroitin sulfate

Chondroitin sulfate has a molecular weight of 5-50 kDa. It consists of *n* repeats of *D*-glucuronic acid and *N*-acetyl galactosamine disaccharides [86, 88]. It is commonly sulfated on either carbon 4 and/or carbon 6 of the *N*-acetyl galactosamine. Chondroitin sulfate binds to proteins such as collagen to form protein aggregates and has a role in collagen fibrillogenesis through facilitating collagen crosslinking [86, 93, 96, 100].

Heparin/Heparin sulfate

Heparin and Heparin sulfate are linear polysaccharides with repeating uronic acid and glucosamine disaccharides [92]. They are the most structurally complex GAG with 24 different uronic acid (1-4)-D-glucosamine disaccharides due to the fact that they can contain both *N* and *O* sulfated hydroxyls as well as *N*-acetyl groups [92]. Proteoglycans containing heparin or heparin sulfate have roles in cell adhesion, regulation of cell growth, coagulation and angiogenesis [92]. One study suggests that heparin has a role in inhibiting collagen fibrillogenesis by hindering lysyl oxidase activity [90] whilst another identifies heparin/heparin sulfate binding sites in fibrillin-1 indicating it may have a role in the assembly of microfibrils.

Keratan sulfate

Keratan sulfate has a molecular weight of 4-19 kDa, and is the most heterogenous GAG [86]. It is typically found in other tissues such as the cornea, however small amounts are present in skin/hide [89]. Keratan sulfate has repeating disaccharides of *D*-galactose and *N*-acetylglucosamine. The sulfation is primarily on the carbon 6 of the *D*-galactose, and it is *O*-

linked to asparagine residues of core proteins [89]. Its potential roles in skin/hide has not been extensively studied however it is believed to form covalent bonds with lumican and to be associated with fibrillar collagen [89]

Hyaluronic acid (HA)

HA has a molecular weight between 4 and 8000 kDa, it is the only non-sulfated GAG and forms non-covalent bonds to proteins in the ECM [86]. It contains repeating disaccharides of D-glucuronic acid and N-acetyl-D-glucosamine and, due to its lack of sulfation, is less acidic than dermatan sulfate [95]. Unlike other GAGs that are synthesised in the Golgi, HA is synthesised at the cell membrane [95]. It has many functions including cell differentiation and proliferation, regulation of apoptosis and angiogenesis and promotion of tissue integrity [94]. Its major function in the skin/hide is hydration as it forms a large tangled weave that traps large quantities of water [94, 95].

Techniques used to study GAGs in wrinkly and tight skin

Qualitative analysis of GAGs can be achieved using stains such as alcian blue followed by microscopy to observe their structure and localisation [78]. However, such methods do not give any quantitative information. Colorimetric assays and HPLC can be used to quantify GAGs. Different colorimetric assays include the carbazole assay which produces reliable results for uronic-acid containing GAGs but is affected by salt [101] and the alcian blue and dimethylmethylene blue methods which although fast, are only reliable for sulfated GAGs [101, 102]. Although the HPLC-based method provides very reliable results for a range of GAGs, it is time consuming and requires specialist equipment [101].

Evidence that GAGs are associated with wrinkly skin arises from two sets of evidence. Aged skin shows either a loss of GAGs or their accumulation in disorganised aggregates depending on the method of ageing *e.g.* natural over environmental influences such as UV radiation [24, 28] (Figure 1.6C). Studies on chondroitin sulfate suggest that it is modified with age and UV radiation [103, 104]. Shar-Pei dogs and naked mole rats that have naturally wrinkly skin have skins with increased concentrations of HA. Studies suggest that this is due to higher transcription of the *has2* gene resulting in increased activity of hyaluronic acid synthase2 (HAS2) [27, 95]. Naked mole rats, on the other hand produce a very high molecular weight (long chain) HA, over 5 times higher than that of humans, which accumulates in tissue due to the decreased activity of HA degrading enzymes [26, 95].

GAGs in Leather

HA is removed during the processing of leather prior to treatment with alkali. Excess HA in the skin/hide results in stiff leather as chromium tanning salts and other mineral tanning agents react with it. While the effect of other GAGs such as dermatan sulphate on the finished leather products is not as clear, they are also removed during processing as it is known that they bind to other proteins including collagen [7].

1.5.2 Proteoglycans

Proteoglycans are a class of proteins that have at least one GAG molecule covalently linked to the core protein [105]. There are three main categories of proteoglycans; small leucine-rich proteoglycans (SLRPs), modular proteoglycans and cell-surface proteoglycans. They regulate many cellular processes that depend on both the core protein and the attached GAG including regulating collagen fibril formation in skin/hide [105]. Table 1.3 shows the structure and function of proteoglycans in skin/hide.

Table 1.3 Types of proteoglycans and their functions in skin/hide [106, 107].

Name	Class	GAG Chains	Function
Decorin	SLRP	Chondroitin sulfate Dermatan sulfate	Interacts with fibrillar collagen Inhibits collagen fibrillogenesis
Biglycan	SLRP	Chondroitin sulfate Dermatan sulfate	Interact with fibrillar collagen
Lumican	SLRP	Keratan sulfate	Interacts with type I collagen Regulates size of collagen fibrils
Versican	Modular (lectican)	Chondroitin sulfate Dermatan sulfate	Interact with HA Increases viscoelasticity and regulates cell shape

SLRPs

SLRPS have a protein core containing leucine-rich repeat sequences, *N*-terminal cysteine clusters and "ear repeats" as well as at least one GAG chain [105]. SLRPs regulate collagen fibril assembly by binding to collagen at specific binding sites thus delaying fibril formation [108]. They also inhibit cell growth and bind to TGFβ [105]. SLRPs may also have a role in regulating the intermolecular crosslinking of collagen [108]. Of the many different types of SLRPs, only decorin, biglycan and lumican are found in skin/hide [105, 108].

Decorin the major proteoglycan in skin/hide, is localised in the dermal ECM [109]. It consists of a single unbranched GAG which can be either chondroitin sulfate or dermatan sulfate and is linked to the 4^{th} *N*-terminal amino acid of the core leucine rich protein [109]. The core protein binds to specific surface residues on type I collagen fibrils, the interaction being stabilised by electrostatic interactions between collagen and the sulfates of the GAG [109]. This interaction is necessary for the native assembly of collagen microfibrils and prevents the cleavage of collagen fibrils by matrix metalloprotease I [109].

Biglycan contains a core leucine-rich protein attached to two GAGs, either dermatan sulfate or chondroitin sulfate [74, 106]. In skin/hide the biglycans are localized to the epidermis and dermis [109] and have been shown to organise collagen VI microfibrils into a hexagonal network using the two GAG chains [108].

Lumican contains keratan sulfates attached to a core protein [110]. Its roles includes binding to fibrillar collagen, regulating fibrillogenesis and inhibiting the size of collagen fibrils [106, 107].

Modular Proteoglycans

Modular proteoglycans are a diverse group characterized by the assembly of various protein modules in an elongated and often highly glycosylated structure [105]. There are two main groups; the hyalectans which bind lectin and the non-hyalectans. Versican is a hyalectan that is found in skin/hide. It has a tridomain structure consisting of a central domain that carries most of the GAGs surrounded by unique *N*- and *C*-terminal globular regions. The *N*-terminal domain binds HA whilst the C-terminal domain binds lectins [105]. The GAGs are either chondroitin sulfate or dermatan sulfate and its major functions include regulation of cell adhesion, migration and proliferation, ECM assembly and fibrillogenesis of elastic fibres [105].

Cell-surface proteoglycans

There are two main groups of cell-surface proteoglycans: membrane-spanning *e.g.* the syndecans and GPI-linked proteoglycans such as the glypicans [105]. The GAG that interacts with these molecules is heparin/heparin sulfate which acts as a co-receptor facilitating ligand encounters with signalling receptors [105].

Techniques used to study proteoglycans in wrinkly and tight skin

A range of techniques have been used to study proteoglycans in skin/hide including immunoblotting and SDS-PAGE [111]. Another method utilises MS. Both the types and concentrations of various proteoglycans have been shown to change throughout an animal's lifetime. Versicans containing chondroitin sulfate GAGs are known to decrease with age [111] and their structures and concentrations in foetal skins is different to those in mature skins [111]. On the other hand, the concentration of decorin containing dermatan sulphate GAGs increases with age [111] although its molecular size significantly decreases with age. This is thought to be due to a reduction in the size of the GAG chain as the average size of the protein moiety remains constant [109]. Knockout studies of lumican have shown that it has a profound effect on skin laxity and fragility [110].

Proteoglycans in leather

Proteoglycans are typically removed during the pre-tanning stage of leather processing. Studies have shown that 1.2 % of proteoglycans are removed in the pre-tanning stages, and this removal depends on the duration of these processes [112]. As processing is known to contribute to looseness in leather, it is possible that the presence and concentration of proteoglycans in the raw material may have an effect.

1.5.3 Glycoproteins

Glycoproteins are proteins that have complex carbohydrate molecules post-translationally linked to either serine or threonine sidechains (*O*-linked), to the amino nitrogen of asparagine sidechains (*N*-linked) or to the sulfur of cysteine residues (*S*-linked) [113, 114]. Glycoprotein synthesis occurs in the endoplasmic reticulum and the Golgi apparatus where the carbohydrate core is co-translationally attached to the protein [113]. There are a multitude of glycoproteins

in skin/hide including collagen and proteoglycans. The attached carbohydrate molecules give the protein hydrophilicity, make the protein more soluble, resistant to proteolysis and help it to fold correctly [113]. Table 1.4 shows the structure and function of some non-collagenous glycoproteins found in skin/hide.

Table 1.4 Glycoproteins found in skin/hide [74, 79, 115-117].

Type	Protein Structure	Glycans	Function
Fibronectin	230-270 kDa Forms aggregates and fibrils 2 subunits covalently linked by disulfide bridges at the carboxyl terminus Each subunit has 4 globular regions	*O* and *N*-linked ~4-9 % carbohydrate	Cell surface adhesion Migration Growth and differentiation. Binds directly to some sites on collagen and to some GAGs
Fibulin	448 amino acids Integrin ligand 5 potential calcium-binding epidermal growth factor-like domains	Either *O* and/or *N*-linked depending on type	Supramolecular structure formation and or stabilisation Interacts with elastic fibres and basement membranes
Laminin	3 polypeptides Flexible 3 short arms and 1 long arm that contain globular regions	*N*-linked 13 % carbohydrate	Cell-adhesion interactions Laminin-5 localises at filaments between the dermal-epidermal junction and may be involved in binding collagen VII in anchoring filaments.
Fibrillin	~ 350 kDa 3 isoforms 40-80 amino acids. Calcium binding epidermal growth factor domains and eight-cysteine containing motifs.	Mainly *N*-linked, however some types have *O*-linked	Assembly of elastin into elastic fibres.

Fibronectin

Fibronectin is present at the dermal-epidermal junction of skin/hide and is made up of 2 domains that are covalently linked by disulphide bridges. Both domains mediate self-assembly and binding between collagen, heparin, fibronectin and other extracellular molecules [74, 117]. Fibronectin concentrations increase during wound healing and fibrosis [74]. They aid fibrillogenesis initiation, progression and maturation, because their multidomain structure enables them to bind simultaneously to a number of different cell surface receptors [74].

Fibulin

Fibulins are a group of seven glycoproteins that are tightly connected to the basement membrane, elastic fibres and other components of the ECM [74]. Fibulin-5 is the fibulin most common in skin/hide. It is a 448 amino acid glycoprotein with an integrin binding RGD motif (tripeptide Arg-Gly-Asp), six calcium binding epidermal growth factor-like repeats and a globular C-terminal domain [116]. It is found in the basement membrane of most tissues [115, 116]. Fibulin-5 interacts with a wide array of ECM components including fibronectin, laminin, versican, fibrillin and elastin [116]. It has roles in the assembly and stabilisation of the ECM and is involved in regulating organogenesis, vasculogenesis, fibrogenesis and tumorigenesis [116].

Laminin

Laminins are multidomain, heterotrimeric glycoproteins with sizes between 500 and 800 kDa [74]. There are sixteen trimeric isoforms of laminin each consisting of three chains. They form a cross or T shaped molecule with 2 to 3 short arms and one long arm [74]. Common to all laminins is a coiled-coil domain. The variability in the length of the chains is responsible for the large variation in laminin size [74]. They are located in the basement membrane and have

roles that include cell adhesion, interactions with integrins, dystroglycans and sulfated glycolipids. They maintain the structure of the ECM through adhesion, and are involved in differentiation, migration, stability of phenotype and resistance towards apoptosis [74].

Fibrillin

Fibrillin has a molecular weight of approximately 350 kDa, and has 3 different isoforms [74]. The structure consists of 40 – 80 amino acid residues and calcium binding epidermal growth factor domains interspersed with eight-cysteine containing motifs that bind TGFβ [74]. Fibrillin is the major microfibril found in elastic fibre, and interacts with tropoelastin and integrins. It plays an important role in the assembly of elastin into elastic fibres [74].

Techniques used to study glycoproteins in wrinkly and tight skin

The carbohydrate moiety of glycoproteins can be quantified using colorimetric assays and HPLC. Tandem MS enables both the protein and the glycan to be characterized simultaneously [113]. Glycoproteins such as collagen and proteoglycans have been shown to be different in aged or wrinkly skin. A mutation in fibulin-5 is responsible for a recessive form of cutis laxa in humans, that causes elastinopathy and results in loose skin [118]. Excessive glycosylation of proteins is also present in some cutis laxa patients [119].

1.6 Lipids

Lipids or fats are water insoluble substances. They include triglycerides, wax esters, fatty acids and smaller amounts of cholesterol, cholesterol esters, ceramides and squalene [28, 120]. Lipids in skin/hide are mainly concentrated in the epidermis and hypodermis layer [7, 120]. They are synthesised in the sebaceous gland which secretes a fatty mixture called sebum. The composition of the sebum varies among mammalian species [121, 122]. Table 1.5 shows the common lipids found in skin/hides [120]. Lipids play a number of important roles in skin/hides

including waterproofing, membrane formation, antimicrobial functions and energy storage [123-125].

Table 1.5 Composition of lipids found in skin/hide [120, 123-126].

Classification	Function
Triglycerides	Fat cells located in subcutaneous layer Synthesised in epidermis
Phospholipids	Membrane formation
Free fatty acids	Antimicrobial properties Located in outer layer of epidermis Role in permeability barrier homeostasis
Wax esters	Hydrophobic lipids Protect and lubricate skin Important for the survival of sebaceous glands
Cholesterol	Membrane formation

Triglycerides are synthesised in the epidermis by the sebaceous glands [123, 124]. Their role in permeability barrier homeostasis is poorly defined. Triglycerides are also the major ingredient of fat cells located in the hypodermis layer of skin [61, 120].

Phospholipids are important for the formation of membranes. They are produced by lamellar bodies (secretory organelles in keratinocytes) [124]. Phospholipases turns phospholipids into free fatty acids and glycerol which plays a role in keeping skin hydrated [124].

Free fatty acids are found in the outer layer of the epidermis (stratum corneum). They are saturated, straight chained molecules containing 20-28 carbons [123, 124] and give the skin/hide antimicrobial protection. They are required for normal stratum corneum structure and provide a permeable barrier [124].

Wax esters are unique to the sebum, and account for approximately 25 % of sebaceous gland lipids [125]. They are the most hydrophobic of all the lipids and aid in lubricating and protecting the skin/hide [122].

Cholesterol is also found in skin/hide and plays a role in membrane formation [122]. It is located in the lamellar bodies of the stratum corneum and plays a role in the permeable barrier [123].

Techniques used to study lipids in wrinkly and tight skin

Lipids can be analysed using a variety of different techniques. Histological stains and microscopy enable the distribution of lipids to be detected, and can give some insight into the types of lipid present in the tissue depending on the stain used [78]. Analyses such as TLC enable the different types of lipids to be separated and quantified [121, 127, 128]. Multiple studies using a variety of different techniques give conflicting results on changes in lipid concentration and composition in aged and wrinkly skin. Some studies suggest that the overall lipid content decreases with age, while others suggest there is no change in the amount, but rather a change in the composition [28]. It is clear that the concentration and composition of lipids is species specific [121]. One study found a possible relationship between fat content and looseness in ovine skins [11]. Sheep tend to have a greater percentage of lipids than other species such as cows due to a layer of large lipocytes in the grain-corium junction [7]. Removal of these lipids during processing is thought to create a void space resulting in loose leather.

Lipids in leather

Natural lipids in the raw material tend to be removed during processing in the degreasing step. This step is important as too many natural lipids tend to cause leather with fatty based stains,

bad odour, poor preservation and lack of inner softness, whilst too few natural lipids cause looseness, coarseness of the grain and a decrease in physical properties such as tensile strength and tear resistance [7, 120].

1.7 Research Aims and Objectives

Looseness is a defect found in 7 % of New Zealand cattle hides, that has an impact on the leather industry economy. Determining the molecular basis of looseness by qualitative and quantitative comparison of specific molecular components of the raw hide will hopefully aid in developing biomarkers for its early detection which will save money and time for the leather industry. Because previous research had shown there are changes in the collagen structure in loose leather, it was thought that that looseness could be caused by a change in specific molecular components that make up the hide. Collagen, elastin and GAGs are molecular components that are heavily implicated in causing wrinkles in human skin, a similar phenotypic condition to looseness in leather. These molecules were therefore analysed in tight and loose raw hides in order to identify differences in their concentration distribution or structure that may be related to looseness. Figure 1.10 illustrates the experimental design of this project.

The main objectives of this project were as follows:

1. Investigate the structure, concentration and distribution of collagen in loose and tight hides.
2. Isolate and characterise the natural crosslinks in loose and tight hides.
3. Analyse the amino acid composition, specifically the concentration of hydroxyproline in loose and tight hides.
4. Analyse the different types of proteins found in loose and tight hides, specifically the different types of collagen.
5. Analyse, quantitate and compare elastin in loose and tight hides.

6. Analyse and compare the different types of carbohydrates found in loose and tight hides.

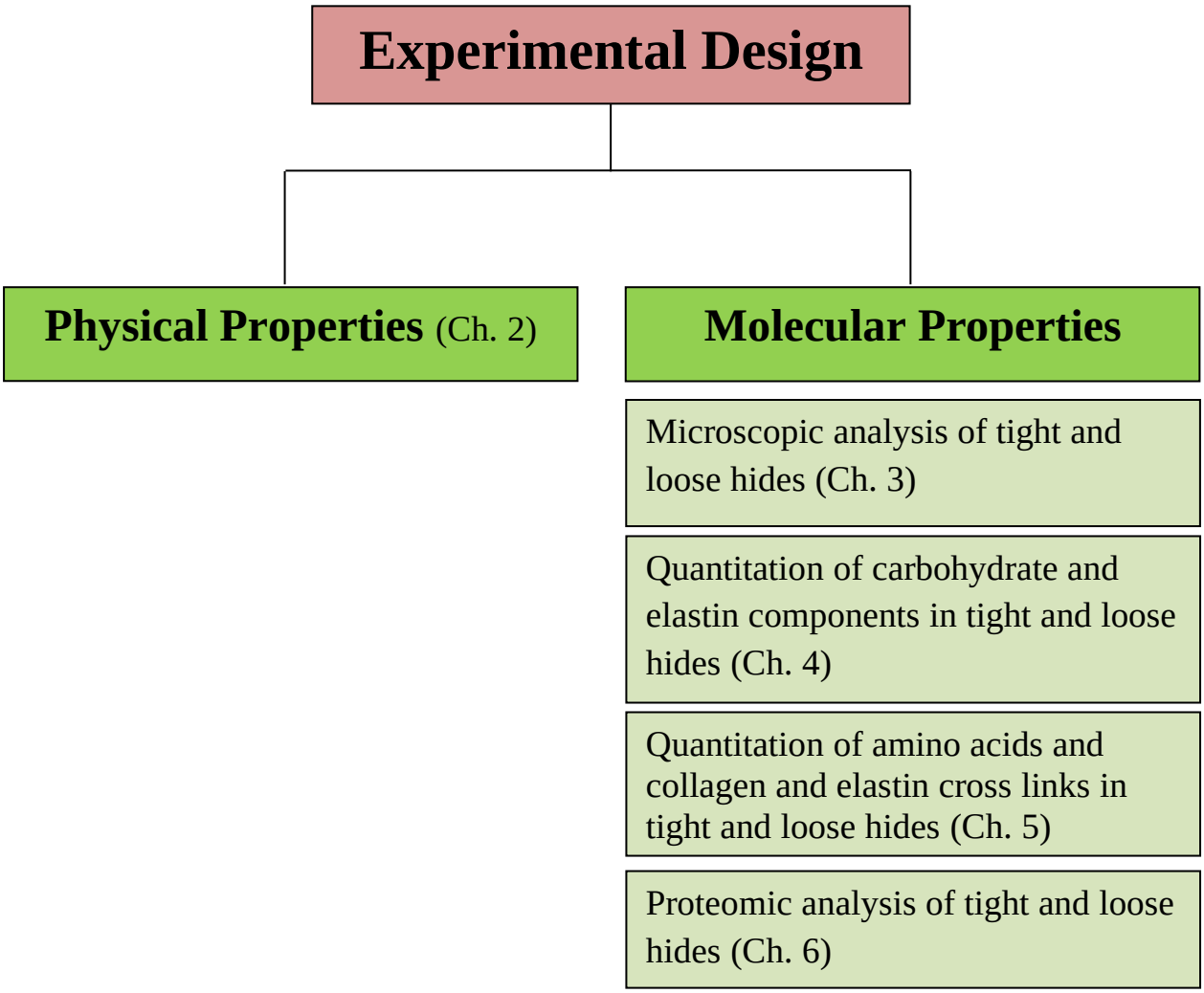

Figure 1.10 Diagram illustrating the experiment design for this research project and their location in this thesis**.**

2. Sample Collection and Analysis

2.1 Introduction

A big problem encountered at the start of this project was how to obtain both loose and tight hides at the raw stage. Work is currently in progress to identify looseness early on in the processing of hides through techniques such as ultrasound [10, 18] and NMR transverse relaxation analysis [129]. However, none of these have been sufficiently developed for industrial use. Currently, the only readily available method for determining looseness is to process the raw hide into leather and then check it using a subjective grading procedure called the SATRA break scale [11]. To overcome this, it was decided to select a number of hides, cut them in half, then process half of the hide into leather to check for looseness while keeping the other half in its raw state (at - 20 °C to prevent putrefaction) for later analysis. In this way, matched halves of one hide should have a similar molecular composition and structure, providing a basis for comparison [7]. Multiple locations throughout the finished leather were examined, as reference to the literature has shown that different regions of the hide are more prone to looseness than others [10-12].

Unfortunately, the number of biological replicates that could be obtained was limited due to the hit and miss potential of getting loose samples, and the cost of the hide. On the plus side, the ability to accurately determine looseness provided a distinct advantage. Although the low number of biological replicates was not sufficient to give statistical significance to findings of this study it proved to be an adequate screening mechanism to determine which molecular components for future focus.

The strengths of the loose and tight leather samples and their corium to grain ratios were measured to determine if apart from appearance there were any other readily available physical

properties that differentiated loose and tight leather. Both of these tests have previously been shown to be strongly correlated to the structure of collagen in skin/hide [22, 130, 131].

2.2 Methods

2.2.1 Chemicals and Equipment

The chemicals utilised during the leather processing were obtained from NZ Leather and Shoe Research Association (LASRA) and to the best of our knowledge they are sourced from the suppliers stated in Table 2.1. Equipment used is listed in Table 2.2.

Table 2.1 Chemicals used in chapter 2.

Supplier	Country	Chemical
Carpetex Lederhilfsmittel GmbH	Germany	Merpin 8016
Clariant-Chemcolour	Auckland, NZ	Feliderm DP Mimosa (Clarotan) Syntan Tanicor Tergolix CA surfactant
Clark Products	Napier, NZ	Ammonium chloride Hydrogen peroxide Formic acid, 85 % Sodium bicarbonate ($NaHCO_3$) Sulphuric acid, 95 %
Dominion Salt	Tauranga, NZ	Sodium Chloride (NaCl)
Farmlands	NZ	Magnesium oxide (MgO)
Lanxess	Cologne, Germany	Chromium (III) sulphate
Leatherchem International	Auckland, NZ	Tetrapol LTN
McDonalds Lime	Te Kuiti, NZ	Lime (CaO)
Redox Pty Ltd	Auckland, NZ	Sodium hydrosulfide, 70 % Sodium sulphide
Smit and Zoon	Weesp, Netherlands	Polyol AK Sulphirol EG60
Sigma-Aldrich	Steinheim, Germany	2-thiocyanotomethylthiobenzothiazole (TCMTB), 30 %
Trumpler	Germany	Trupozym CB
Zauba	Spain	Melioderm HF yellow-brown dye Rp

Table 2.2 Equipment used in chapter 2.

Supplier	Country	Equipment
Bray Leather Instruments	Northamptonshire, UK	Bray leather substance gauge
Instron	Massachusetts, USA	Instron 4467
Japan Optical Industries Co., Ltd	Japan	Nikon optiphot 134528 light microscope
SATRA Technology	Northamptonshire, UK	SATRA STD174 Break/Pipiness scale

2.2.2 Sample collection

Four random hides that had already been removed from the carcass were obtained from Tasman Tannery; Whanganui, NZ on the 12th May 2015. The hides were labelled and cut in half, with one half being processed to finished leather using a standard processing procedure at LASRA as described in section 2.2.3 whilst the other half was stored at -20 °C for later analysis as shown in Figure 2.1.

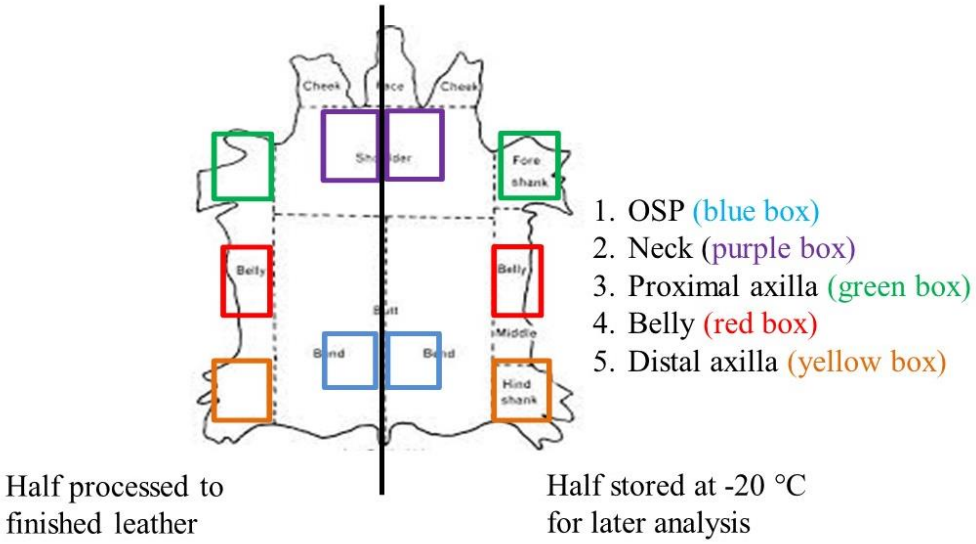

Figure 2.1 Diagram of a hide illustrating how it was sampled and stored.

2.2.3 Leather Processing

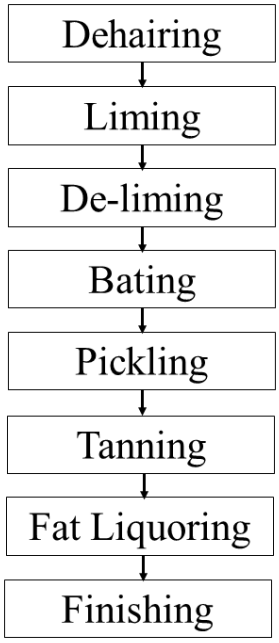

Figure 2.2 Schematic diagram of leather processing [7, 8].

The half hides, each weighing approximately 10 kg, were green fleshed to remove excess fat and then processed using a conventional method (Figure 2.2). All values below give the chemicals used for tanning as a percentage of the weight of the hide. The raw hides were placed in 4 m height by 3.8 m diameter drums, and rotated at 30 rpm with approximately 2 times their weight (200%, v/w) of water for 30 minutes at 28 °C to remove dirt, blood and dung. After draining off the water, a solution of 1.5 % (w/w) sodium hydrosulphide, 2 % (w/w) sodium sulphide, 1.5 % (w/w) CaO and 0.5 % (v/w) Merpin 8016, a liming auxiliary with reducing activity, was added to remove the hair from the hide by increasing the pH. After being left in the solution overnight with intermittent rotation, the solution was removed and the hides washed twice in fresh water. A final wash was undertaken using 0.5 % (w/w) ammonium chloride in surplus water to remove any excess sodium sulphide.

A solution of; 0.5 % (v/w) hydrogen peroxide, 2.5 % (w/w) ammonium chloride and 0.2 % (v/w) neutralising detergent tetrapol LTN in 35 % water (v/w) was then added to the hides and incubated at 30 °C for 90 minutes with rotation at 12 rpm. The bating enzyme, 0.04 % (w/w) Trupozym CB, in 100 % (v/w) water was then added and the hides incubated for a further 20 minutes at a temperature of 35 °C to remove non-collagenous proteins. The solution was then drained, and excess chemicals removed by repeated washing in water at 20 °C for 20 minutes. The hides were then pickled by first immersing them in an 8 % NaCl solution for 10 minutes, followed by 1.2 % sulphuric acid. After incubation in the pickling solution for 120 minutes, the hides were chrome tanned by adding 6 % (w/w) chromium sulphate for 180 minutes followed by 0.05 % (v/w) of the biocide TCMTB and 0.35 % (w/w) tanbase MgO. The temperature of the drum was then increased to 40 °C and the hides left rotating at 16 rpm overnight. The chrome tanned hides were then transported to Tasman Tannery where the excess water was removed using a machine called a throughfeed sammying press after which they were shaved and split to 2.2 mm to get evenly thick hides.

The following steps were all done in the drums at a temperature of 35 °C and a speed of 10 - 12 rpm. First the hides were wet back with a solution of 0.3 % (v/v) Tergolix CA surfactant and 200 % (v/v) water for 30 minutes. The solution was then drained and a solution containing 5 % (v/v) feliderm DP, 0.5 % $NaHCO_3$ and 150 % v/v of water was added to the hides and incubated for 60 minutes to neutralise the pH. After this time an extra 0.15 % (w/v) $NaHCO_3$ was added to the drum and the hides left overnight in this solution to further neutralise the pH. The solution was then drained, and the hides were washed twice for 10 minutes each wash.

The hides were then exposed to a solution containing 2 % (w/v) vegetable tannin mimosa, and 4 % (w/v) syntan tanicor for 60 minutes. Melioderm HF yellow-brown dye (2 % (w/v)) was

then added to the solution, and left for a further 120 minutes. Fat liquor, made up from 4 % (v/v) polyol AK, a natural animal oil and 1 % (v/v) sulphirol EG60, a synthetic oil, was then added to the drum, the temperature increased to 60 °C, and the hides exposed to the solution for 90 minutes. Finally, two volumes of 0.5 % formic acid were added to the hides for two 20-minute incubations, to adjust the pH. The solution was then drained and after a final wash in water, the hides were dried and mechanically softened.

2.2.4 Grading for Looseness

The finished leather was analysed for looseness using the SATRA break scale, which is widely used to measure the wrinkling of leather. It consists of a graded selection of leather replicas numbered one to eight with one having the least severe wrinkles and eight having the most severe as illustrated in Figure 2.3. Five different locations on the hide were tested for looseness; the official sampling position (OSP) which is situated near the lower half of the backbone, the neck, the belly, and the proximal and distal axilla (Figure 2.1). Results under 4 were considered tight whilst those 4 and over were considered loose.

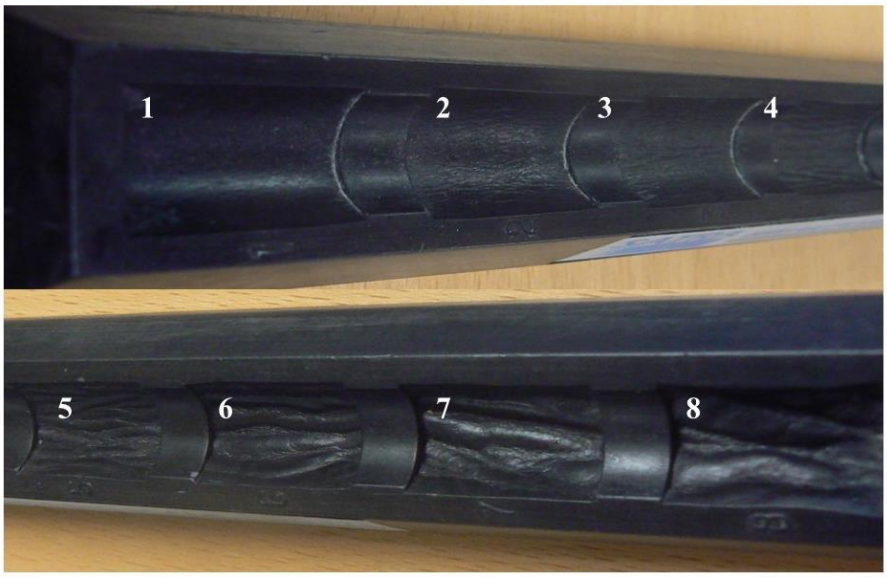

Figure 2.3 SATRA break scale.

2.2.5 Tear and Tensile Strength

Tear Strength

The tear strength of the finished leather samples was measured using the international standard method known as the double edge tear strength method. Samples were cut into 50 x 25 mm sized pieces with a hole in the middle by a press. The samples were incubated at 20 °C overnight, then the thickness was measured using a Bray leather substance gauge which has an error of ± 0.02 mm. The sample was placed in an Instron 4467 between two tear strength hook attachments. These attachments separate at a user-determined constant rate until the sample tears. The maximum load is recorded by the machine and normalised to the sample thickness. The average tear strength was calculated from duplicate readings.

Tensile Strength

The tensile strength of the finished leather samples was measured using the international standard method as follows: Samples were cut into bone shaped pieces 100 mm by 20 mm using a press. After incubation at 20 °C overnight, the thickness was measured using a Bray leather substance gauge. The sample was attached to specific tensile strength clamp attachments in the Instron 4467. These were then separated at a constant rate until the sample ripped giving the force required to break the sample in Newtons, which was then normalised to the sample thickness. The average tensile strength was calculated from duplicate readings.

2.2.6 Corium to Grain Ratio

The total sample thickness was calculated using the Bray leather substance gauge as before. The thickness of the grain and corium was then measured using the ruler inbuilt in the Nikon optiphot 134528 light microscope using the 4-x microscope lens. 8 replicates of each sample were averaged to calculate the ratio of the corium to grain.

2.3 Results and Discussion

2.3.1 Looseness grade

The looseness grade of four different hides was assessed using the SATRA break scale. They were measured in five different locations; the OSP, belly, neck, proximal axilla and distal axilla (Figure 2.1). Hide 1 and 4 displayed average looseness grades below 4 (3.4 and 3 respectively) and were considered tight. Hide 2 and 3 displayed average looseness grades over 4 (4.1 and 5.75 respectively) and were considered loose (Figure 2.4A).

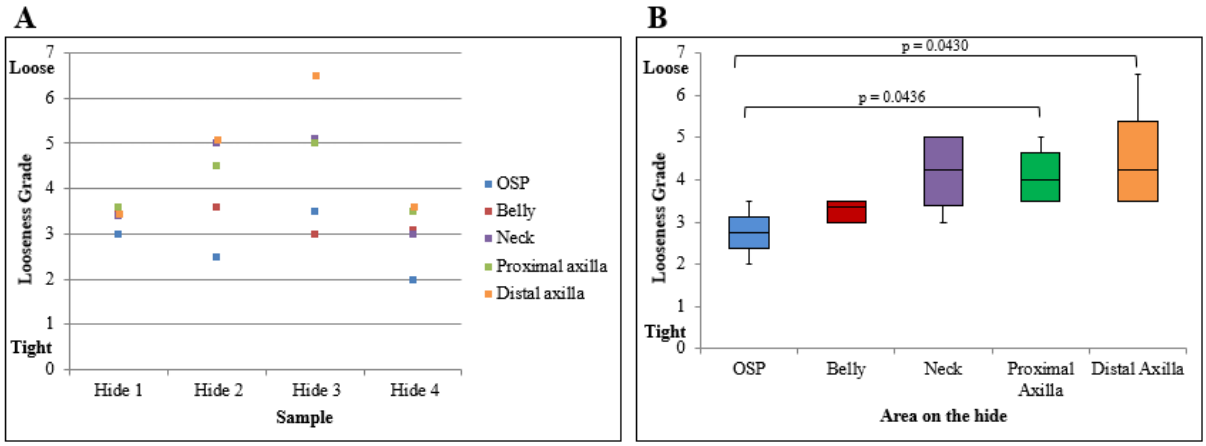

Figure 2.4 (A) Looseness grade of each sample in the five different sampling locations. Hides 2 and 3 exhibit more loose areas than hides 1 and 4. (B) Box plot showing the grade of looseness of five different sampling locations on the hide; OSP, belly, neck proximal axilla and distal axilla. At least three different measurement were taken in each location to ascertain the looseness grade.

Multiple locations on the hide were examined for looseness as previous work has illustrated that certain areas are more prone to looseness than others, specifically the shoulders and flanks [10]. Some studies also implicate the belly as being prone to looseness due to the orientation of the collagen fibres [11, 12]. Figure 2.4B shows the variation in looseness grade at different locations for the 4 biological replicates. In this study the neck, proximal and distal axilla are more prone to looseness than the OSP and belly, however the only significant difference is between the OSP and proximal axilla and distal axilla (p value 0.0436 and 0.0430 respectively),

an observation that may reflect the small sample size. Most notably, all samples taken from the belly were tight, which does not concur with the literature. This could either be due to the small sample size, or due to loose belly hide being influenced by other factors such as breed, age, nutrition or season.

2.3.2 Strength tests

The strength of leather is an important characteristic when evaluating its quality [7, 61]. Typically, end products such as shoes and bags require strong leathers that have a resistance to tearing. Two methods are commonly used when determining the strength of a leather sample. Tear strength which measures the resistance of leather to tear forces, and tensile strength which measures the maximum force required to stretch the sample until it breaks [7]. Determining how looseness affects the strength of leather could provide an indicator to its underlying cause(s) in raw hide, as various factors such as crosslinking and collagen concentration have been shown to correlate to skin/hide strength [61]. Strength tests were only done on finished leather for two reasons. Firstly, the samples were frozen prior to testing commencing. It was not known how the subsequent thawing would affect the measurements and secondly, the machinery used is not designed to accurately determine the strength of raw hide.

Tear Strength

The results showed no significant differences between the tear strength of leather produced from tight and loose hides (Figure 2.5A), although the average strength was slightly higher for loose compared to tight hides. This correlates with other studies which have shown that tear strength is higher in loose hides compared to tight [10, 132]. Figure 2.5B showed that the samples taken from different locations on the hide, had different tear strengths especially the OSP which had a significantly lower tear strength compared to almost all other areas (p-value

range between 0.0216 and 0.0056). This is most likely due to changes in the orientation of collagen fibres in these regions.

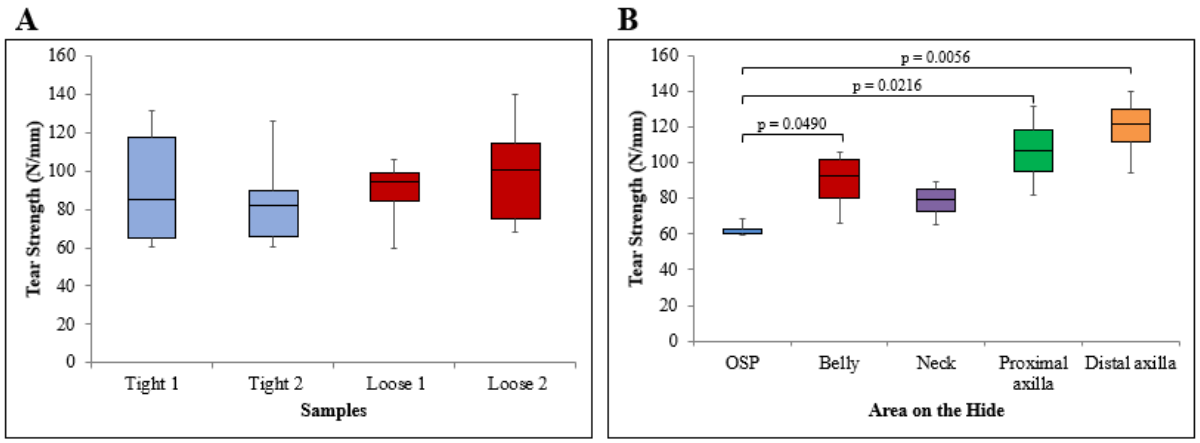

Figure 2.5 (A) Tear strength of tight and loose samples. Results from 2 biological replicates are shown. Each bar graph shows the variation within for 5 technical replicates. (B) Tear strength of five different areas on the hide; OSP, belly, neck, proximal axilla and distal axilla. Results from four biological replicates are shown as box plots.

Tensile strength

Tensile strength measurements (Figure 2.6A and B) were consistent throughout the different areas of the hide and regardless of whether the hides were loose or tight which agrees with a previous study [13]. One study, however, did show that the location of the hide does have an effect on tensile strength with the strength of the OSP region being much higher than other areas [131]. This was **not** observed in this study, perhaps due to small sample size, different technique used, or the breed or sex of the animal.

Relationship with looseness grade

Figures 2.7A and B show the correlation between tear strength (A) and looseness as well as tensile strength (B) and looseness. Although the results indicate that there is a positive correlation between strength and looseness it is not statistically significant with R^2 values of

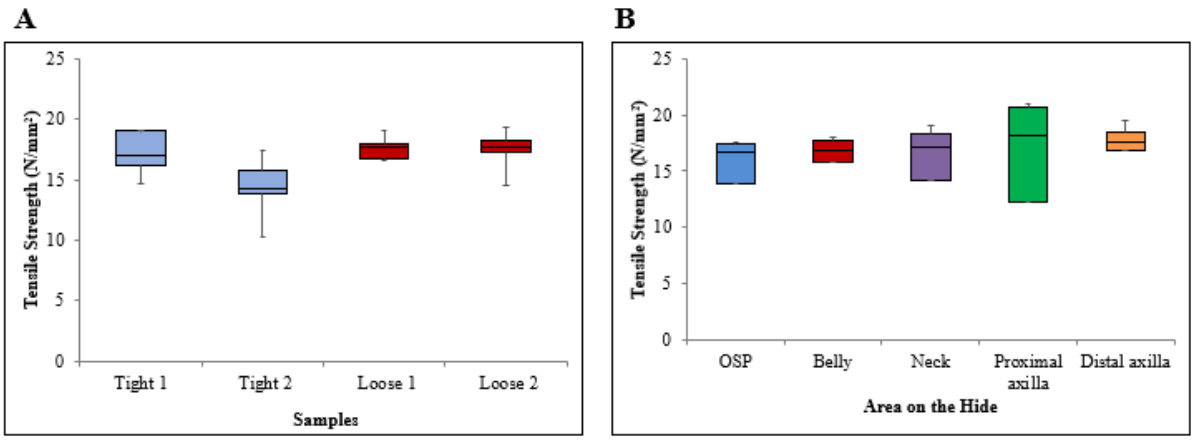

Figure 2.6 (A) Tensile strength of samples from tight and loose hides shown as a box plot. Measurements included the average tensile strength of 5 different regions sampled throughout the hide. (B) The tensile strength of hide samples from the OSP, belly, neck, proximal axilla and distal axilla from 4 different hides shown as box plots. Each box plot represents the average tensile strength of 4 biological replicates.

0.2611 and 0.1049 for (A) and (B) respectively. With a greater sample size this correlation could change. The significance between samples with looseness grades below 4 (tight) and above 4 (loose) regardless of hide sampled from was also analysed for both tear and tensile strength. In both instances they were insignificant with p-values of 0.25 and 0.40 respectively. These results indicate a greater variation in the strength of different locations on the hide rather than looseness grade.

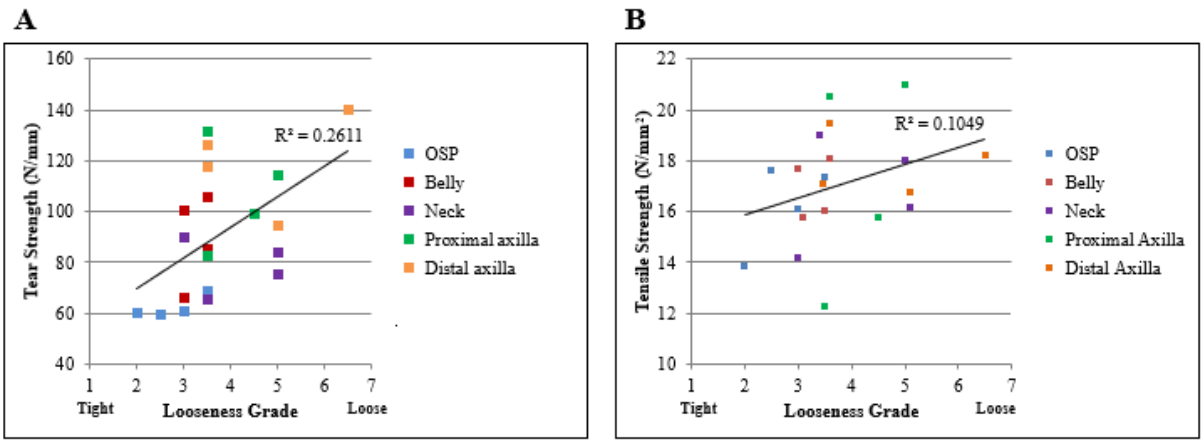

Figure 2.7 (A) Relationship between tear strength and looseness grade. (B) Relationship between tensile strength and looseness grade.

2.3.3 Corium to Grain Ratio

There are two main layers to hide that have importance in leather. The grain which is made up of small, interwoven collagen fibres and the corium made up of a network of large collagen fibres [22]. The corium is the strongest part of the hide whilst the grain affects the appearance of the finished leather [7, 22]. As the corium to grain ratio may be a characteristic of looseness, it was measured in all raw hides and finished leather samples. A significant difference was found between the corium to grain ratio in raw hide versus the finished leather (p-value of 0.0120). Finished leather tends to have a greater corium to grain ratio compared to raw hide most likely due to changes in hide composition during processing, especially the loss of water and interfibrillary substances many of which are found in the grain layer [7, 21]. While there appears to be no change in the corium to grain ratio between loose and tight finished leathers, in the raw hides, the average corium to grain ratio was higher than in loose hides. This could be due to differences in the structure and/or composition of molecular components found in raw hide.

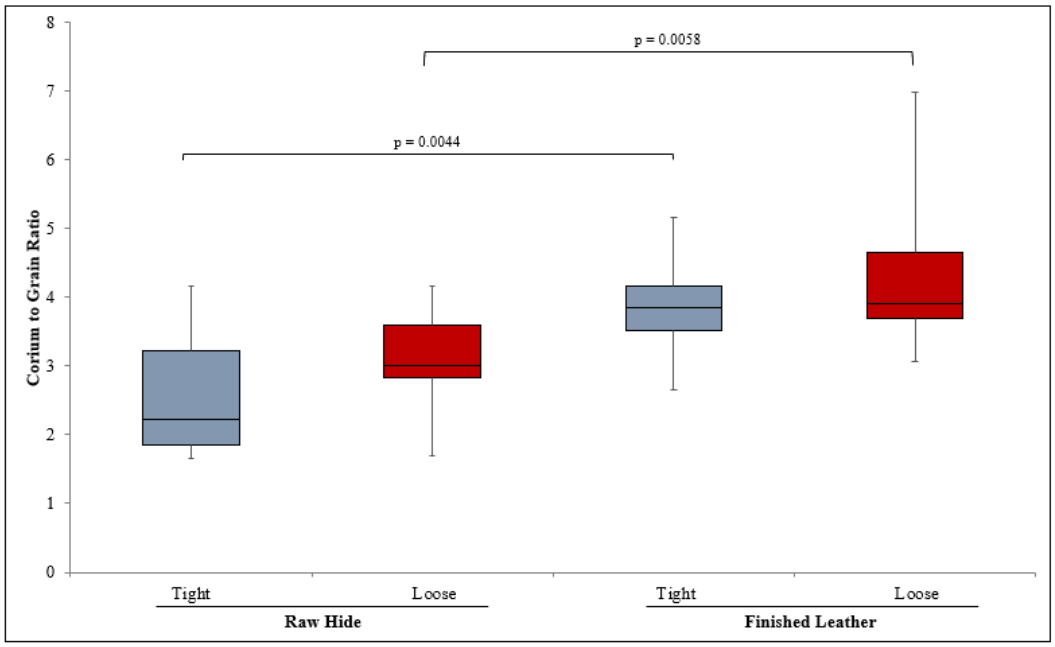

Figure 2.8 Corium to grain ratio of tight and loose samples in raw hide and finished leather. The box plots represent 2 biological samples from tight and loose hides each measured with 8 technical replicates.

The significance between samples with looseness grades below 4 (tight) and above 4 (loose) regardless of sampling position was also analysed for differences in the corium to grain ratio for both raw hides and finished leathers. In both instances they were insignificant, with p-values of 0.256 and 0.105 respectively.

The corium to grain ratio was also investigated in the different locations of raw hide and finished leather (Figure 2.9). In the raw hide the OSP had the highest corium to grain ratio, followed by distal axilla, neck, proximal axilla and belly (Figure 2.9A). In the finished leather the distal axilla had the greatest corium to grain ratio, with the remaining areas all having similar corium to grain ratios (Figure 2.9B). Why the different parts of raw hide have different ratios of corium to grain is unknown, but as they will be reflected in the concentration and composition of the molecular components making up these regions, it is useful information. Studies have shown that the grain layer has only 20 % of the tear capacity of the corium [22], and it is widely believed that the corium to grain ratio of the finished leather should match the tear and tensile strength measurements of finished leather in the different locations. In this study, the distal axilla had a greater corium to grain ratio in finished leather and a higher tear strength. Samples taken from other locations with similar corium to grain ratios don't however, exhibit tear strengths that correlate. The tensile strength however is similar for sample taken from all locations. During processing the leather is split and shaved at the wet blue stage, and it is possible that this results in uniform corium to grain ratios. The results for the distal axilla which has a higher corium to grain ratio and subsequently a higher tear strength may be due to inefficient splitting and shaving in this region.

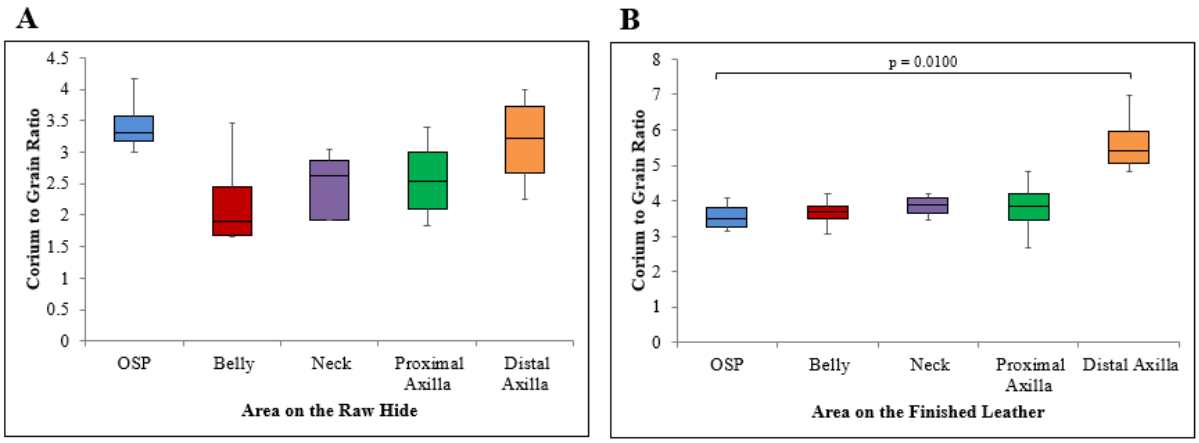

Figure 2.9 (A) Box plot of the corium to grain ratio of raw hide samples in five different areas; OSP, belly, neck, proximal axilla and distal axilla. The value for the 4 biological replicates was obtained from the average of 8 technical replicates. (B) Box plot of corium to grain ratio of finished leather in five different areas; OSP, belly, neck, proximal axilla and distal axilla. The value for the 4 biological replicates was obtained from the average of 8 technical replicates.

3. Analysing molecular components through microscopy

3.1 Introduction

A combination of histochemical staining and microscopy is a technique that is frequently used to study the distribution and organisation of specific hide macromolecules such as proteins, carbohydrates and lipids.

Collagen is the dominant structural protein found in hide and subsequently leather. The size of the fibres, organisation and their orientation all play important roles in the mechanical properties of the tissue conferring strength and flexibility [61]. The dye picrosirius red is commonly used to stain collagen due to its ability to enhance the natural birefringence of collagen, as well as its ability to form strong interactions between the sulfonic acid groups on the dyes and the basic amino acid sidechains of collagen molecules [133, 134]. This dye in combination with various microscopy techniques such as confocal laser scanning microscopy [135-137] enables the bundle pattern, orientation and weave of collagen fibres to be visualised [61, 137]. Previous studies using microscopy showed that loose leather has excess space between collagen fibre bundles compared to tight leather as well as a pronounced gap between the grain to corium junction [10, 12, 13]. Aged or wrinkly human skin is characterised by fibre bundles that are less consistent in size and are packed less densely than those seen in normal skin [62, 63].

Elastin is responsible for the elastic properties of hide, and is typically removed during bating in leather processing because its presence is said to result in rigid leather [7]. In age-related wrinkly skin, elastin is thought to accumulate as the skin suffers damage [28]. Interestingly

another study reported that loose ovine skins tend to have greater amounts of elastin [80]. However, yet another study reported that excessive elastin removal during bating results in loose leather [11]. Multiple staining agents can be used to study the distribution and morphology of elastin in hide including Weigert's reagent, resorcin, fuchsin, orcein and Verhoeff's reagent [78, 81]. Aldehyde fuchsin was chosen for this study due to previous reports showing success with this dye [80, 138, 139]. Although the exact mechanism by which aldehyde fuchsin binds to elastin is not clearly understood it is believed to be covalent rather than non-covalent [78, 140].

Lipids are typically hydrophobic molecules that have important roles in hide including waterproofing, antibacterial action and energy storage [123-125]. In ovine skin they are thought to be responsible for looseness due to the large concentration of fat in the grain to corium junction which when removed during processing often leaves gaps [11]. This is unlikely to be the case in bovine hides because of the significantly lower concentration of lipids [120]. The hydrophobic properties of lipids enable coloured non-polar substances to dissolve in them rendering them visible under the microscope. There are many different types of dyes that can be used to stain lipids, the most well-known of these being Sudan. Sudan III and IV are lysochrome diazo dyes which stain neutral fats, and esters of cholesterol whose acetyl groups are unsaturated pink as well as weakly colouring hydrophilic phospholipids [78, 141].

Although these studies enable the distribution and organization of macromolecules in hide to be examined, they do not give quantifiable results.

3.2 Methods

3.2.1 Chemicals and Equipment

The chemicals and equipment used in this section are listed in Table 3.1 and 3.2 respectively.

Table 3.1 Chemicals used in chapter 3.

Supplier	Country	Chemical
Acros Organics	New Jersey, USA	Alcian blue 8GX
Ajax Finechem	NSW, Australia	Gelatin
BDH Ltd	Poole, UK	Paraldehyde Potassium Permanganate Sodium dihydrogen orthophosphate Sudan III Sudan IV
Damar Industries Ltd.	Rotorua, NZ	Oxalic acid
Fisher Scientific	UK	Basic fuchsin/Schiff's reagent
Hopkins and Williams	Essex, UK	Phosphomolybdic acid
Labscan analytical sciences	Bangkok, Thailand	Analytical grade xylene
Merck	Darmstadt, Germany	DPX
PanReac	Barcelona, Spain	Hydrochloric acid (HCl), 37 %
Pure Science	Wellington, NZ	Acetone Ethanol absolute, min 99.8 % Di-sodium hydrogen orthophosphate Phenol crystals
Sharlau	Barcelona, Spain	Formaldehyde, 40 %
Sigma-Aldrich	St. Louis, USA	Fast green FCF dye
Spectrum chemical MFG Corp	California, USA	Sirius red F3B spectrum
Vickers Laboratory Ltd	West Yorkshire, UK	Glycerol
VWR Chemicals	Pennsylvania, USA	Picric acid

Table 3.2 Equipment used in chapter 3.

Supplier	Country	Equipment
Leica Microsystems	Wetzlar, Germany	Leica CM 1850 UV cryostat Leica SP5 DM6000B scanning confocal microscope
Olympus Australia PTY Ltd.	Melbourne, Australia	Olympus BX51 microscope

3.2.2 Preparing samples on microscope slides

2 cm by 2 cm samples of hide were cut and fixed in 40 % formaldehyde, made up in 30 mM di-sodium hydrogen orthophosphate and 30 mM sodium dihydrogen orthophosphate (pH 7.4) for approximately 24 hours. After fixation samples were sectioned using a Leica CM 1850 UV cryostat to 40 µm thick cross sections. These sectioned samples were then placed on a microscope slide in two rows of 7, ready for staining.

3.2.3 Picrosirius red stain for visualising collagen

The slides were rinsed with H_2O then placed in 1 % (w/v) potassium permanganate for 5 minutes. After removal, they were washed with H_2O then placed in 1 % (w/v) oxalic acid until all the colour had dissipated. The samples were rewashed with H_2O then placed in a 0.2 % (w/v) phosphomolybdic acid solution for 10 minutes, after which they were stained with 1.2 % (w/v) picric acid containing 0.1 g Sirius red F3B spectrum. Picrosirius red is a strongly acidic azo dye containing six sulfonic groups (Figure 3.1) [133, 134] that forms a strong interaction with the basic groups of collagen molecules [133, 134]. Samples were then placed in 0.01 N HCl before being washed with 100 % absolute ethanol. They were then placed into a 100 % xylene solution. Coverslips were attached using DPX containing dibutyl phthalate (10-20 %) and xylene (100 %) as the mounting solution.

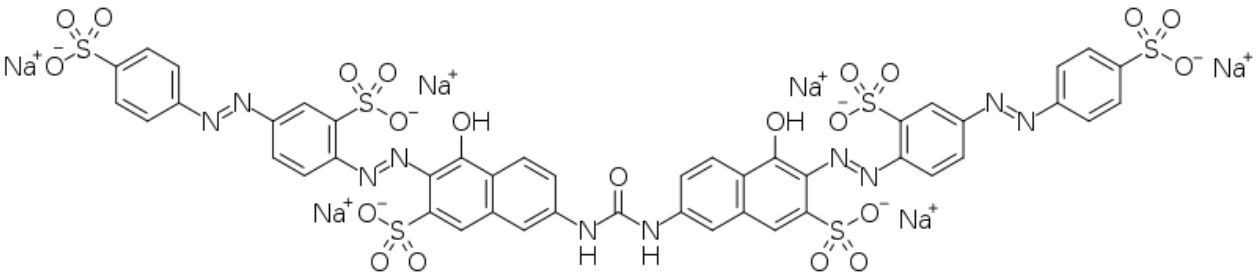

Figure 3.1 Structure of picrosirius red stain.

3.2.4 Sudan III/IV stain for visualising lipids

The glass slides containing the samples were rinsed in H_2O then placed in a sudan III/IV solution containing 0.025 g sudan III, 0.025 g sudan IV, 80mL acetone and 60 mL ethanol (100 %), for 10 minutes. Sudan III and IV are lysochrome diazo dyes (Figure 3.2) which stain lipids (primarily fats) pink [78, 141]. They were then washed twice with H_2O for 5 minutes before being placed in 1 % alcian blue 8GX for 30 minutes. The samples were then rewashed with H_2O twice for 5 minutes before a coverslip being attached using a glycerol mix (10 g gelatin, 60 mL H_2O, 70 mL glycerol and 0.25 g phenol crystals) as the mounting solution.

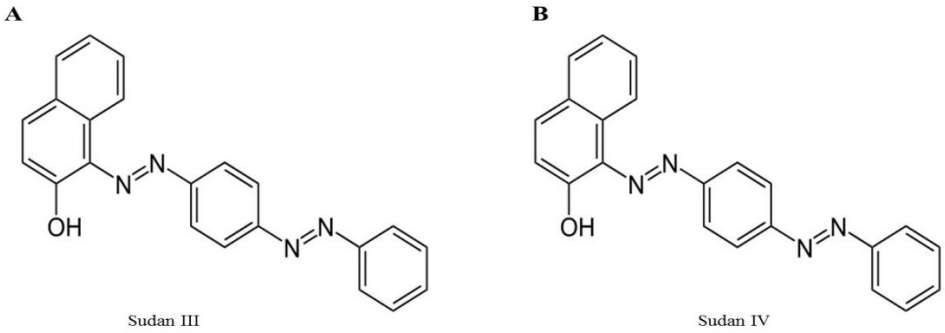

Figure 3.2 Structure of (A) sudan III and (B) sudan IV.

3.2.5 Aldehyde fuchsin stain for visualizing elastin

Samples were rinsed with H_2O then placed in 1 % (w/v) potassium permanganate. Potassium permanganate is used to oxidise the many disulfide bonds in elastin to their anionic sulfonic acid derivatives which can then selectively react with the basic dye aldehyde fuchsin [78]. Samples were then washed with H_2O before being placed in 1 % (w/v) oxalic acid until they became colourless. They were then immersed in 70% ethanol for 2 minutes before being placed in aldehyde fuchsin (1 g basic fuchsin/Schiff's reagent, 70% absolute ethanol, 1 mL HCl and 2 mL paraldehyde) for 7 minutes to stain the elastin fibers purple. The samples were then rinsed in 70 % ethanol, followed by H_2O until no more colour could be seen coming out of the sections. Samples were then placed in 0.1 % fast green stain (0.08 g fast green and 5 mL picric

acid) for 10 minutes as a counterstain to stain the collagen green. They were then placed in 0.2 % phosphomolybdic acid for 10 minutes to stain the phenolics, hydrocarbon waxes, alkaloids and steroids yellow. The samples were then placed in 1.2 % saturated picric acid for 60 minutes after which time they were placed into a 0.01 N HCl solution for 15 minutes before being washed in increasing concentrations of ethanol (70 %, 90 %, ending in absolute ethanol). The samples were then placed in xylene before being covered with a coverslip using DPX as the mounting solution.

3.2.6 Light microscopy images

The stained samples were examined using an Olympus (BX51) microscope, magnification 4x. The images were taken using a Nikon camera and analysed using image J [142]. The picrosirius red and aldehyde fuchsin stained samples were analysed using the following plugins: microscope correction [143], extended depth of field [144], bright field [145], mosaic [146] and orientation [147] to determine the angle of the collagen fibres in the corium and the distribution of the elastin fibres. The sudan III/IV stained samples were analysed using the following plugins: microscope correction [143], extended depth of field, [144] bright field [145], mosaic [146], colour deconvolution [148] and calculator plus for demasking [149] to determine the amount and distribution of lipids found throughout the cross section of the hide.

3.2.7 Two-dimension (2D) Confocal Images

The picrosirius red stained samples were further examined using a Leica SP5 DM6000B scanning Confocal Microscope with LAS AF software (version 2.7.1.9723). Images were acquired using a 20x lens with a 3x optical zoom and standard filters set at an excitation and emission wavelengths of 561 nm and 571 - 653 nm respectively [137]. Several images were

taken using cross sections of hide including the grain, the grain to corium junction and the corium. The results were analysed using ImageJ.

3.2.8 Three-dimensional (3D) Confocal Images

Using the same machinery as above 3D images were also taken by scanning 80 different cross sections of the hide and over-laying them in ImageJ. Several images were taken using cross sections that included the grain, the grain: corium junction and the corium.

3.3 Results

3.3.1 Microscopy results for collagen, lipids and elastin

The combination of staining and microscopy is a powerful tool that is routinely used to study the organisation and distribution of different molecules within hide. Figure 3.3 illustrates three different stains used to study (A) the organisation of collagen fibres, (B) the location and distribution of lipids and (C) the organisation and distribution of elastin fibres.

While collagen and lipids were successfully stained and studied, the elastin fibres were not quite so readily visible under the microscope. Several fresh aldehyde fuchsin stains were made up and trialled on the basis of literature reports which suggested that the age of the aldehyde fuchsin stain can have an impact on its specificity and binding [78, 138]. As there was no improvement in the results a more quantitative method was used to analyse elastin such as biochemical assays and analysis of the specific elastin crosslinks.

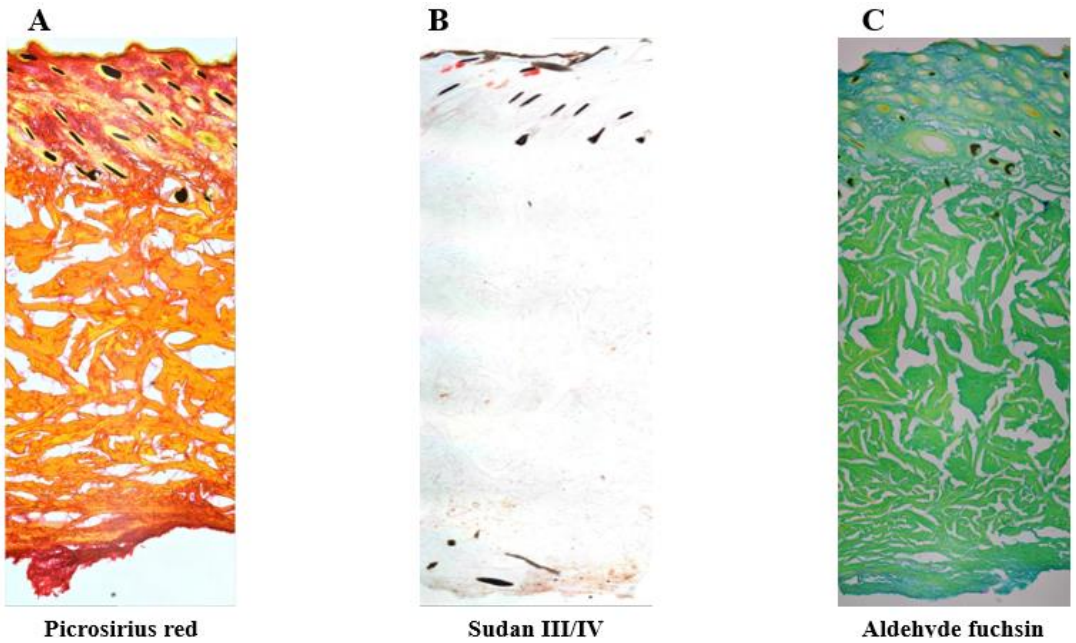

Figure 3.3 Images of stained raw hide using light microscopy, at 4x magnification. (A) Collagen fibres stained with picrosirius red. (B) Lipids stained with sudan III/IV (pink). (C) Elastin stained with aldehyde fuchsin (purple). In all images the black lines represent hairs.

3.3.2 Organisation of collagen fibres

Angle of weave

The organisation of collagen fibres and bundles has been shown to change depending on the layer of the hide, and during different leather processing stages [21, 73]. Changes in the angle of weave of collagen bundles have been linked to a change in the strength of the leather [11, 150] and are different between loose and tight bovine leather [10, 11].

Measurements of the angle of weave taken from from images of samples from loose and tight raw hide and finished leather were calculated using Image J and the associated plugins. The loose samples generally showed a lower angle of weave in both raw hide and finished leather (Figures 3.4A and B), although the results are not significant (R^2 values of 0.0402 and 0.1981 respectively). Nevertheless, they support the literature which reports that highly orientated collagen fibres with a low angle of weave are seen in loose leather [10, 11]. The differences in the angle of weave of both raw hide and finished leather between samples with looseness grades

below 4 (tight) and above 4 (loose) regardless of position were insignificant with p-values of 0.71 for raw hide and 0.94 for finished leather.

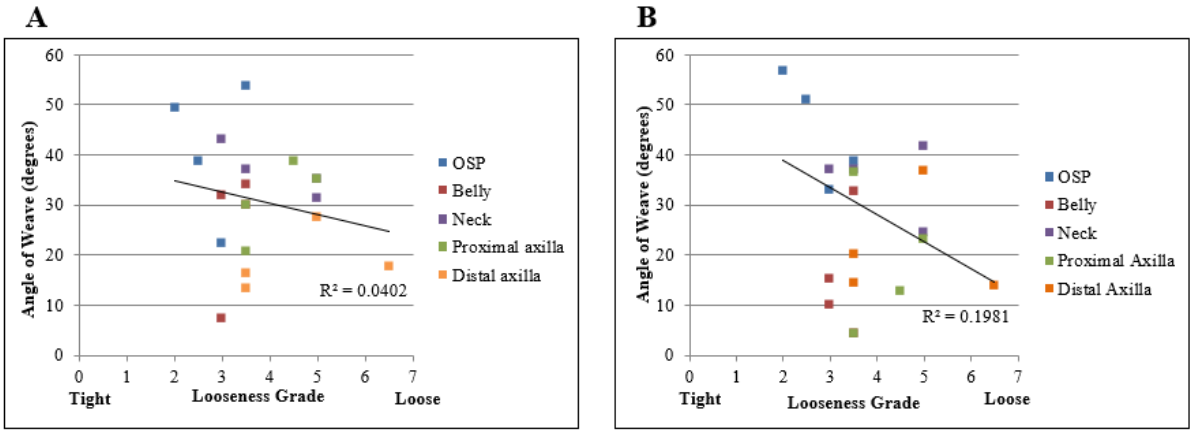

Figure 3.4 The average angle of weave of collagen fibres in the corium versus the looseness grade of the samples in (A) raw hide and (B) finished leather. Each data point is the average of three different images.

Interestingly, samples with a low angle of weave in both raw hide resulted in stronger leather (figure not shown (R^2 0.37)) supporting the results of other studies that suggest a lower angle of weave results in stronger leather [11, 150]. There was little difference seen between the angle of weave in raw hide and finished leather, with samples having a low angle of weave in the raw material also having a low angle of weave in the finished leather. These results suggest that either there is little change in the organisation of the collagen fibres as a result of processing or that if there are changes during processing they return to a similar state at the end.

Figure 3.5 shows the varying angles of weave in the five different locations sampled. In both the (A) raw hide and (B) finished leather the OSP region had a higher angle of weave than the other four regions. In raw hide, the sample from the OSP had an angle of weave that was significantly higher than that of the distal axilla (p-value 0.027) whilst in finished leather the angle of weave of hide from the OSP was significantly higher than that of hide from the belly, proximal and distal axilla (p-values 0.012, 0.027 and 0.022 respectively). The change in angle

of weave in these locations is likely due to the armpits and belly being required to have more flexibility than the OSP region, thus resulting in the lower angle of weave.

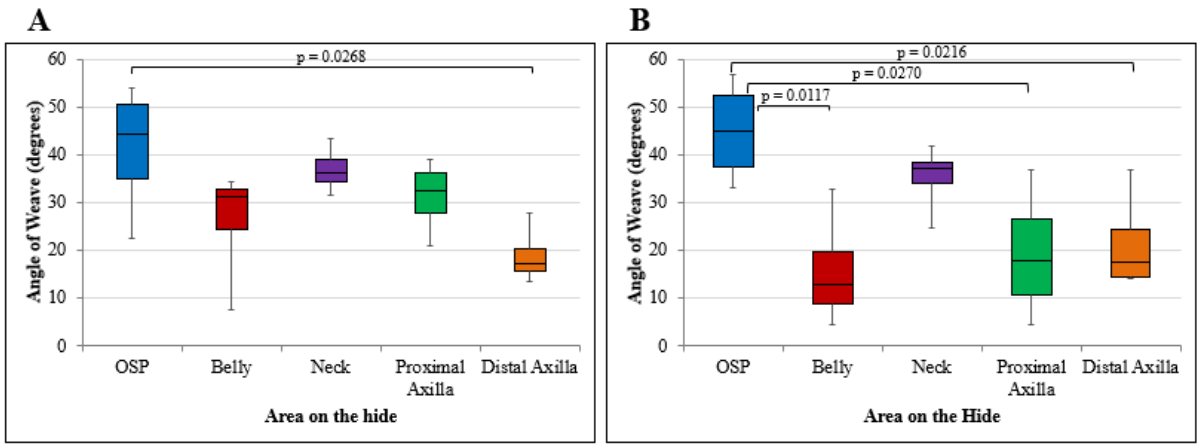

Figure 3.5 (A) The angle of weave of raw hide from the OSP, belly, neck proximal axilla and distal axilla of 4 biological replicates. (B) The angle of weave of finished leather from the OSP, belly, neck proximal axilla and distal axilla of 4 biological replicates.

An in-depth study of the collagen bundles and fibres.

To further examine the organisation of the collagen fibres and bundles in loose and tight hides, 2D and 3D confocal microscopy images were analysed. As 3D confocal microscopy gave more detailed images of the collagen fibres and bundles (Figures 3.6 A and B), only the images obtained using this technique are reported.

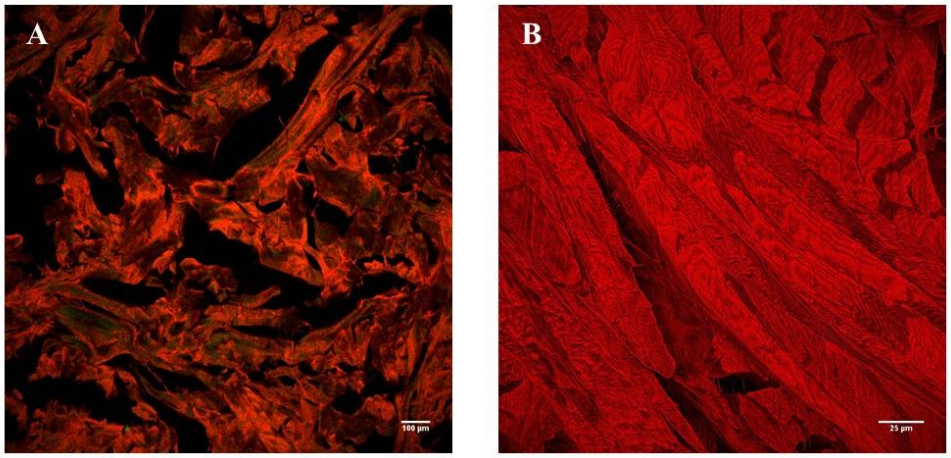

Figure 3.6 Example of 2D and 3D confocal microscopy images: (A) 2D image, scale bar 100 µm and (B) 3D image, scale bar 25 µm.

Collagen fibres in the different layers of hide

The size and organisation of the collagen fibres throughout the layers of the hide are clearly different with thinner, less organised fibres being found in the grains of raw hide and finished leather (Figures 3.7 A and D) and slightly larger collagen fibres organised into well-defined bundles being found in the corium of raw hide and finished leather (Figures 3.7 C and F). The collagen fibres visualised in raw hide (Figures 3.7 A-C) are less well defined than those in the finished leather and appear to be almost glued together due to the high concentration of water and interfibrillary components.

No discernible differences between the grain layers of loose and tight hides were observed, which is possibly because the fibres are too thin for the scanning microscope to differentiate them. The grain to corium junction was found to be too varied between sections, even within the same sample to easily examine differences between loose and tight samples. Part of this could be due to the sectioning technique, as this area is very fragile and tends to be easily torn during sample preparation. Typically experiments that have reported differences in the grain to corium junction between loose and tight leather samples have used scanning electron microscopy [10, 13]. However, differences in fibre bundle architecture were found in the corium layer and will be expounded on later in this chapter.

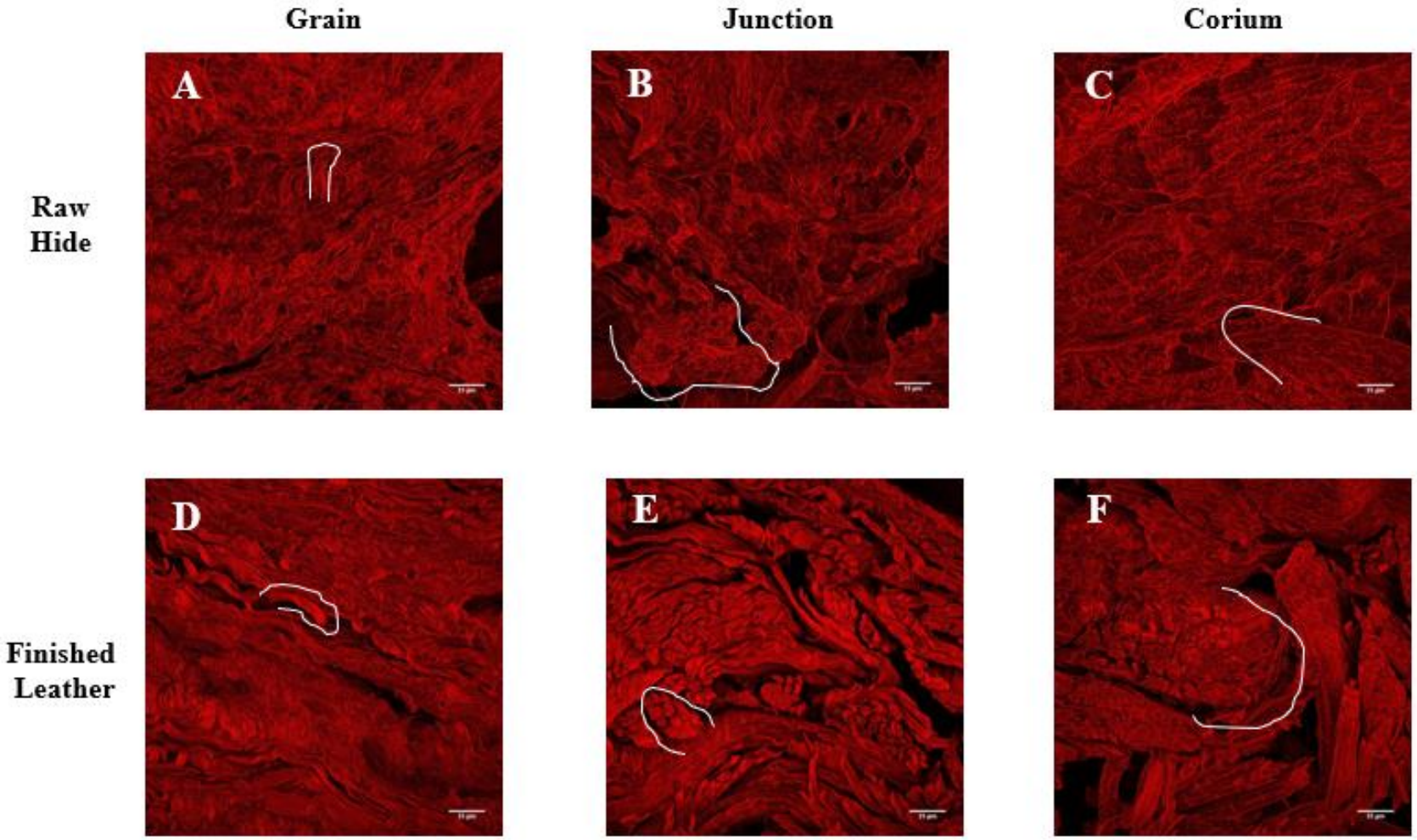

Figure 3.7 Examples of 3D Confocal Microscopy images of raw hide; (A-C) and finished leather (D-F). (A&D) grain, (B&E) grain to corium junction (C&F) corium. Scale bar 25 µm. The white marks indicate areas where fibres are grouped into bundles.

Differences in organisation of collagen fibres in loose and tight cattle hide and its subsequent finished leather

3D images were visualised at all 5 locations on both the raw hide and finished leather (Appendix 9.A). Minor differences in the organisation of the collagen fibres and bundles were observed in all the locations. However, the most obvious differences were those found in the proximal and distal axilla. In raw hides samples taken from these locations had an increase in space found around the collagen bundles while in both raw hide and finished leather the directionality of the collagen fibres and bundles were more consistent compared to samples taken from the other regions; OSP, neck and belly. A more in-depth analysis of the collagen fibres and bundles organisation was carried out on samples from the OSP and distal axilla as they showed very different results at almost all stages of analysis; average looseness grade, strength and angle of weave.

The organisation of the collagen fibres between the OSP and distal axilla are slightly different with the OSP regions having more densely packed collagen bundles compared to the distal axilla as seen in both the raw hide (Figure 3.8) and finished leather (Figure 3.9). Figure 3.10A shows that the distal axilla appears to have a greater amount of space between the collagen fibre bundles as calculated by imageJ although the value is not statistically significant (p-value 0.088). This could be due to the OSP region having a greater concentration of collagen or the distal axilla region having a greater concentration of interfibrillary substances.

Loose samples appear to have regions of poorly defined collagen bundles that are less densely packaged than the tight samples in both the raw hide and the finished leather (Figure 3.9 and 3.10), similar to the change in collagen organisation found in wrinkly human skin [62, 63]. Loose samples also appear to have a greater amount of space between the collagen bundles, as

measured using imageJ (Figure 3.8B). Although a greater number of replicates would be needed to confirm this, the correlation between looseness and the space between collagen bundles appears significant with an R^2 of 0.6048 and a p-value of 0.032 between samples with looseness grades under 4 (tight) and over 4 (loose). This finding agrees with previous reports that suggest that there is an excess of space between the collagen fibres in loose leather, most likely filled with molecules that are not stained with picrosirius red such as GAGs, proteoglycans and other non-collagenous proteins. Further analysis of these molecules will enable a more thorough understanding of the cause of looseness in cattle hide.

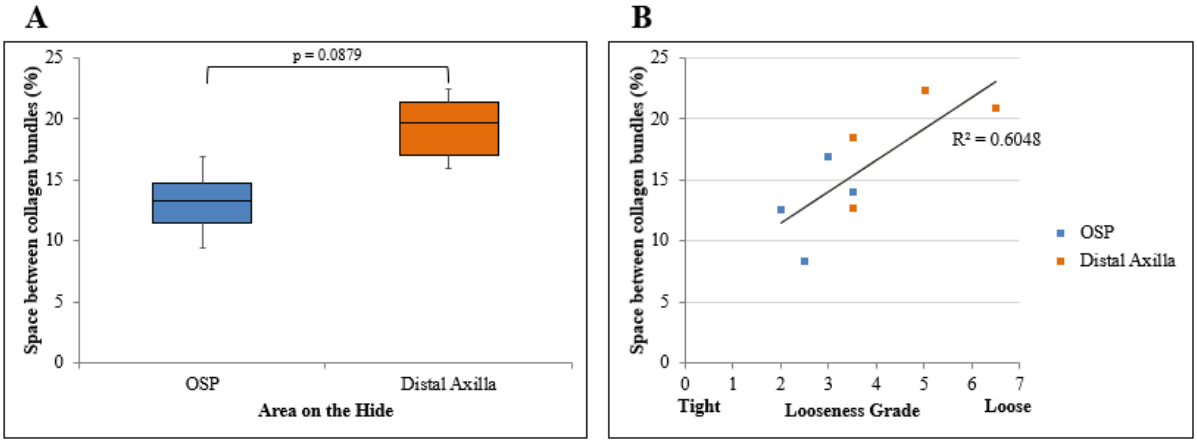

Figure 3.8 (A) Box blot of the percentage of blank space found between the collagen bundles in raw hide between the OSP and distal axilla location, average of at least four technical replicates for four biological replicates. (B) Relationship between looseness grade and space between the collagen bundles. Data averaged from four slides from four hides in two different locations.

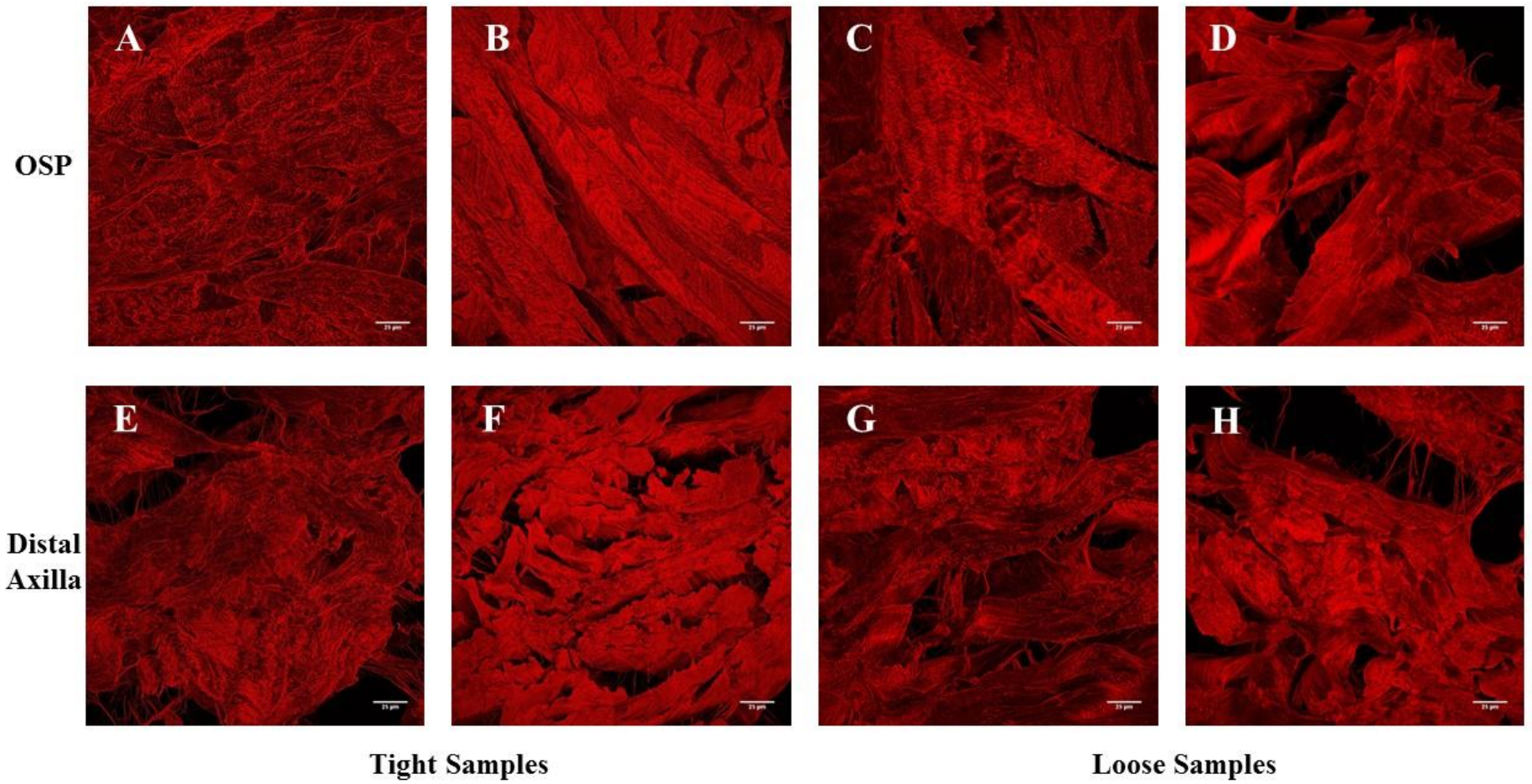

Figure 3.9 Organisation of collagen fibres in the corium of loose and tight raw hide. (A-B) tight OSP; (C-D) loose OSP;(E-F), tight distal axilla; (G-H) loose distal axilla. Scale bar 25 µm.

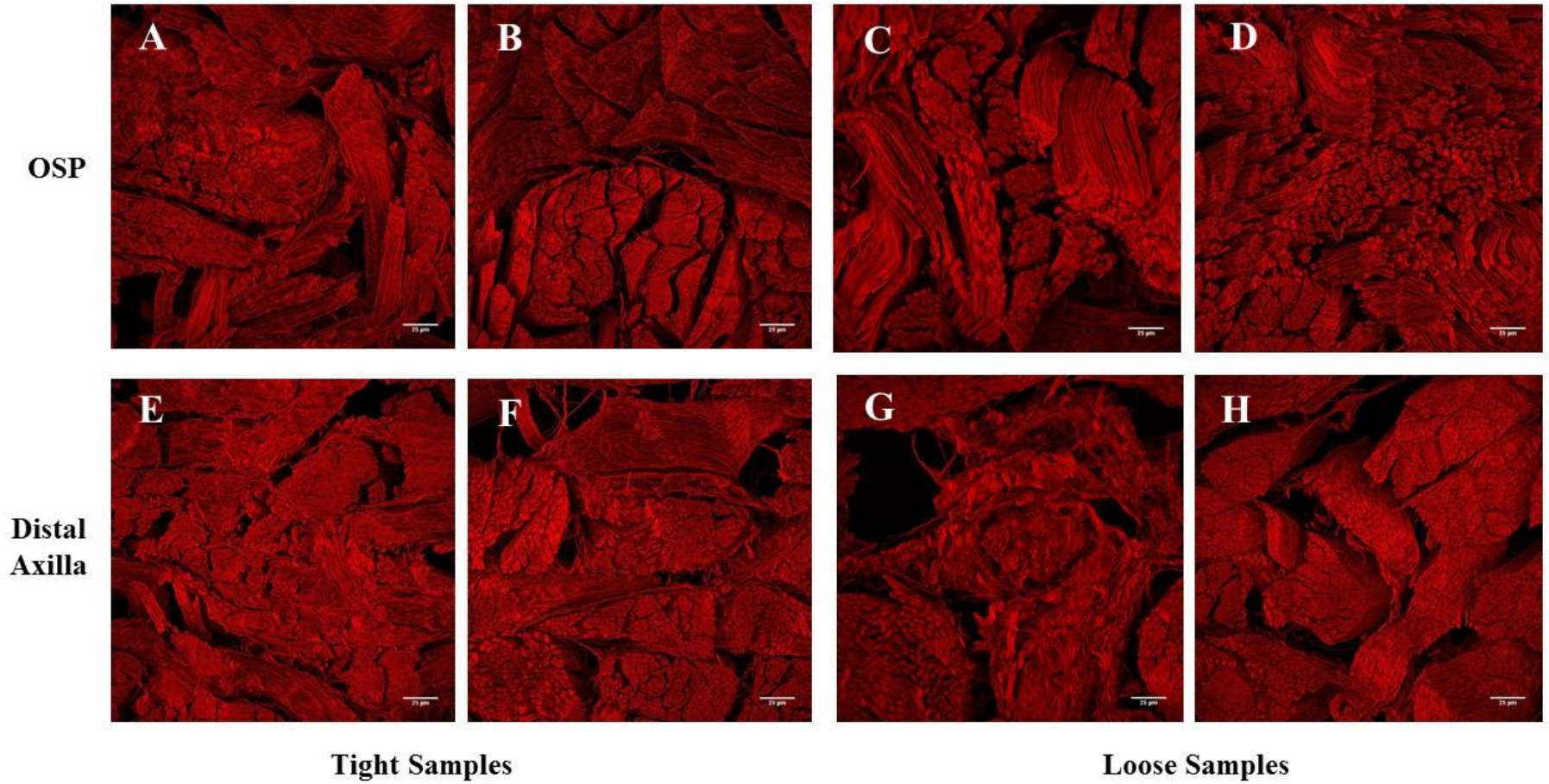

Figure 3.10 Organisation of collagen fibres in the corium of loose and tight leather. (A-B) tight OSP; (C-D) loose OSP; (E-F), tight distal axilla; (G-H) loose distal axilla. Scale bar 25 µm.

3.3.3 Distribution of lipids in loose and tight hides

The distribution of lipids in loose and tight raw hide were investigated using sudan III/IV dye. The majority of the lipids are found in the grain region (as shown during the grain-corium ratio and thickness tests) and in the hypodermis region, consistent with literature for the distribution of lipids in hide (Figure 3.11) [151]. Cooper [11] reported that higher levels of fat are present in looser sheepskins compared to tight sheepskins. However, our studies showed no consistent differences between the relative fat content of loose and tight hides (Figures 3.11A and B). This difference is most likely due to the lower amount of fat found in bovine hides compared to sheepskin, as well as the difference in fat distribution. Sheepskins can have up to 30 % fat (wet weight) in the skin with large quantities present in the grain to corium junction whilst bovine hides typically have 5-10 % fat (wet weight) which is mainly located in the grain and lower regions of the corium [11, 120].

There appears to be a greater amount of fat present in the distal axilla region than the OSP, especially in the lower part of the corium. However, this could be due to poor fleshing (removal of fat from hypodermis layer) in this region.

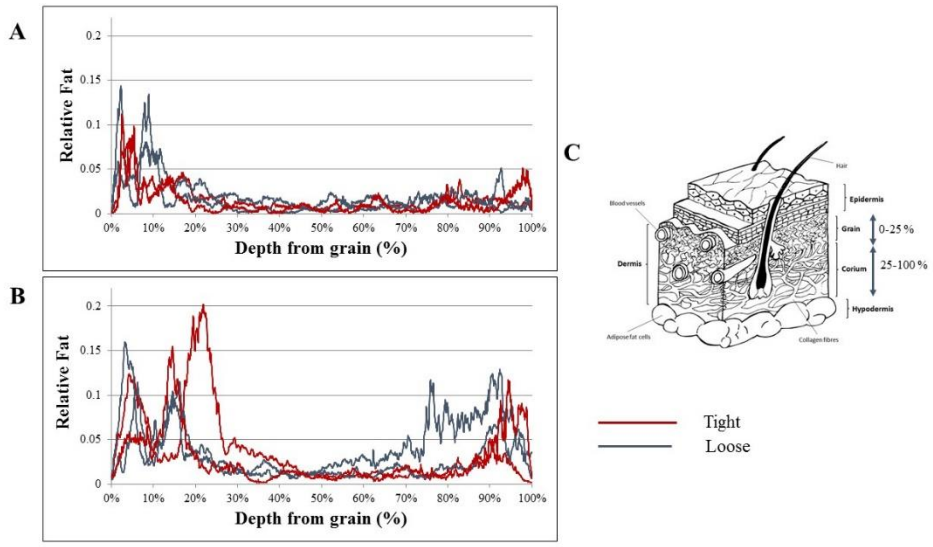

Figure 3.11 Graphs illustrating relative fat content in the (A) OSP and (B) distal axilla regions of cattle hide. (C) Diagram of cross section of hide illustrating the different layers.

4. Quantitation of carbohydrate and elastin molecules in loose and tight hides

4.1 Introduction

In the literature so far, collagen has been investigated as the most likely culprit for causing looseness in leather with various studies indicating that it is differences in the organisation of collagen fibres that cause the change in the leather's appearance [10, 12, 13]. The focus on collagen is due to the fact that most other molecules get removed during leather processing. However, as this study found that there was a greater amount of separation between collagen fibre bundles in loose leather compared to tight leather [10, 12], a finding that agreed with other studies, it is possible that before processing there was a greater amount of non-collagenous material such as GAGS present in the hide. This possibility was investigated in several ways; first colorimetric assays were used to determine any differences between certain non-collagenous material such as carbohydrates including GAGs, hyaluronic acid and elastin in loose and tight hides. Secondly, amino acid analysis and shot-gun proteomics were used to analyse the proteins in loose and tight hides (elaborated on in chapter 5 and 6).

Colorimetric assays are useful tools for determining the concentration of specific macromolecules in a sample. For this project, the phenol-sulfuric acid method was used to measure total carbohydrates, the Blyscan^{TM} assay using 1,9-dimethylmethylene blue (DMMB) dye was used to measure sulfated GAGs, HA was measured using the Purple-Jelley^{TM} method with the Stains-all dye, and elastin was measured using the Fastin^{TM} kit using the 5,10,15,20-tetraphenyl-21H,23H-porphine tetra-sulfonate (TPPS) dye. Whilst colorimetric assays are quick, they have several disadvantages including the necessity for extraction of the compound to be measured which limits accuracy, and limited specificity due to the dyes used and their

ability to bind specifically to the substrate [65, 83, 101]. These disadvantages were very apparent when using these tests on the loose and tight hides.

4.2 Methods

4.2.1 Chemicals and Equipment

The chemicals and equipment used in this section are listed in Table 4.1 and 4.2 respectively.

Table 4.1 Chemicals used in chapter 4.

Supplier	Country	Equipment
Ajax Finechem	NSW, Australia	Sulfuric acid, 98 % Sodium acetate NaCl Sodium phosphate
BDH Lab supplies	Poole, UK	Oxalic acid Phenol Papain Sodium formate
Biocolour Life Science	Carrickfergus, Northern Ireland	Chondroitin sulphate Elastin
Emsure	Germany	Glacial acetic acid
Fisher Scientific	Leicestershire, UK	Formic acid, 98-99%
J. T. Baker	USA	EDTA, disodium salt
Merck	Germany	Ethanol, 96 %
Pure Science	Wellington, NZ	Tris
SERVA	New York, USA	α-D-glucose
Sharlau	Barcelona, Spain	Propan-1-ol
Sigma-Aldrich	St. Louis, USA	Ascorbic acid, 99 % Cetylpyridinium chloride (CPC) Cysteine hydrochloride 1,4-Dioxan 2,6-di-tert-butyl-4-methylphenol DMMB Guanidine hydrochloride HA Proteinase K Stains-all
Thermo Fisher; Milli-Q Ultra-Pure	Massachusetts, USA	Milli-Q H_2O

Table 4.2 Equipment used in chapter 4.

Supplier	Country	Equipment
BioTek Instruments, Inc.	Vermont, USA	PowerWave XS microplate Spectrophotometer

4.2.2 Phenol-sulfuric acid assay for total carbohydrates

Carbohydrate content was measured using the phenol-sulfuric acid method in a microplate format [152]. Depilated lyophilized hide pieces (25 mg) was hydrolysed with 2 mL of 1.0 M sulfuric acid at 100 °C for 8 hours to extract the carbohydrates. After cooling, undissolved particles were removed by centrifuging for one hour at 14,100 x g at room temperature. The supernatant was transferred to a fresh microcentrifuge tube and the pellet discarded. 10 µL of supernatant was placed in a 96-well microplate to which 150 µL of sulfuric acid followed by 30 µL of 5 % phenol was added. The microplate was sealed then incubated at 90 °C for 10 minutes before measuring the absorbance at 490 nm. Three separate extractions were carried out on each sample. All samples and standards were prepared in triplicate and the results averaged. A standard curve was created using 0, 5, 10, 20, 40, 60, 80 and 100 nM of α-D-glucose (Figure 4.1).

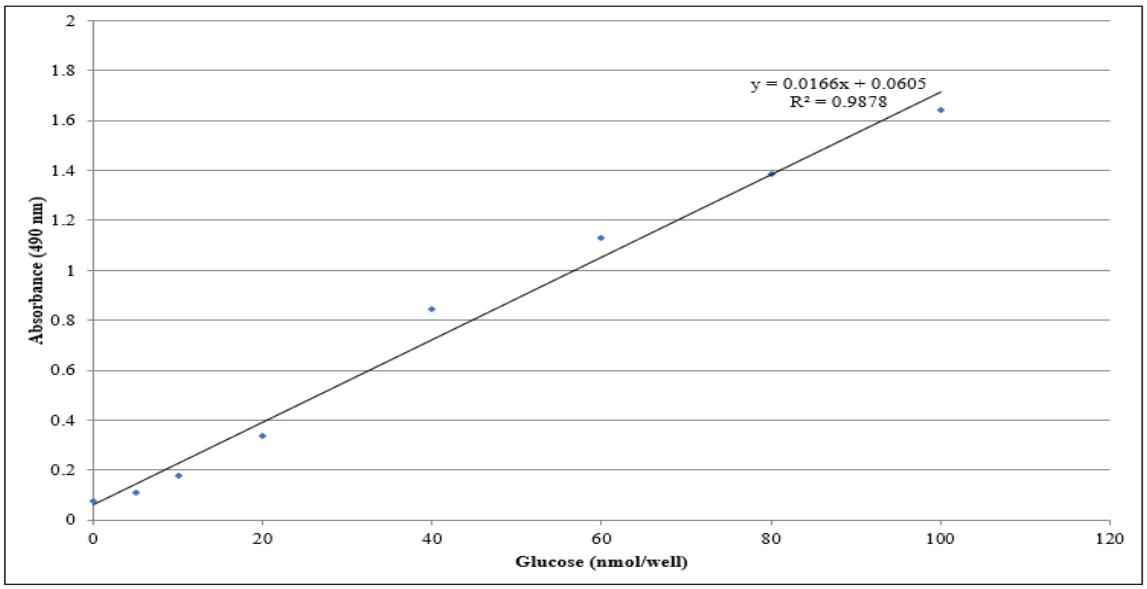

Figure 4.1 Carbohydrate standard curve of glucose at 490 nm.

4.2.3 GAG assay

GAGs were extracted from lyophilized depilated hide using the method recommended by the manufacturers of the Bicolour life science assay kit and Hyanuh *et al*. [153]. 50 mg of sample were mixed with a papain extraction reagent made up of 0.2 M sodium phosphate buffer (pH 6.4) containing 100 mM sodium acetate, 50 mM EDTA, 5 mM cysteine HCl and 5 mg of papain at a 20:1 volume ratio (papain: hide) and incubated for 24 hours at 65 °C. After this time, the insoluble material was removed by centrifugation at 13,800 x g for 30 mins and the supernatant was placed in a clean tube. This extraction was repeated three times to ensure all GAGs had been removed from the sample.

It was subsequently found that the majority of GAGs were extracted in the first extraction with insignificant amounts being found in the latter two extractions. 50 µL from the first extraction was made up to 100 µL then mixed with 1 mL of DMMB solution (1.85 mM DMMB dye, 0.2 M guanidine hydrochloride, 0.2 % formic acid and 0.5 % sodium formate). After mixing for 30 min on a mini labroller, the pellet was isolated by centrifugation at 16,500 x g for 30 min, then dissolved in 250 µL of GAG-precipitating solution (4 M guanidine hydrochloride, 50 mM sodium acetate and 10% propan-1-ol). The absorbance of each sample was recorded at 656 nm. Three separate extractions were carried out on each sample. All samples and standards had triplicate absorbance readings. These were then averaged. A standard curve was prepared using 0, 10, 20, 30, 40 and 50 µg of chondroitin sulfate (Figure 4.2).

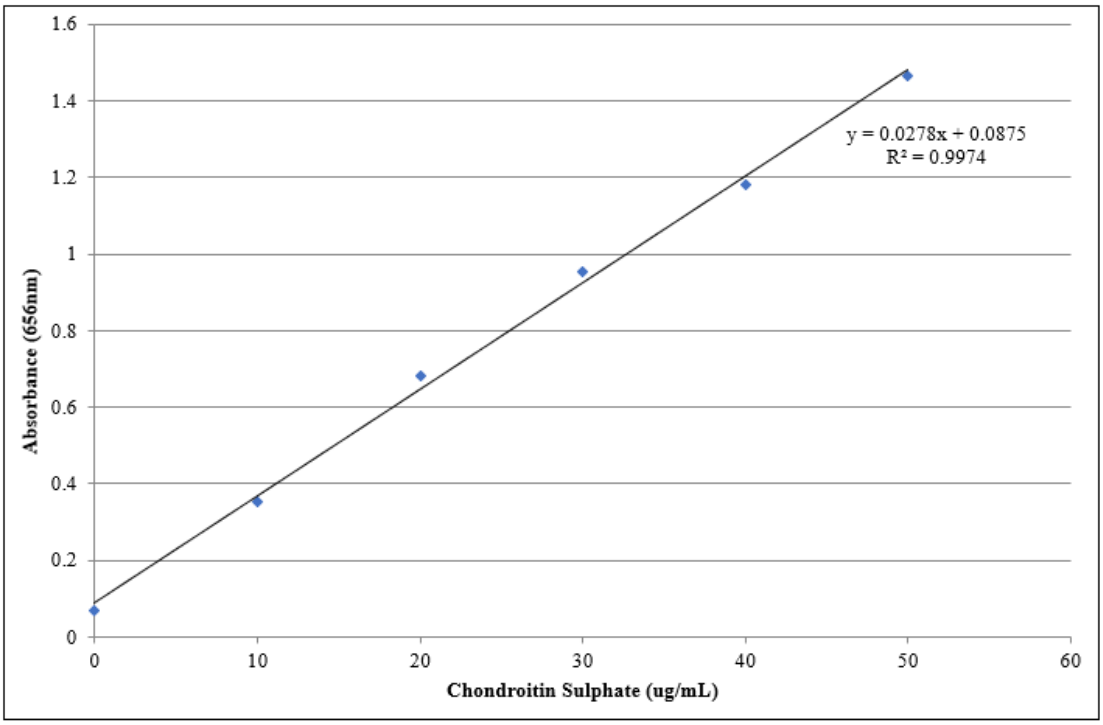

Figure 4.2 GAG standard curve of chondroitin sulphate at 656 nm.

4.2.4 HA assay

Hyaluronic acid was extracted and assayed using the Biocolour Purple-Jelley^{TM} method according to the manufacturer's instructions as seen in figure 4.3. First the proteins were removed from the sample by treatment with Proteinase K. The GAGs were then isolated and hyaluronic acid purified by repeated treatment with GAG precipitation reagent (55.5 % saturated sodium acetate in 44.5 % ethanol, concentrated NaCl and CPC (Figure 4.3). The HA was then resolubilised in Milli-Q H_2O. 20 µL of sample was placed in a 96-well microplate followed by 180 µL of Stains all dye, using a recipe adapted from Homer, Denbow and Beighton [154] (0.1 mM Stains all added to a 50 % Milli-Q H_2O / 50 % 1,4-dioxan mix containing 25ppm 2,6-di-tert-butyl-4-methylphenol followed by 1 mM acetic acid and 0.5 mM ascorbic acid) followed by addition of 100 µL water. The absorbance was measured at 620 nm and compared against a standard curve of 2, 4, 6 and 8 µg HA (Figure 4. 4). Three separate extractions were carried out on each sample.

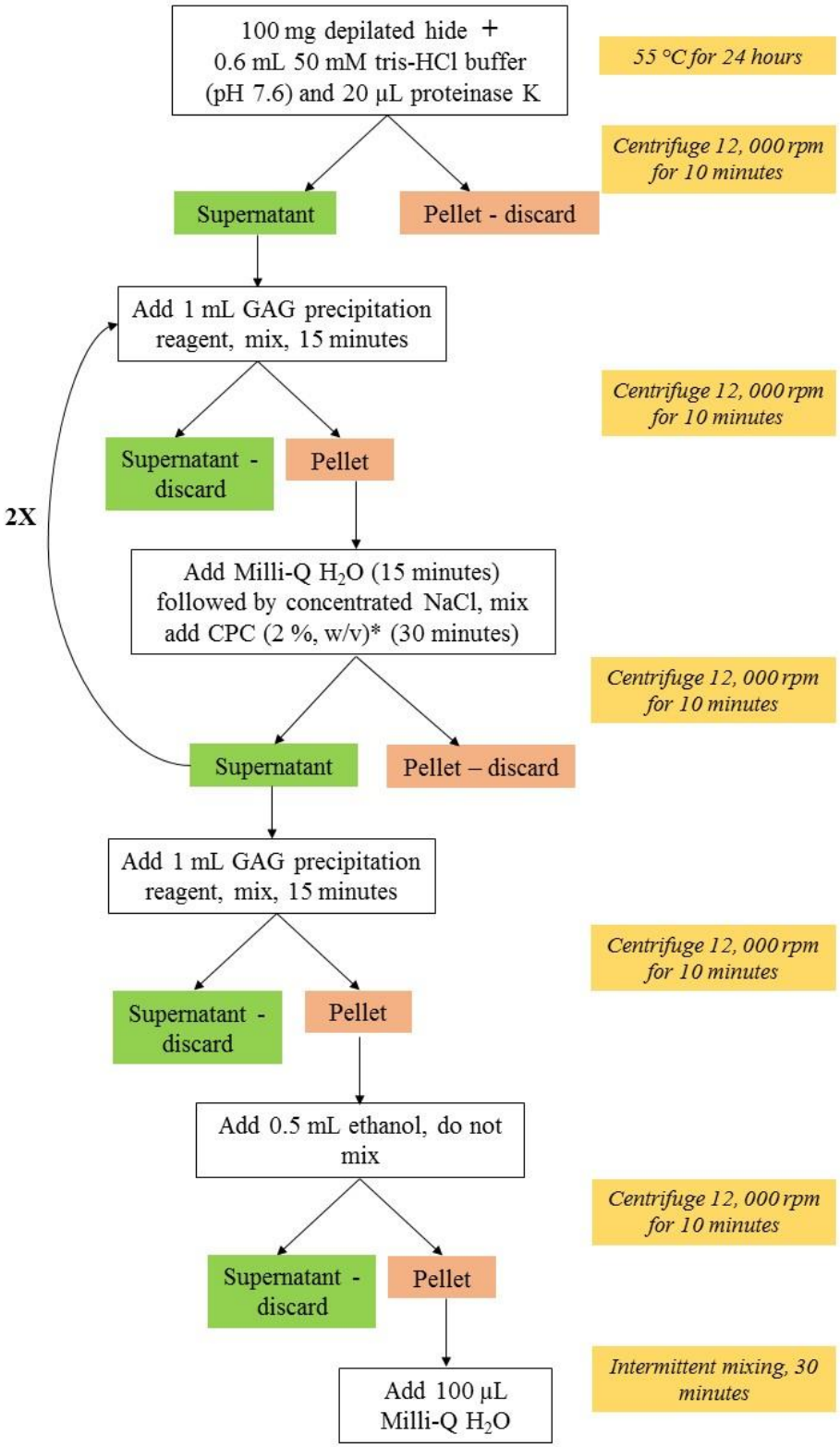

- *1 extraction add 360 µL Milli-Q H_2O, 40 µL concentrated NaCl and 95 µL CPC (2 %, w/v)*
- *2 extraction add 300 µL Milli-Q H_2O, 33 µL concentrated NaCl and 77 µL CPC (2 %, w/v)*

Figure 4.3 HA extraction and purification protocol from Biocolour - Purple-Jelley™ method.

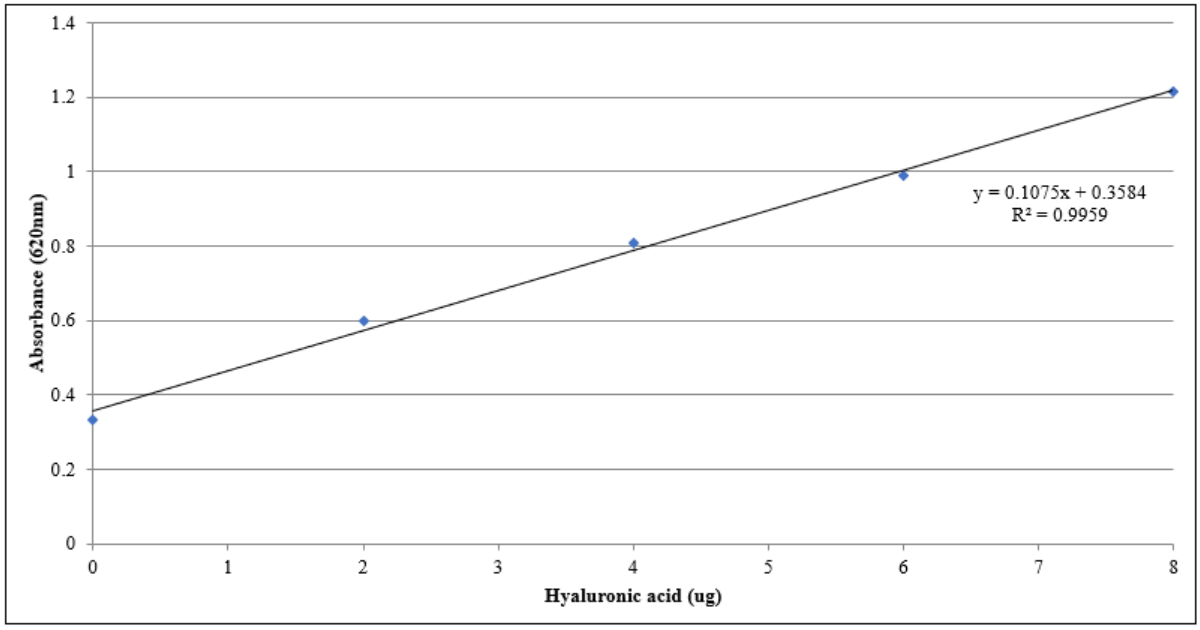

Figure 4.4 Standard curve of HA at 620 nm.

4.2.5 Elastin assay

Elastin was extracted from hide samples using the Fastin^{TM} assay kit.100 mg of lyophilized depilated hide was added to 1 mL of 0.25 M oxalic acid and incubated at 100 °C for 60 minutes. The insoluble material was pelleted by centrifugation at 900 x g for 10 minutes and the supernatant collected. The pellet was then treated with two more rounds of oxalic acid to extract all of the elastin from the hide whilst the supernatant was kept for further analysis. Equal volumes of elastin precipitation reagent and supernatant containing the extracted elastin was added to a fresh microcentrifuge tube, vortexed and left for 10 minutes. The pellet was then isolated by centrifugation for 10 minutes at 9, 600 x g and the supernatant discarded. 500 µL of dye reagent was added to the pellet, and vortexed followed by mechanical mixing for 90 minutes. Insoluble material was removed by centrifugation at 6000 x g for 10 minutes, and after discarding the supernatant, 250 µL of dye dissociation reagent was added, vortexed and left to incubate at room temperature for 10 minutes. 200 µL of each sample was added to a 96-

well microplate which was read at 513 nm. The results were compared against a standard curve of 12.5, 25, 50 and 100 µg of elastin (Figure 4.5).

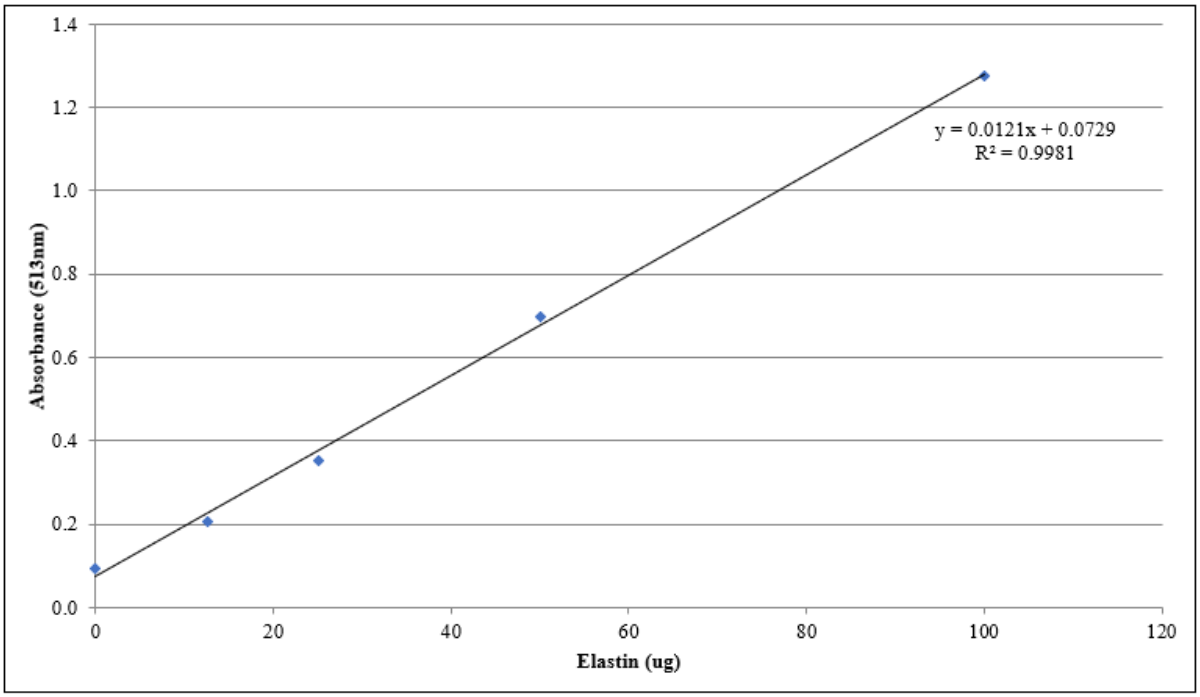

Figure 4.5 Standard curve of elastin at 513 nm.

4.3 Results and Discussion

4.3.1 Assays for carbohydrate components

Although carbohydrates are only present in small amounts in hides, when attached to proteins, they play fundamental roles in a diverse array of processes such as enzyme regulation, cellular adhesion, growth, migration and differentiation [87, 88]. Three different assays were used to analyse the different carbohydrate components present of loose and tight hides and for all of these methods, the variation between readings was very large. To compensate, three separate extractions were carried out on each sample with triplicate absorbance readings for each to give 9 results which were then averaged. The correlation coefficient (CV %) between readings could be as high as 10 % while between extraction methods, it could be as high as 25 % despite all care being taken with both sample extraction and preparation. Because the CV % of HA results

was typically even higher than this, and it was very easy to lose the sample due to the extended extraction and purifying process, quantitation of HA was not continued.

Figure 4.6A illustrates that no significant differences in the total carbohydrate concentrations were found between samples taken from the OSP and distal axilla (p-value 0.330). Figure 4.6B shows no significant differences in the total carbohydrate concentrations of loose (samples above 4) and tight (samples below 4) hides, with p-values of 0.860 and R^2 of 0.1705. This indicates that the total carbohydrate content does not play a role in hide looseness. However, it must be noted that this value was obtained using the standard phenol-sulfuric acid method presented in terms of glucose-equivalent concentrations, which has potential limitations when dealing with complex carbohydrates that are not simple polymers of glucose [155]. It also does not negate the potential for specific differences, for example in the glycosylation patterns of collagen, that may be related to looseness. To investigate such specific differences tandem MS was used (Section 6.3.5).

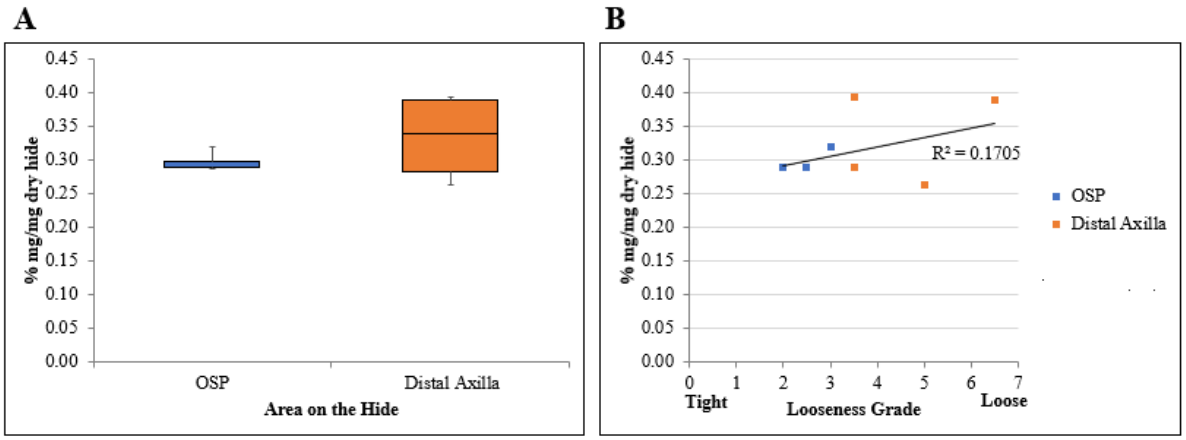

Figure 4.6 (A) Box plot illustrating the total carbohydrates in OSP and distal axilla region. Each box blot shows the result of four biological replicates. (B) Relationship between looseness grade and total carbohydrates.

Figure 4.7A illustrates that the results for the sulfated GAGs showed more variation between samples, and although not significant (p-value 0.322), on average, samples from the distal

axilla contained a higher concentration of GAGs (0.213 % mg GAGs/mg of dry hide) than the OSP (0.136 % mg GAGs/mg dry hide). No correlation was found between looseness grade and sulfated GAGs (Figure 4.7B) with a p-value of 0.915 and R^2 of 0.0022. Because of the difficulties in measuring HA, no conclusions could be made concerning the concentrations of nonsulfated GAGs in the samples.

While it was disappointing that there were no significant differences in the concentrations of GAGs in loose and tight skins, it must be remembered that these results are derived from a very small sample size, and it is possible that there may be subtle differences in, for example, the sulfation pattern of the GAGs in loose and tight skins. A more sophisticated analysis involving HPLC or MS could be used in the future to look into such differences [156].

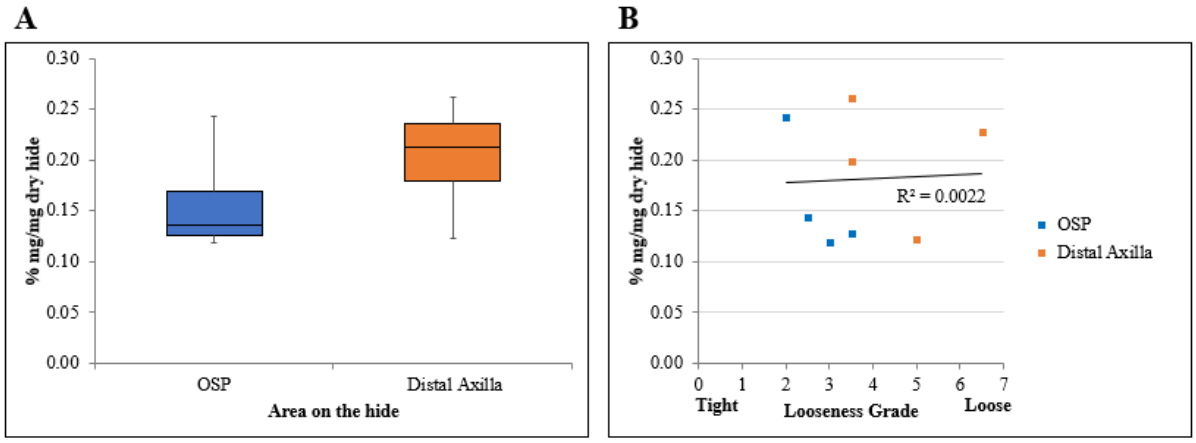

Figure 4.7 (A) Box plot illustrating sulfated GAGs in OSP and distal axilla region. Each box blot shows the result of four biological replicates. (B) Relationship between looseness grade and sulfated GAGs.

4.3.2 Elastin assay

During the course of this project three different methods were attempted to determine whether any differences were found between elastin in tight and loose cattle hide. One of these experiments was an elastin assay which is used to determine the concentration of elastin. Two

different colorimetric assay methods are commonly used. One of these, the bio-colour kit Fastin^{TM}, uses the dye TPPS to quantitate elastin concentration. The manufacturers state that the dye binds to the 'basic' and 'non-polar' amino acid sequences found in elastin and can measure three different elastin forms including soluble tropoelastins, lathyrogenic elastins and insoluble elastins. The other method involves the extraction of elastin, then further ensures removal of collagens from the extract through an autoclaving step [83]. Two problems were identified with both these techniques. In the Fastin^{TM} kit even after 5 sequential treatments with oxalic acid, elastin was still being removed from the sample indicating that the oxalic acid method was not stringent enough to remove all of the elastin from the samples. Also, in both methods the elastin specific dye and collagen specific dye both had positive results indicating that these dyes are not sufficiently specific to separate these proteins and that the extraction method was not able to isolate each protein. Only one paper was found that suggests that the TPPS dye is specific to elastin and does not interact with collagen [157]. Elastin and collagen concentrations were therefore analysed using more specific techniques.

5. Quantitation of amino acids and collagen and elastin cross links in loose and tight hides

5.1 Introduction

Proteins are the most abundant macromolecule found in hide, comprising 33 % of the wet weight [8]. They play a variety of roles to give hide strength, elasticity and flexibility [61]. Protein structure, concentration and composition is implicated in the phenomenon of looseness, through microscopy studies on loose and tight leather [10, 13] as well as on wrinkly human skin [24, 28].

One method that can be used to investigate protein concentration and composition is the analysis of the amino acid profile. As amino acids are the primary building block of proteins, and as collagen, the predominant protein found in hide has a unique amino acid profile [8, 158], compositional differences are likely to be reflected in the amino acid profile. Whilst collagen contains all the regular amino acids, except for tryptophan, it also contains two unique amino acids, hydroxyproline and hydroxylysine [61]. Hydroxyproline plays a role in maintaining the hydrothermal stability of collagen by forming hydrogen bonds with water molecules [45]. It is also frequently used to determine the collagen concentration of skin and hide due to it only being found in collagen, and to a lesser degree in elastin [159, 160]. Hydroxylysine helps to maintain the stability of collagen through its role in the formation of covalent crosslinks between collagen fibrils. [161, 162]. Investigating the amino acid composition of loose and tight hides in different areas of the animal and layers of the hide may give information about how the molecular components of the hide affect its physical properties. The amino acid composition of hides is typically analysed using two steps; hydrolysis of the substrate followed by chromatographic separation and detection of the individual acids that are labelled with a chromophore either pre- or post-separation [163-166]. This study used the method of Cohen

[167] to determine the amino acid composition of loose and tight hides. It uses 6-aminoquinolylcarbamyl (AQC) to pre-label amino acids as it rapidly reacts with both primary and secondary amino acids to produce a stable fluorescent derivative that can later be separated and detected by RPHPLC [61, 167, 168].

Collagen and elastin crosslinks, formed during biosynthesis of the macromolecules, aid in the development of the complex mesh-like structure characteristic of skin and hide [35, 44]. They also contribute to its physical properties such as its flexibility and strength, which is largely due to collagen structure. Changes in the profile and concentration of collagen crosslinks have been linked to ageing in a variety of types of skins, including human and bovine, with mature crosslinks such as HHL and HHMD being more prevalent in aged skin than immature crosslinks such as HLNL and DHLNL [53, 71]. The elastin crosslinks desmosine and isodesmosine are frequently used to determine the concentration of elastin, as they are unique to the elastin molecule [59, 61]. Analysis of the concentrations of crosslinks in loose and tight hide may indicate whether the difference in hide quality is due to a structural difference in the collagen and/or elastin molecules. A wide variety of techniques have been used to investigate collagen and elastin crosslinks including ion-exchange chromatography, and RPHPLC[71]. This study used the recently developed technique reported by Naffa [57, 61] which isolates all of the known collagen and elastin crosslinks using a CF-11 column then separates and detects them using silica hydride chromatography in conjunction with MS (LCMS).

5.2 Methods

5.2.1 Chemicals and Equipment

The chemicals and equipment used in this section are listed in Tables 5.1 and 5.2 respectively.

Table 5.1 Chemicals used in chapter 5.

Supplier	Country	Equipment
Ajax Finechem	NSW, Australia	Ammonium acetate NaCl n-Butanol
BDH Lab supplies	Poole, UK	Phenol
Emsure	Germany	Ammonium hydroxide, 28-30 % Glacial acetic acid
Fisher Scientific	Leicestershire, UK	Formic acid, 98-99% HCl, 37 % MS grade H_2O
GE Whatman	UK	CF-11 fibrous medium cellulose powder
PanReac applichem	Barcelona, Spain	Acetone Acetonitrile
Sigma-Aldrich	Stenheim, Germany St. Louis, USA	Amino acid standard Boric acid Norleucine Sodium borohydride Sodium hydroxide Sodium phosphate
Synchem	Germany	AQC
Thermo Fisher; Milli-Q Ultra-Pure	Massachusetts, USA	Milli-Q H_2O

Table 5.2 Equipment used in chapter 5.

Supplier	Country	Equipment
BH Medical Supplies	Essex, UK	10 mL Syringe, sterile with Luer lock tip
Leica Microsystems	Wetzlar, Germany	Leica CM 1850 UV cryostat
Thermo Fisher	Massachusetts, USA	Ultimate 3000 HPLC system with Dionex RF 2000 fluorescence detector
Phenomenex	California, USA	Gemini® 5 µm C18 110 Å liquid chromatography column, 150 x 4.6 mm
Microsolv technology corp.	North Carolina, USA	Cogent Diamond Hydride™, 2.2 µM 120 Å column, 150 x 2.1 mm
Thermo Fisher Scientific	Massachusetts, USA	Dionex UltiMate™ LPG-3400RS rapid separation quaternary pump (LC system) Q Exactive Focus mass spectrometer Xcalibur software suit (version 4.1.31.9)

5.2.2 Amino acid analysis

Amino acid extraction from hide

Samples were sectioned used the Leica CM 1850 UV cryostat to 40 µm thickness separated into grain, middle and corium sections utilising the data obtained from total thickness of the hide and grain to corium ratio (Figure 2.8-9), then lyophilized. 100 mg of each grain, junction and corium sections were then hydrolyzed in 5 mL of 6 M HCl containing 3 % (w/v) of phenol for 24 hours at 110 ^{0}C. Phenol is used to minimize the destruction of amino acids by oxidation during hydrolysis [166]. The hydrolyzed samples were then filtered to remove particles and lyophilized. The lyophilized samples were dissolved in 1000 µL of 0.1 M of HCl, and any particles were removed by centrifugation (16,500 x g for 30 minutes) before being diluted 10 x with Milli-Q H_2O.

Derivatization of amino acids

Derivatization was achieved by mixing 10 µL sample or standard (2.5 nmol/µL of each amino acid, 1.25 nmol/µL cysteine, 12.5 nmol/µL hydroxyproline and hydroxylysine), 100 pmol/µL of norleucine, 0.2 M borate buffer pH 8.85 and 15 pmol/µL AQC. These were incubated for 10 minutes at 55 ^{0}C, to ensure complete conversion and production of the stable derivatives [167] then diluted 10 x with Milli-Q H_2O.

Separation of AQC derivatized amino acids

1 to 5 µL of standards and 1 µL of samples were injected on to a Phenomenex 150 x 4.6 mm Gemini C18, 5µ HPLC column. The analysis was performed at 37 ^{0}C using the following gradient: Mobile phase A: 5 mM ammonium acetate, 1 % acetic acid, pH 5.05 adjusted using concentrated ammonia hydroxide. Mobile phase B: 60 % (v/v) acetonitrile in water. Eluted peaks were monitored using a fluorescence detector (Dionex RF 2000) with excitation and

emission wavelengths set at 245 nm and 395 nm respectively. Table 5.1 shows the gradient profile used for the analysis. Amino acid concentrations were determined using calibration curves calculated using Dionex CHROMELION version 6.80 SR13 Build 3967. Figure 5.1 shows the separation of the AQC-amino acid derivatives of the standard (A) and the samples (B) using this method.

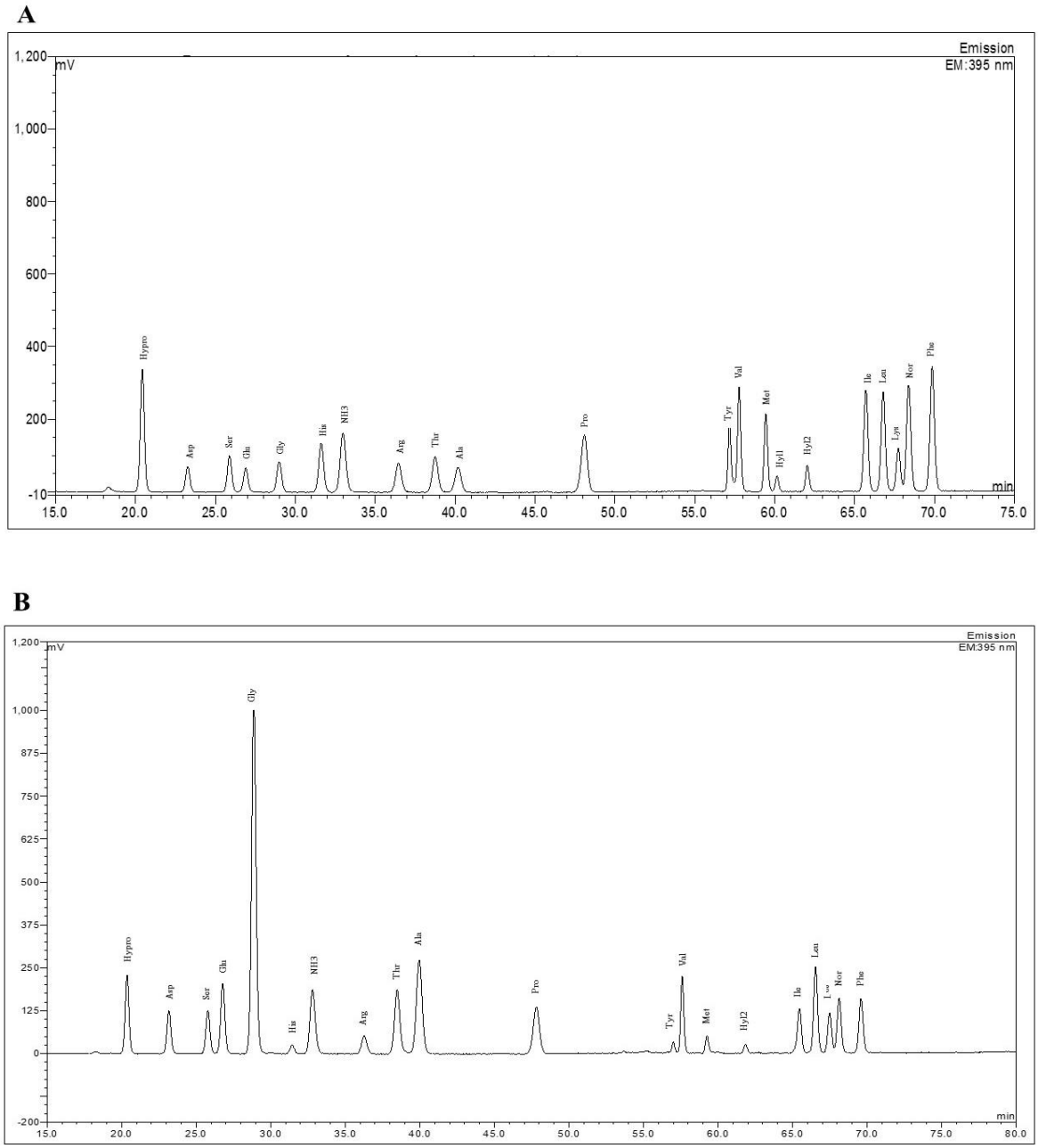

Figure 5.1 Separation of AQC-amino acid derivates using buffer A: 5 mM ammonium acetate, 1 % acetic acid (pH 5.05), buffer B: 60 % acetonitrile, column temperature 37 °C, flow rate 1.0 ml/min, Gemini C18 column. (A) Amino acid standard with norleucine as internal standard. (B) Hide hydrolysate with norleucine as internal standard.

Table 5.3 Gradient profile of Gemini column used for amino acid analysis.

Time (min)	Flow (ml/min)	% B	Curve
0	1.00	0	*
25	1.00	5	Linear
45	1.00	12	Linear
52	1.00	22	Linear
57	1.00	31	Linear
67	1.00	45	Linear
75	1.00	60	Linear
76	1.00	100	Linear
81	1.00	100	Linear
86	1.00	0	Linear
90	1.00	0	Linear

5.2.3 Cross link separation and detection via MS

Reduction of hide sample

Raw hide samples were shaved to remove the hair, then cut into small pieces (5 mm by 5 mm), washed with acetone and lyophilised. 100 mg of sample were rehydrated in 10 volumes of phosphate buffered saline (0.15 M sodium chloride, 0.05 M sodium phosphate, pH 7.4). Sodium borohydride was dissolved in the minimum amount of 1 mM sodium hydroxide at 4 °C then added to the samples at a 1:30 ratio. The mixture was then incubated at 37 °C for 2 hours to reduce the samples then quenched by adjusting the pH to 3 using glacial acetic acid. The solid material was pelleted by centrifugation (23,000 x g for 30 minutes) and the supernatant discarded. The pellet was then washed three times with Milli-Q H_2O to remove excess acetic acid and salt.

Hydrolysis of hide sample

The reduced hide was lyophilized then hydrolysed as per section 5.2.2. 10 µL of sample was removed for amino acid analysis on the HPLC as described in section 5.2.2 (from derivatization step). The remaining 990 µL was used for crosslink analysis.

Crosslink Isolation

The amino acids were removed from the remaining solution by CF-11 column chromatography. A 10 mL syringe was filled with a 5 % CF-11 slurry prepared by suspending 5 g of CF-11 powder in 100 mL of n-butanol acetic acid-water (BAW) (4:1:1, v/v). The column was washed three times with 5 mL of BAW (4:1:1, v/v), before the samples were loaded on to the column bed, taking care not to disturb it. Once the solution had been adsorbed, the column was washed with 10 x 5 mL of fresh BAW before the crosslinks were eluted with 15 mL of water After lyophilisation the crosslinks were dissolved in 1 mL of 0.1 % formic acid then analysed by MS.

Detection of crosslinks via MS

The extracted crosslinks (1 µL and 3 µL injection volume) were separated using a Diamond Silica Hydride column with the following conditions: 20-60 % buffer A (0.1 % formic acid) for 10 minutes then 60-90 % buffer A for 5 minutes at 25 °C. The Dionex LC system directly connects to the Q Exactive Focus mass spectrometer. The peaks from each run were collected in Full MS scan mode over a mass range of 100-600 *m/z* with detection at a resolution setting of 70,000. Full details for the chromatography and MS settings are listed in Appendix 9.B. Crosslink ions were extracted from the chromatogram using the Qual Browser from the Xcalibur software suit (example of mass spectrum and chromatogram of extracted crosslinks shown in Figure 5.2A and B) and integrated by area for quantitation using a standard curve of purified crosslink standards (Figure 5.3) containing 0.98 µM HLNL, 0.61 µM DHLNL, 5.11 µM HHL, 1.15 µM HHMD and 0.75 µM Des.

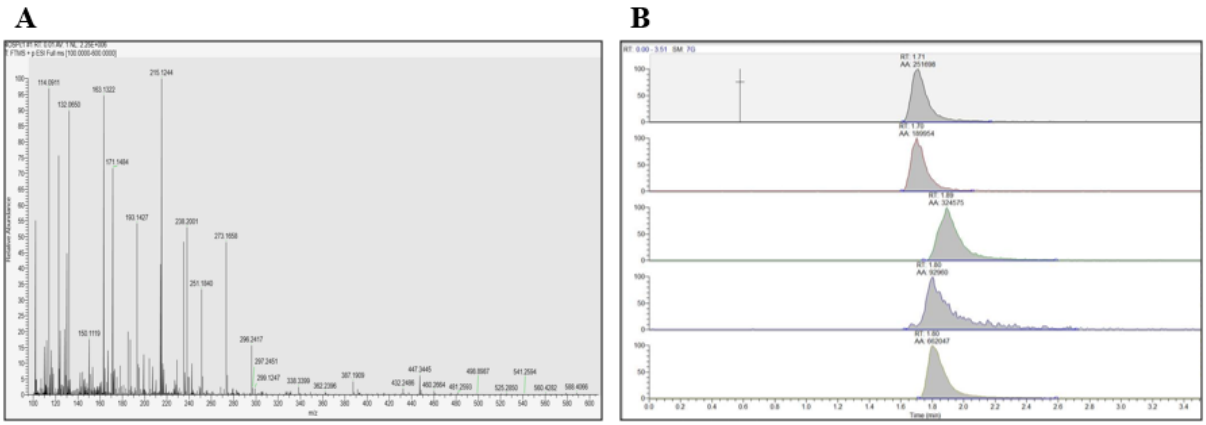

Figure 5.2 Example of (A) mass spectrum and (B) extracted chromatogram of crosslinks extracted from samples and separated on the Cogent Diamond Hydride HPLC column. The crosslink concentrations were calculated from the peak area of the extracted chromatogram.

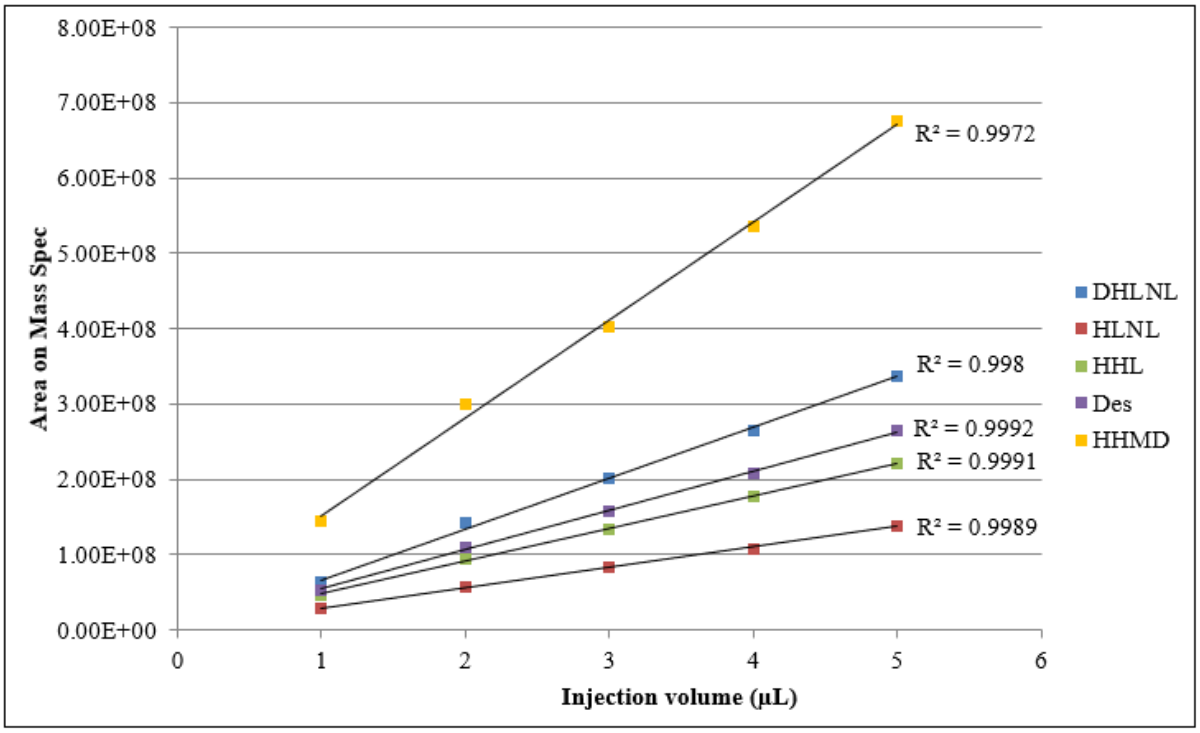

Figure 5.3 Standard curves of crosslink standards.

5.3 Results and Discussion

5.3.1 Collagen content in tight and loose hides

All amino acids were quantified as described in section 5.2.2, and the collagen content was estimated using the hydroxyproline concentration. Hydroxyproline is not found in any other protein except for small amounts in elastin and previous studies have shown that the hydroxyproline content of collagen from various mammals averages about 13.5 % (w/w) [160]. The calculation is:

Collagen % = weight of hydroxyproline/ dry weight of hide x (100/13.5) x 100

The concentration of collagen was compared between the OSP and distal axilla region, loose and tight samples and different layers of the hide. Figure 5.4A illustrates that although the OSP on average has a slightly higher collagen content (65.53 %) compared to the distal axilla (60.33 %), the difference is not significant (p-value 0.279). This supports a previous study by Wong *et al.* [169] which state that different areas of skin show different degrees of laxity despite having similar collagen contents. Figure 5.3B shows that loose hides typically contain a lower concentration of collagen than tight hides with a R^2 value of 0.7432. The p-value between tight (under 4) and loose (above 4) samples was significant at 0.003. These results are reflected in the images obtained using confocal microscopy which show there is greater space between the collagen fibres in loose samples, indicative of a lower collagen content. A decrease in collagen concentration has also been linked to ageing in humans [24, 28, 66], potentially contributing to wrinkly skin. It is possible that lower levels of collagen cause a change in the organisation of the collagen fibres and bundles which results in loose leather, although it must be noted that some studies dispute this.

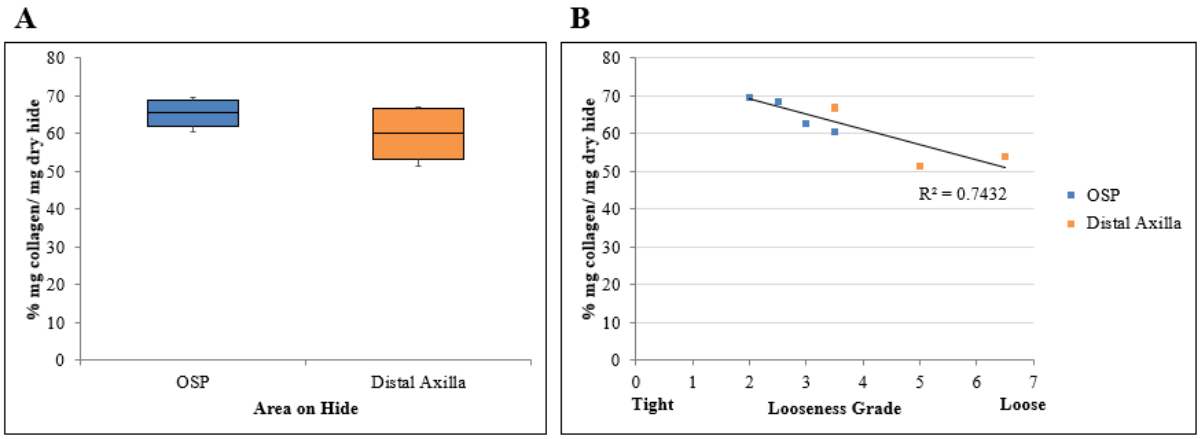

Figure 5.4 (A) Collagen concentrations of hides sampled from the OSP and distal axilla regions. Each box plot shows the results of four biological replicates, with three technical replicates each. (B) Relationship between collagen concentration and looseness grade. Each sample is the average of three technical replicates. The collagen concentrations were calculated on the basis of hydroxyproline concentration.

The collagen content of samples taken from the grain, grain to corium junction and corium layers of the hide were also measured individually as it is known that these layers have a different molecular composition, manifested in the structure of collagen fibres and their composition [5, 169]. The loosest and tightest samples from the OSP and distal axilla were selected for analysis. Figure 5.5 shows there is a greater concentration of collagen in the corium compared to either the grain to corium junction (p-value: 0.0031) or the grain layer (p-value: 0.0027), supporting previous studies which suggest that the grain is low in collagen [170]. This is likely due to the other structures present in the grain such as the arteries and veins [5, 7]. Figure 5.6 shows the correlation between each layer of the sample and its looseness grade. Interestingly, although the grain to corium junction and corium layer show that the samples taken from loose hides have a lower collagen concentration similar to that of the whole hide (R^2 of 0.5104 and 0.8402 respectively), samples taken from the grain layer do not show this trend. The grain appears to have an increase in collagen concentration, although the correlation is very weak (R^2 of 0.2864).

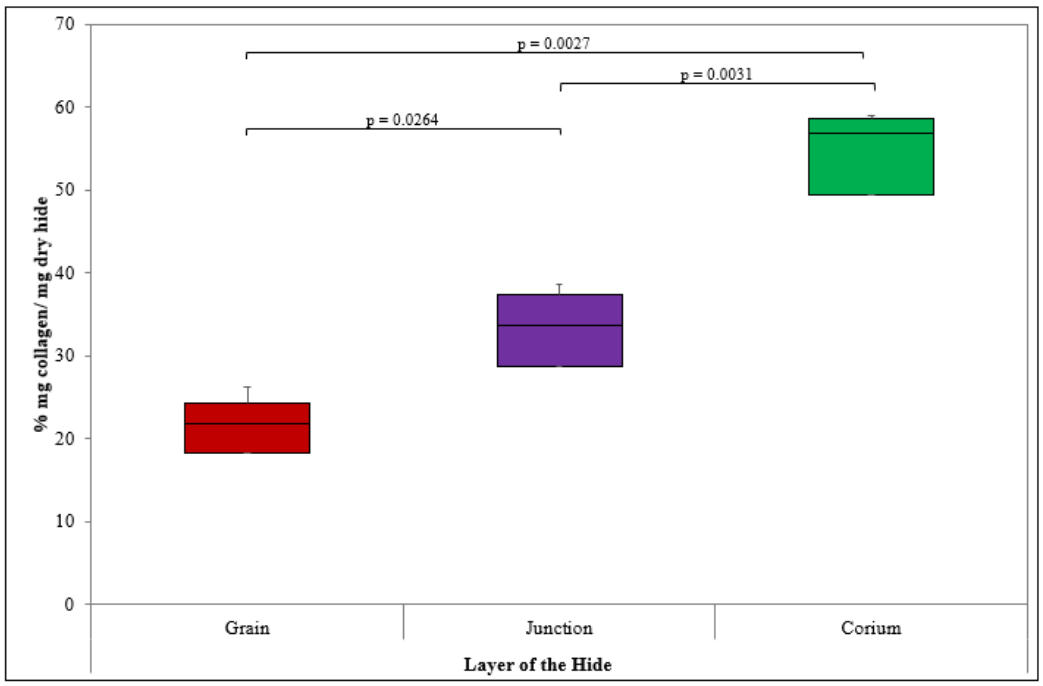

Figure 5.5 Box plots showing the collagen content of the three different layers of hide; grain, grain to corium junction and corium. Combined results of two biological replicates in two different areas. Each value is the average of three technical replicates.

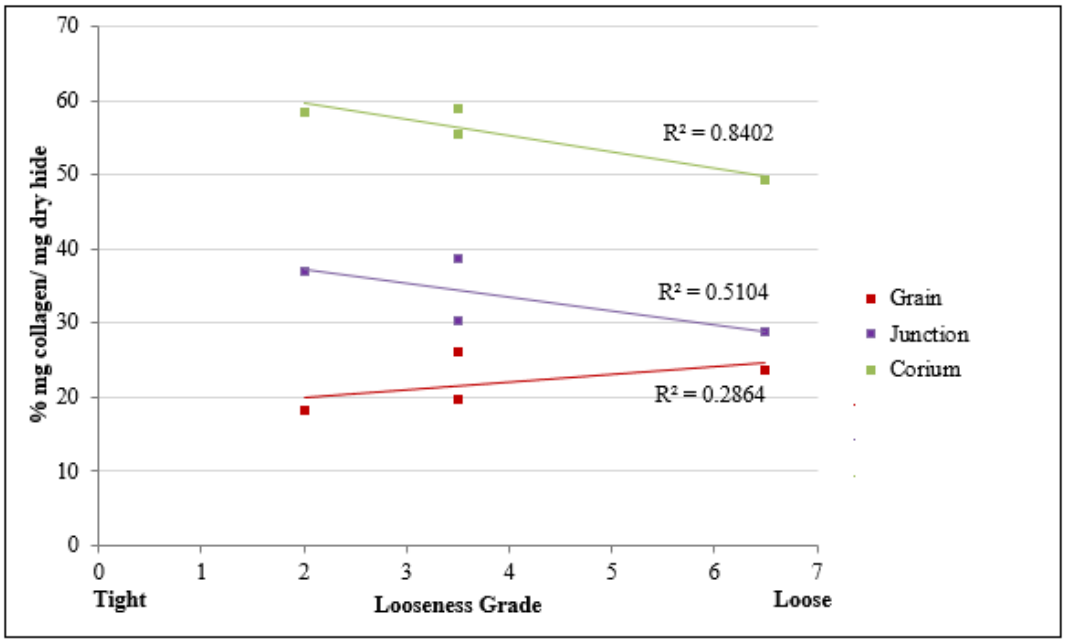

Figure 5.6 Relationship between collagen concentration (%mg/mg dry hide) in the three different layers of hide; grain, grain to corium junction and corium and looseness grade. Each sample is the average of three technical replicates.

A brief examination of the collagen concentration in samples taken from the OSP and distal axilla regions for each of the three layers show that the OSP has less collagen in the grain than

the distal axilla but more collagen in the grain to corium junction and corium layer. None of these differences are significant, however, with p-values of 0.053, 0.992 and 0.173 respectively.

These results suggest that collagen plays an important role in causing looseness in cattle hide. To further validate these results, particularly throughout the layers of the hide, and to examine in more detail the proteins that could contribute to looseness in-gel LCMS/MS was performed (chapter 6).

5.3.2 Hydroxylysine diastereomers in tight and loose hides

PTMs of lysine residues including hydroxylation and glycosylation are important in the formation of collagen crosslinks, which stabilise the molecule [52, 171]. Two diastereomers of hydroxylysine (HyLys) are reported to exist in collagen referred to as hydroxylysine (HyLys1) and allohydroxylysine (HyLys2) [172]. Differences in the concentrations of the HyLys diastereomers have been found in collagens extracted from different sources, different species, different tissue, within tissues and different collagen types [52, 165, 171, 173, 174].

Only trace amounts of HyLys1 were found present in all of the samples tested in this study. Varying concentrations of HyLys2, 0.63 – 1.24 % mg/ mg dry hide, were found in raw hide. However, no differences were detected between the OSP and distal axilla regions or between loose and tight hides.

Figure 5.7A shows the concentration of hydroxylation found in samples taken from the different layers of hide. The concentration of HyLys was higher in the corium layer of hide compared to the grain to corium junction (p-value: 1.20×10^{-3}) and grain layer (p-value: 1.57

x 10^{-5}). Figure 5.6B shows the relationship between concentration of HyLys and the looseness grade of the three different layers. Both the corium and grain to corium junction show a decrease in the concentration of HyLys in looser samples, with the relationship being more prominent in the junction (R^2: 0.8258) than the corium (R^2: 0.3121). No correlation was observed in the grain.

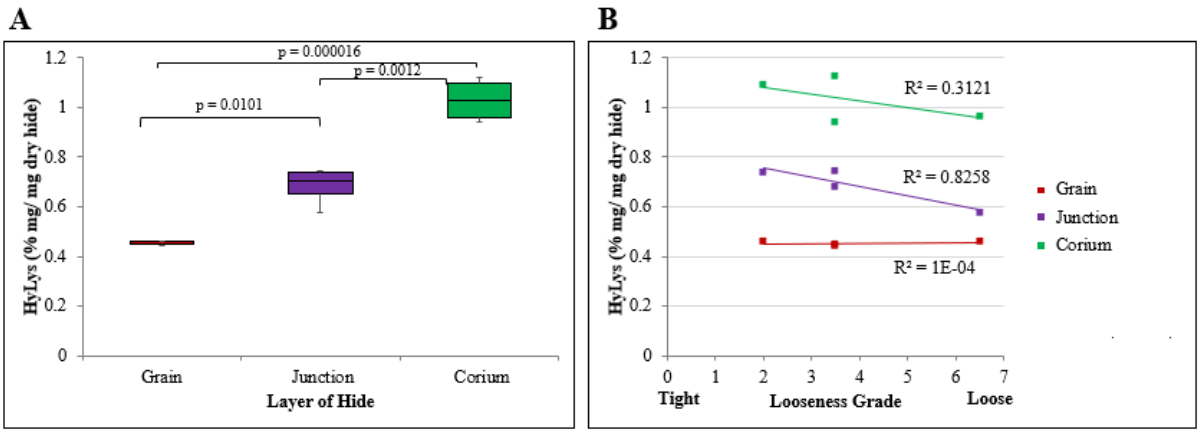

Figure 5.7 (A) Concentration of HyLys in the different layers of hide. Each box plot contains the results of two biological replicates in two different areas. Each value is the average of three technical replicates. (B) Relationship between concentrations of HyLys in the different layers of hide versus the looseness grade. Each sample is the average of three technical replicates.

This increase in hydroxylation in the corium is likely to be due to the increase in collagen content as noted in Figure 5.4. It could also be due to a decrease in crosslinking, as any HyLys involved in crosslinking will not show up in amino acid analysis. Changes to hydroxylation of lysine could also be due to changes in the composition of collagen as different types of collagen have been noted to have different hydroxylation concentrations, varying as much as 75 % [52] However, this increase was not observed across the whole hide, with the HyLys concentration remaining stable regardless of the concentration of collagen.

5.3.3 Amino acid content in tight and loose hides

Other than hydroxyproline (used to quantitate collagen, section 5.3.1) and HyLys 1 and 2 (section 5.3.2), 17 other amino acids, listed in Tables 5.4 and 5.5 were detected in hide samples. Due to the number of amino acids, challenges were faced when attempting to get good separation of all the peaks. Adjustments of buffer pH, gradient and column temperature were all tested, however in some instances complete separation was still unsuccessful; for example, in total hide the resolution between arginine and threonine was poor, thus the value calculated for these two residues was combined. Since this work was completed, a study detailing the optimum conditions for running amino acid analyses of skin and hide using AQC and RPHPLC resulting in shortened run times and complete resolution of all 19 amino acids has been reported [175]. The CV % of the concentrations measured for the technical replicates was typically below 5 % with few exceptions while that for the biological replicates was higher as expected, typically below 10 %. Only 10 % of the amino acids had a CV % above this value and these were always the low abundance amino acids such as HyLys or histidine.

In all whole-hide samples, the most abundant amino acids were glycine, proline, hydroxyproline, alanine, arginine+threonine and glutamic acid. As these amino acids are abundant in collagen the predominant protein found in hide, this is not surprising. The least abundant amino acids in the whole-hide samples were tyrosine, histidine, methionine, hydroxylysine and cysteine.

Table 5.4 Average concentration (% mg/ mg dry hide) of amino acids in lyophilized hide of different areas of hide (OSP and distal axilla) and tight and loose samples using AQC labelling and RP-HPLC as described in section 5.2.2. Area of hide data represents the mean of 4 biological replicates where the average of 3 technical replicates were measured for each biological replicate, whereas the looseness grade consists of 6 replicates for tight but only 2 for loose.

	Area of Hide				**Looseness**			
	OSP	*CV %*	*Distal Axilla*	*CV %*	*Tight*	*CV %*	*Loose*	*CV %*
Hyp	8.66	5.67	8.64	4.86	8.66	4.41	8.63	8.40
Asp	5.12	4.77	5.25	3.22	5.12	3.70	5.37	3.09
Ser	2.23	6.23	2.47	8.47	2.28	8.43	2.56	0.94
Glu	10.17	6.09	10.48	4.80	10.14	4.82	10.89	2.55
Gly	18.24	4.14	18.17	6.56	18.00	4.29	18.82	7.48
His	0.41	9.39	0.87	12.15	0.56	44.95	0.88	0.59
Arg & Thr	15.60	4.20	15.45	4.79	15.36	4.34	16.00	2.44
Ala	7.27	5.15	7.15	5.64	7.16	5.15	7.35	6.18
Pro	10.68	5.64	10.02	4.27	10.36	6.52	10.29	4.56
Cys	0.62	20.12	0.63	8.87	0.63	16.01	0.60	10.53
Tyr	0.87	4.98	0.98	7.76	0.89	4.52	1.04	2.20
HyLys1	traces	-	traces	-	traces	-	traces	-
Valine	1.90	3.16	2.00	5.02	1.91	2.84	2.08	1.56
HyLys2	0.98	27.66	1.09	2.77	1.03	21.60	1.07	1.07
Met	0.69	4.15	0.70	7.97	0.68	5.96	0.73	1.73
Lys	2.56	2.23	2.64	5.14	2.55	2.45	2.74	0.26
IIe	1.40	5.85	1.43	2.87	1.41	4.57	1.45	4.15
Leu	2.90	2.76	2.94	6.07	2.87	3.18	3.09	1.38
Phe	1.66	3.56	1.69	4.15	1.65	2.99	1.75	1.56

Table 5.4 displays the concentration (% amino acid (mg)/ mg dry hide) for all 19 amino acids for the OSP and distal axilla and between tight and loose samples. The only amino acid that showed a significant difference between the OSP and distal axilla was histidine, with a greater amount being found in the distal axilla (p-value: 1.7×10^{-4}). As histidine is involved in the formation of mature collagen crosslinks [59] this could be due to a decrease in the number of mature crosslinks in the distal axilla. Nine amino acids, serine, glutamic acid, histidine, tyrosine, valine, methionine, lysine, leucine and phenylalanine, have significantly different concentrations in tight and loose samples (p-values below 0.05). All of these amino acids were

more concentrated in samples from loose hides than those from tight hides. These results potentially indicate that loose hides have a different proteomic profile than tight hides. As this result could be a consequence of the low number of biological replicates in this study the protein profile of tight and loose hides was further investigated by in-gel LCMS/MS (chapter 6).

The amino acid profile of samples from the different layers of hide showed great variation. Table 5.5 displays the concentration of all 19 detected amino acids in the different layers of hide, irrespective of area or looseness. The corium contained more hydroxyproline, glycine, proline, alanine and hydroxylysine, than the grain to corium junction or the grain, all amino acids that are predominant in collagen. The grain, on the other hand, contained more histidine, arginine, tyrosine, valine, methionine, lysine, serine and isoleucine, indicative of a more varied cohort of proteins. The concentrations of the two acidic amino acids, aspartic acid and glutamic acid, were similar in the grain and corium but were slightly lower in the grain to corium junction. Whilst there were no significant differences in any of the amino acids in the grain or grain to corium junction between the OSP and distal axilla regions, 9 amino acids were found in significantly lower amounts in the distal axilla than in the corium. These amino acids included; aspartic acid, serine, glutamic acid, arginine, proline, valine, HyLys2, leucine and phenylalanine. These differences indicate potential differences in the proteomic profile of these two regions, especially in the corium layer. As the distal axilla is thought to be more prone to looseness than the OSP, it could potentially be indicative that the different layers of hide have different proteomic profiles in tight and loose hide, a fact that is explored in chapter 6.

Table 5.5 Average concentration (% mg/ mg dry hide) of amino acids in lyophilized hide of different layers of hide using AQC labelling and RP-HPLC as described in section 5.2.2. Each data point represents the mean of two biological replicates, in two different areas.

	Grain	CV %	Junction	CV %	Corium	CV %
Hyp	2.97	16.46	4.54	14.59	7.50	7.96
Asp	4.04	8.35	3.57	11.29	3.98	6.72
Ser	3.56	7.47	2.50	9.86	2.56	5.70
Glu	8.46	7.50	7.59	11.93	8.39	6.23
Gly	10.86	5.50	12.41	8.28	15.68	2.98
His	0.82	9.77	0.56	12.33	0.52	6.40
Arg	2.86	12.62	2.03	12.69	1.85	5.15
Thr	3.87	8.08	3.57	11.62	4.46	7.64
Ala	4.27	3.76	4.91	10.72	6.83	8.21
Pro	5.02	5.24	6.28	13.74	9.50	10.12
Tyr	1.58	14.66	0.92	15.80	0.59	4.45
Hyl1	traces	-	traces	-	traces	-
Valine	2.29	10.73	1.76	11.35	1.68	3.69
Hyl2	0.45	1.73	0.68	11.37	1.03	8.90
Met	0.65	8.60	0.56	13.21	0.57	3.88
IIe	1.68	11.05	1.23	12.34	1.13	3.31
Lys	3.67	12.28	2.74	14.39	2.39	2.96
Leu	2.76	8.29	2.46	11.85	2.57	4.86
Phe	1.67	10.04	1.35	11.32	1.38	4.06

5.3.4 Analysis of collagen crosslinks in tight and loose hides

Collagen crosslinks have been linked to age. Enzymatic crosslinks have been shown to change composition, with an increase in mature crosslinks such as HHL and HHMD and a decrease in immature crosslinks such as DHLNL and HLNL [53, 71]. Nonenzymatic crosslinks are thought to increase with age [54, 56]. These changes in crosslink concentration and composition have been linked to changes in the mechanical strength, flexibility and stability of the collagen molecule, skin defects and ageing [53, 54, 56, 71]. It is therefore possible that they may also affect leather quality.

Enzymatic crosslinks were investigated using a technique that isolates the crosslinks using a CF-11 column then separates and detects them using LCMS (as outlined in section 5.2.3). This

method only detects the enzymatic crosslinks found in hide; thus, it does not show the complete picture of collagen crosslinking. Figure 5.8A shows that no significant differences were found in the "total" collagen crosslink concentration between the OSP and distal axilla region (p-value: 0.402). Figure 5.8B illustrates a slight negative correlation between the looseness grade and concentration of collagen crosslinks, with looser samples having a decreased concentration of collagen crosslinks. This is likely due to the correlations found previously, where looser hides have lower amounts of collagen, and all less histidine, resulting in fewer collagen crosslinks.

The different types of collagen crosslinks were also investigated individually; DHLNL, HLNL, HHL and HHMD, in Figure 5.9. In all samples HHL was present in the greatest concentration compared to the other three crosslinks in contrast to previously reported results [57, 61, 168] that show that in bovine hide, HHMD has the higher concentration. The reason for this is unclear. The biological variation found in HHL and HLNL is also very high, particularly in the OSP region.

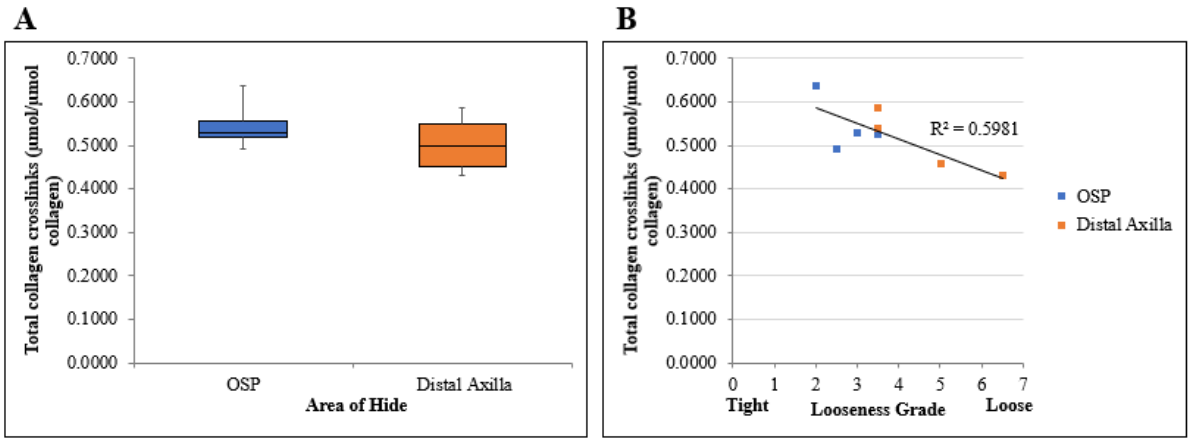

Figure 5.8 (A) Total concentration of collagen crosslinks sampled from the OSP and distal axilla areas of hide. Each box plot represents an average of four biological replicates, each with three technical replicates. (B) Relationship between looseness grade and total concentration of collagen crosslinks. Each data point is the average of three technical replicates. All values are normalised to the collagen content based on the hydroxyproline content of the hides.

Although these hides were collected at the same time, the age, sex or breed of the animal was not recorded by the abbatoir. As age is known to affect both crosslink concentration and composition [53, 71], differences in the age of the hides could account for the differences observed in these samples. If this was the case however, samples taken from the distal axilla of these hides should also be vastly different which is not the case. It is therefore likely that the differences observed are related to the structure of the skin and thus to looseness.

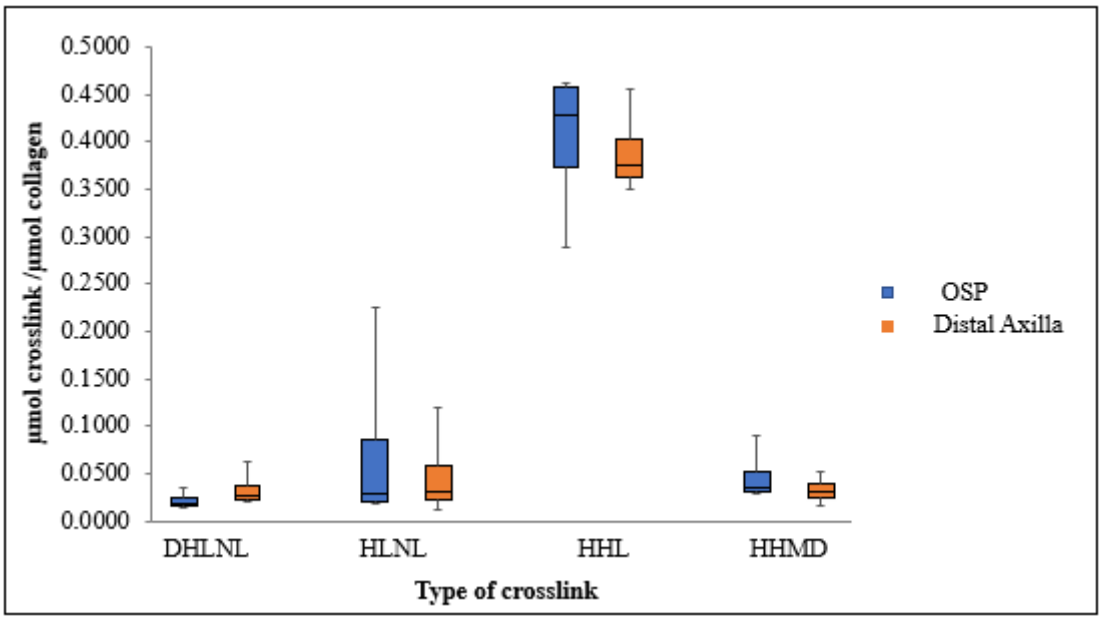

Figure 5.9 Collagen crosslinks in hide from the OSP and distal axilla regions. All values are normalised to the collagen content based on the hydroxyproline content of the hides. Each box plot represents an average of four biological replicates, each with three technical replicates.

No significant differences in the concentrations of individual crosslinks, were identified between samples taken from the OSP and distal axilla regions of hide and no significant correlation was discovered between looseness grade and the concentrations of individual crosslinks. The R^2 values were 0.0246, 0.2718, 0.0056 and 0.4228 for DHLNL, HLNL, HHL and HHMD respectively (figures not shown).

Different collagen crosslinks in loose and tight hides and even between the different areas of the same hide, showed no significant differences. Although there was a slight negative correlation between the total enzymatic crosslinks and looseness grade, it is more likely due to the concentration of collagen in the sample rather than changes in the crosslinking of the collagen molecule itself. This study shows, therefore, that enzymatically formed crosslinks are not an effector of looseness in leather. It is possible, however, that non-enzymatic cross links could play a role in causing looseness in leather. As this study only investigated the crosslinking pattern of the whole hide, it would be interesting to investigate whether there are any differences in the different layers of the hide which are known to contain different compositions of collagen, and which in turn may have different crosslinking patterns [54].

5.3.5 Analysis of elastin crosslinks in tight and loose hides

The elastin crosslinks in loose and tight hides were analysed using the same method as that to investigate collagen crosslinks. As the elastin crosslinks desmosine and isodesmosine have similar retention times and the peaks cannot be separated, the concentration calculated is the sum of both of these crosslinks. These crosslinks are typically used to determine the concentration of elastin in a sample as they are specific to elastin [59]. Figure 5.10A illustrates the differences in these crosslink concentrations in samples from the OSP and distal axilla regions. The sample from the distal axilla contained significantly more elastin (p-value 0.0147) suggesting that this whole region contains more elastin than other areas of the hide. This is most likely because it needs to be more flexible than the OSP as it moves a lot during the animal's life. Figure 5.10B shows the correlation between looseness grade and elastin crosslinks (R^2 0.671) with samples from tight hides containing fewer elastin crosslinks than samples from loose hides. This result could, however, be influenced by the significant difference seen in the concentrations of elastin crosslinks in the OSP and distal axilla. In order

to get a greater understanding of how the elastin concentration and elastin crosslinks affect looseness, more samples or more areas of the hide would need to be tested.

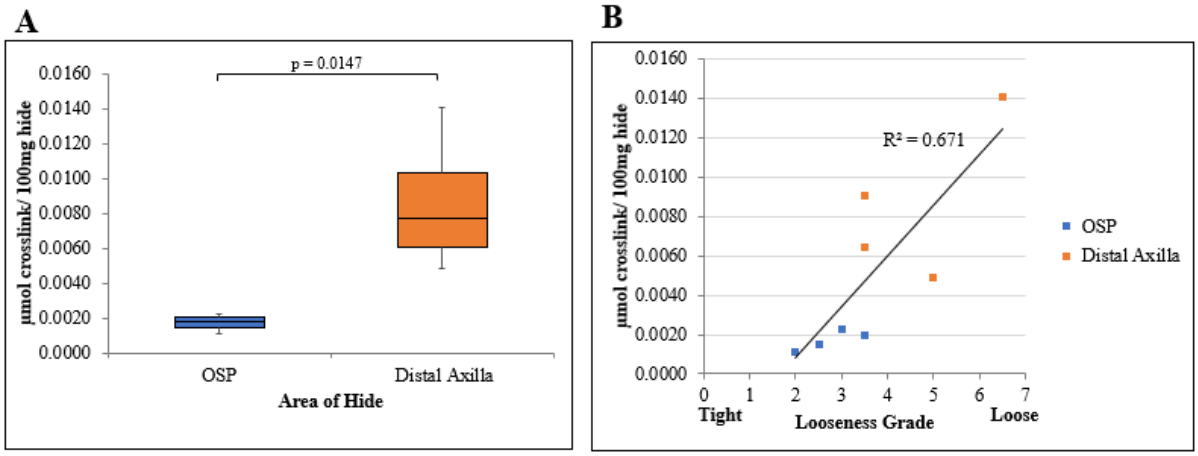

Figure 5.10 (A) Elastin crosslinks sampled from the OSP and distal axilla area of hide. Each box plot represents an average of four biological replicates, each with three technical replicates. (B) Relationship between looseness grade and elastin crosslinks. Each data point is the average of three technical replicates. All values are normalised to the collagen content based on the hydroxyproline content of the hides.

6. Proteomic analysis of loose and tight hides

6.1 Introduction

The diverse array of proteins found in skin and/or hide play roles in the multitude of functions that skin and/or hide perform, including scaffolding, elasticity and strength [3-5]. Collagen, elastin, proteoglycans and glycoproteins are the predominant proteins in leather, and have a significant and known impact on the quality of leather [7, 8]. However, a wide range of other proteins are present in low concentrations in skins and hides that have only been identified in recent years due to the growing capabilities of proteomic techniques more specifically MS, which has been used to show that a wide range of proteins are affected by skin diseases, ageing and stress [30, 31, 176, 177]. The techniques used during this study to analyse the proteins in loose and tight skins were shot-gun proteomics (gel LC-MS/MS) and western blotting.

Shot-gun proteomics enables the study of a wide range of proteins, some of which would not have previously been easily identified using prior techniques due to their low abundance. The large-scale study of proteins from the level of composition, structure and function helps to understand the link between the genomes, proteins and structure [178]. In recent years, technological developments in MS has largely improved the sensitivity, speed and affordability of proteomics [178]. This method allows identification and quantitation of proteins but also provides information about their isoforms, and PTMs including proteolytic cleavage [29]. However, even with the recent advances a full analysis is time consuming and requires specialised equipment. Western blotting on the other hand whilst comparatively quicker does not provide nearly as much data and is prone to false positives. It can identify only those proteins that have available antibodies and consequently requires prior knowledge of the proteins likely to be present in a sample. It is therefore a technique that is not so useful for

discovery, but is often used as validation of identifications made from a shot-gun proteomic study. In this study western blotting was used to investigate the presence of different types of collagen in hide, because of its structural role in leather.

6.2 Methods

6.2.1 Chemicals and equipment

The chemicals and equipment used in this section are listed in Tables 6.1 and 6.2 respectively.

Table 6.1 Chemicals utilised in chapter 6.

Supplier	Country	Chemical
Anchor	Auckland, NZ	Low fat milk powder
Abcam	Cambridge, UK	Antibodies (see Table 6.13)
Ajax Finechem	NSW, Australia	Glycerol Glycine NaCl Orthophosphoric acid, 85 %
Affymetrix Inc.	Ohio, USA	Sodium dodecyl sulfate (SDS)
BDH Lab supplies	Poole, UK	Ammonium sulphate
BDH Prolabo	Manchester, UK	Calcium chloride, dry
Bio-Rad	California, USA	3-[(3-cholamidopropyl) dimethylammonio]-1-propanesulfonate (CHAPS detergent) Coomassie blue G-250 Clarity ECL substrate Clarity max ECL Precision Plus Protein™ Dual standards
Emsure	Germany	Glacial acetic acid
Fisher Scientific	Belgium	Acetonitrile (Optima® LC/MS) H_2O (Optima® LC/MS) Formic acid, 98-100 % Methanol (Optima® LC/MS)
	Leicestershire, UK	Acetone HCl, 37 %
GE Healthcare life Sciences	Buckinghampshire, UK	Iodoacetamide PlusOne Thiourea
	Uppsala, Sweeden	PlusOne Urea
Gold biotechnology	St. Louis, USA	DL-Dithiothreitol (DTT)

Supplier	Country	Chemical
Merck	Germany	Acrylamide: Bis (29.1:0.9), 40 % Ethanol, 96 %
PanReac AppliChem	Germany	MS grade glacial acetic acid
Promega	Wisconsin, USA	Trypsin Gold, (MS grade)
Pure Science	Wellington, NZ	Methanol Tris
Roche Diagnostics GmbH	Mannehim, Germany	cOmplete® protease inhibitor tablets
Sigma-Aldrich	China	N, N, N'N'-tetramethylenediamine (TEMED)
	Steinheim, Germany	Trichloroacetic acid (TCA)
	St. Louis, USA	Ammonium Bicarbonate Ammonium persulfate (APS) Bromophenol Blue N-cyclhexyl-3-aminopropane sulfonic acid (CAPS) Glass Beads, acid washed Sodium phosphate Tween-20
Thermo Fisher (Milli-Q Ultra-pure)	Massacheusetts, USA	Milli-Q H_2O

Table 6.2 Equipment utilised in this section.

Supplier	Country	Equipment Name
Azure Biosystems, Inc.	California, USA	Azure c600
Bio-Rad	California, USA	PROTEAN II casting apparatus and electrophoresis chamber Mini trans-blot® cell
Elma, Ultrasonic	Germany	Elma, S 15 H, elmasonic (sonication bath)
Eppendorf	Hamburg, Germany	0.1 ml Lobind protein tubes
IKA Laboratory technology	Germany	VXR basic vibrax®
Leica Biosystems	Wetzlar, Germany	Leica CM 1850 UV cryostat
Sigma-Aldrich	St. Louis, USA	PDVF membrane

Supplier	Country	Equipment Name
Thermo Fisher	Masacheusetts, USA	DNA speed vac®, DNA 110, Savant Q Exactive Plus mass spectrometer and appropriate attachments including nano-LC system, ionization source, trapping cartridge and analytical column MS grade 2 mL glass vials with 400 µL vial inserts and ultraclean 9 mm caps

6.2.2 Preparing samples

Raw hide samples were shaved to remove the hair, then cut using the Leica CM 1850 UV cryostat to 10 µm thick sections and separated into grain, grain to corium junction and corium layers utilising the data obtained from the total hide thickness and the grain to corium ratio (Figure 2.8A).

6.2.3 Protein Extraction

After the samples (four different hides – OSP and distal axilla regions of varying looseness grades) were separated into the three different layers (section 6.2.1) the protein was extracted using two different methods.

One method involved incubating 100 mg hide in 1 mL of lysis buffer (Table 6.3) overnight at 4 °C. Glass beads (acid washed, approximately 50 mg) and gentle rotation were used to enhance the extraction. Pellets and beads were removed by centrifugation (16,500 x g for 30 minutes) and the supernatants were decanted into clean tubes. Each pellet was then treated with a second volume of lysis buffer while the supernatant was mixed with 25 % TCA in acetone at a ratio of 1:9 and incubated at -20 °C overnight, to precipitate the proteins. Precipitated protein was separated by centrifugation (5,000 x g for 20 minutes) and then washed with cold acetone three

times. The pellets from the sequential lysis extractions were combined and resuspended in a modified lysis buffer (Table 6.3) that did not contain Tris.

Table 6.3 Lysis Buffer.

Component	Concentration
Urea	7 M
Thiourea	2 M
DTT	40 mM
CHAPS detergent	4 %
Tris	30 mM
cOmplete® protease inhibitor tablet	1 x

In the second method, 100 mg hide was incubated in 1 mL of NaCl buffer (Table 6.4) overnight at 4 °C with glass beads (acid washed, approximately 50 mg) and gentle rotation. Pellets and beads were removed by centrifugation (16,500 x g for 30 minutes) and the supernatant was decanted into clean tubes. The pellet was then treated with urea buffer (Table 6.5) while the supernatant was mixed with 25 % TCA in acetone at a ratio of 1:9 and incubated at -20 °C overnight, to precipitate the proteins. The precipitated proteins were pelleted by centrifugation (5,000 x g for 20 minutes) and then washed three times with cold acetone. The precipitated protein was then re-suspended in a modified lysis buffer (Table 6.3) that did not contain Tris. The NaCl extracted and Urea extracted proteins were kept separate until MS analysis.

Table 6.4 NaCl Buffer.

Component	Concentration
NaCl	1 M
DTT	65 mM
Ammonium Bicarbonate	100 mM
cOmplete® protease inhibitor tablet	1 x

Table 6.5 Urea Buffer.

Component	Concentration
Urea	8 M
DTT	65 mM
Ammonium Bicarbonate	100 mM
cOmplete® protease inhibitor tablet	1 x

6.2.4 Bradford assay

The Bradford assay was used to determine the concentration of protein in each of the samples. Volumes of between 1 to 10 µL of sample diluted in 20 µL Milli-Q H_2O was then added to 200 µL of Bradford reagent (Table 6.6) in a microplate and gently mixed for 5 minutes before the absorbance was read using the PowerWave XS microplate spectrophotometer at 595 nm. Standard curves were created using bovine serum albumin (BSA) dissolved in either water (Figure 6.1A) or lysis buffer diluted 1:10 (Table 6.1, Figure 6.2B) at concentrations of 0, 0.1, 0.2, 0.4, 0.8 and 1 µg/mL.

Table 6.6 Bradford Reagent.

Component	Concentration
Coomassie Brilliant Blue G-250	0.12 mM
Methanol	5 %
Phosphoric acid	10 %

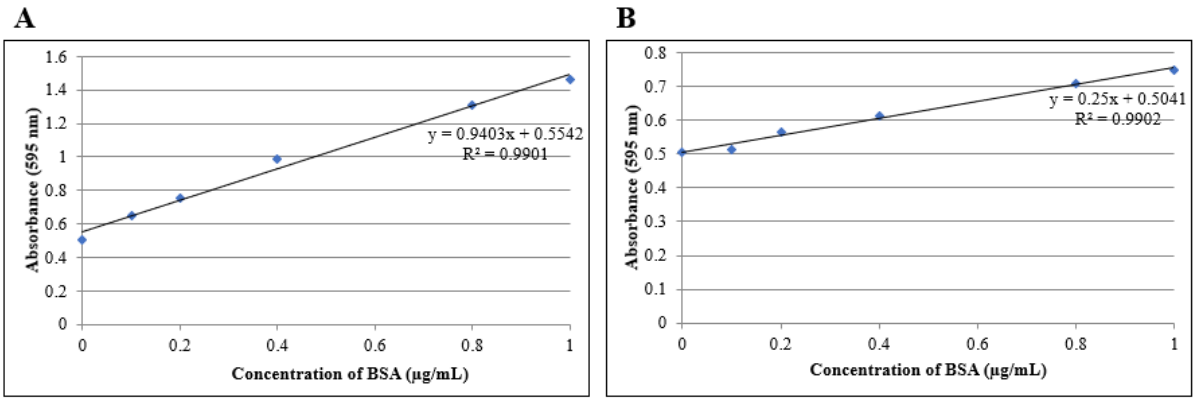

Figure 6.1 Standard curves for Bradford assays using (A) BSA dissolved on H_2O or (B) diluted lysis buffer

6.2.5 1D SDS PAGE gels

One dimensional sodium dodecyl sulphate polyacrylamide gel electrophoresis (1D SDS PAGE) separates proteins based on their molecular weight. Samples to be run on the mass spectrometer were separated on 12 % (v/v) polyacrylamide gels (Table 6.7) while samples being prepared for western blots were separated on 7.5 % (v/v) polyacrylamide gels (Table 6.7). Both 12% and 7.5 % separating gels had 4% stacking gels on top. Prior to addition of APS and TEMED, the gel solutions were degassed for 15 minutes using a water vacuum pump. The separating solution was then pipetted into a Bio-Rad PROTEAN casting apparatus, overlaid with Milli-Q H_2O and allowed to polymerise; Once the gel was set, the separation gel was overlaid with stacking gel solution to a depth of approximately 6 mm. After removing the well former, the gels were placed into a Bio-Rad mini PROTEAN III electrophoresis chamber containing SDS tank buffer (Table 6.8). The wells were loaded with 2 µL of 2 µg protein sample mixed with 1 x sample loading buffer (Table 6.9) alongside 2 µL of Precision Plus Protein^{TM} Dual Standards and 150 V applied across the electrodes for approximately 90 minutes at room temperature until the dye front was within 1 cm of the bottom of the gel. Gels were then removed and placed in fixing solution (40 % ethanol, 10 % acetic acid) for 15 minutes before being placed in colloidal Coomassie stain overnight (Table 6.10). The colloidal Coomassie stain was then removed and the gel de-stained with repeated washes with water until the background was clear. If storage was required 10 % acetic acid was added to the last water wash.

Table 6.7 1D SDS PAGE gel mixtures.

Component	Volume (mL)
Stacking gel (4 %, 10 mL)	
Milli-Q H_2O	6.1
0.5 M tris/HCl pH 6.8	2.5
SDS, 10 % (w/v)	0.2
Acrylamide: Bis 29.1:0.9, 40 % (v/v)	1.0
APS, 10 % (w/v)	0.2
TEMED	0.01
Separating gel (7.5 %, 20 mL)	
Milli-Q H_2O	10.8
1.5 M tris/HCl pH 8.8	5.0
SDS, 10 % (w/v)	0.2
Acrylamide: Bis 29.1:0.9, 40 % (v/v)	3.8
APS, 10 % (w/v)	0.2
TEMED	0.01
Separating gel (12 %, 20 mL)	
Milli-Q H_2O	8.7
1.5 M tris/HCl pH 8.8	5.0
SDS, 10 % (w/v)	0.2
Acrylamide: Bis 29.1:0.9, 40 % (v/v)	6.0
APS, 10 % (w/v)	0.2
TEMED	0.01

Table 6.8 SDS Tank Buffer.

Component	Concentration (g L^{-1})
Glycine	14.4
Tris	3.0
SDS	1.0

Table 6.9 Sample Loading Buffer.

Component	Concentration
SDS	10 %, (w/v)
Glycerol	50 %, (vv/v)
DTT	100 mM
Tris-HCl	0.25 M
Bromophenol blue	0.05 %, (w/v)
pH 6.8	

Table 6.10 Colloidal Coomassie Stain.

Component (stock solution)	Concentration
Ammonium sulphate	10 %
Phosphoric acid	1 %
Coomassie blue G-250 stock	0.1 %
Component (working solution)	**Concentration**
Stock solution	80 %
Methanol	20 %

6.2.6 In-gel tryptic digestion and LC-MS/MS

Each lane of the 12 % gel was cut into 6 or 13 pieces with a clean scalpel blade as shown in Figure 6.2 and transferred into a new 0.1mL Lobind protein tube for trypsin digestion. Trypsin is a serine protease that specifically cleaves the carboxylic site of lysine and arginine residues producing tryptic peptides that contain a C-terminal lysine or arginine residue and are therefore doubly charged. All chemicals and H_2O used in this section were MS grade.

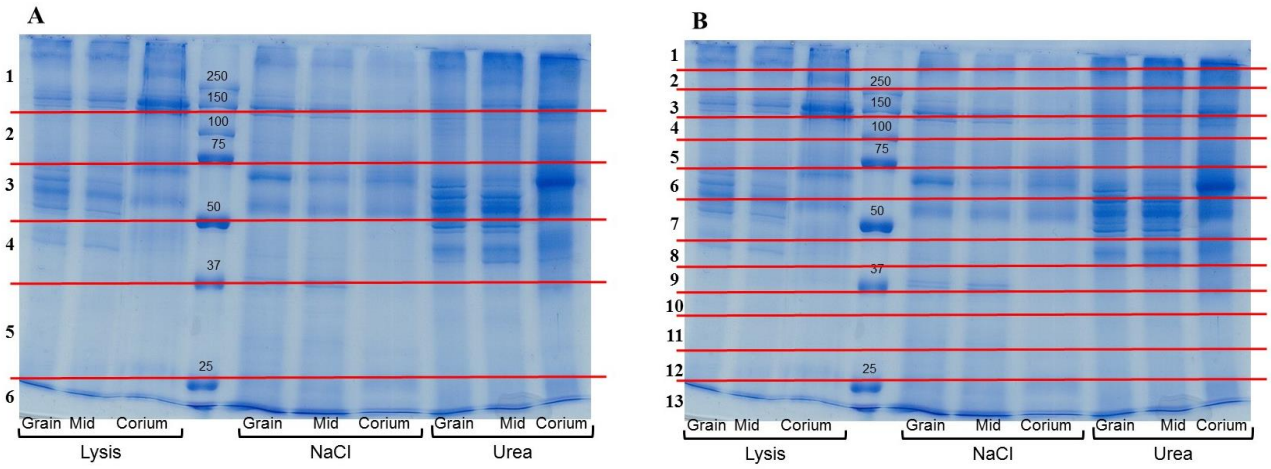

Figure 6.2 Diagram of a 1D SDS PAGE gel illustrating how it is cut in preparation for in gel tryptic digestion and mass spectrometry. (A) Technical replicates 1 and 2 and (B) technical replicate 3. Mid represents grain to corium junction.

The excised bands were further cut up into small pieces and de-stained using a 50 % methanol and 5 % acetic acid solution until no colour was obvious. They were then dehydrated in 200

µL acetonitrile with sonication for 5 minutes. The acetonitrile was then carefully removed and the gel pieces air dried before being reduced in 50 µL of 10 mM DTT in 100 mM ammonium bicarbonate solution for 1 hour at room temperature. After the solution was removed, the gel pieces were alkylated in 50 µL of 55 mM iodoacetamide dissolved in 100 mM ammonium bicarbonate for 1 hour at room temperature in the dark. The solution was again decanted and the gel pieces dehydrated in 200 µL acetonitrile for 5 minutes with sonication. After removal of the solution, the gel pieces were rehydrated in 200 µL of digest buffer with sonication for 5 minutes.

Table 6.11 Digest Solution.

Component	Concentration
Ammonium bicarbonate	50 mM
Calcium chloride	1 mM
Acetonitrile	10 %

Again, the solution was removed and 200 µL of acetonitrile was added to dehydrate the gel pieces with sonication for 5 minutes. The acetonitrile was then discarded and the gel pieces thoroughly air dried. They were then rehydrated in 50 µL of digest solution (Table 6.11) to which 6 µL of trypsin gold (100 µg/mL) was added before the tubes were placed on ice for 10 minutes with occasional vortexing before being incubated at 37 °C overnight. The supernatant was then removed into a clean Lobind Eppendorf tube and 40 µL of 50 % acetonitrile containing 5 % formic acid was added to the gel pieces which were then sonicated for 3 minutes. The supernatant was then carefully removed from the gel pieces and added to the first supernatant. The volume of the combined extracts was then reduced to approximately 20 µL by vacuum centrifugation then transferred to a clean MS glass sample vial.

The digested samples were separated by on-line reversed-phase chromatography for each run using a Dionex nanoLC system with a reversed-phase peptide trap and a reversed-phase analytical column. The liquid chromatography system was coupled to a Q Exactive Plus mass spectrometer equipped with a higher-energy collision-induced dissociation (HCD) collision cell, an Orbitrap mass analyser and a Nano Flex ion source. Details for the chromatographic and mass spectrometric settings are listed in Appendix 9.C.

Data-dependent tandem MS acquisition was used and all analyses were performed at least in duplicate. In all experiments, Full MS1 scans were acquired over a mass range of 375-1,500 *m/z* with a resolution setting of 70,000, while fragment ion spectra produced *via* higher-energy C-trap dissociation (HCD) were acquired with a resolution setting of 17,500. For data-dependent acquisition of HCD spectra, the top ten most intense ions were selected for fragmentation in each scan cycle and full MS as well as fragment ion spectra were detected by the Orbitrap mass analyser. Exclusion conditions were optimised according to the observed peak width (typically 10s).

6.2.7 Database Search

The raw data files were searched using Proteome Discoverer™ v. 2.2. The search parameters applied in the database searches are listed in Appendix 9.D. The reverse database search option was enabled by default, and all data were filtered to satisfy a false discovery rate (FDR) of 1% or better. Due to potential inconsistent loading onto the 1D SDS- PAGE gels, a manual normalisation step was added after the data was searched as shown in Appendix 9.E.

6.2.8 Dot blots

Prior to western blotting the antibodies to collagen I, III and V were tested for responsiveness to the respective collagen standards using dot blots. 2 µL of a 1 mg/mL collagen solution was applied to a PDVF membrane which was then placed in blocking solution (BS) containing 2.5 % low fat milk powder dissolved in 1 x phosphate buffered saline (PBS) (Table 6.12) for 1 hour at room temperature with gentle rotation on a vibrax® shaker. After this time, the solution was discarded and the membrane washed in 1 x PBS 3 times for 5 minutes each wash. The primary antibody was then added using the concentrations shown in Table 6.13, and the blot incubated for 1 hour at room temperature with gentle rotation. This solution was then removed and the membrane washed in PBS 3 times for 5 minutes each. The secondary antibody was then added using the concentrations shown in table 6.9 and incubated for 1 hour at room temperature. After removal of the solution the membrane was washed in 1 x PBS 3 times for 10 minutes each wash. The protein was detected using chemiluminescence. The membrane was submersed in a solution made up from Clarity™ ECL and Clarity™ max ECL substrates mixed in a 1:1 ratio, for 5 minutes then imaged using the Azure c600.

Table 6.12 1 x PBS.

Component	Concentration
Sodium phosphate	10 mM
NaCl	9 g/L
Tween 20	0.05 %

Table 6.13 Antibody concentrations.

Antibody	Concentration in BS
Collagen I	1:5000
Collagen III	1:5000
Collagen V	1:5000
Secondary Antibody (Goat Anti-Rabbit IgG H&L (HRP)	1:10,000

6.2.9 Western Blotting

Protein samples prepared as described in sections 6.2.3 and 6.4.4 were analysed on a 7.5 % SDS PAGE gel as described in section 6.2.5. After the samples were run, the gel was placed immediately in transfer buffer (Table 6.14) instead of fixing solution. The proteins were then transferred onto the membrane. First the PDVF membrane was wetted in methanol for 15 seconds, before being placed in Milli-Q H_2O for 2 minutes then in transfer buffer for at least 5 minutes. The Bio-Rad Mini Trans-Blot® Cell, sponges and filter paper was also equilibrated in the transfer buffer for 10-30 minutes. A sandwich was then made with the cassette; a sponge was laid on either side of the cassette with the filter paper on top of the sponge. The membrane was placed on the cathode side of the cassette whilst the gel was placed on the anode side of the cassette. The apparatus was then subjected to 60 V for 1 hour at 4 °C. Efficient transfer of proteins to the blot was confirmed by staining the gel with colloidal Coomassie to check for residual bands. The samples were then probed with the antibodies using the same method as that in the dot blot (section 6.2.8).

Table 6.14 Transfer buffer.

Tris-Glycine		**CAPS**	
Component	**Concentration**	**Component**	**Concentration**
Tris	25 mM	CAPS	10 mM
Glycine	190 mM	Methanol*	10 %
Methanol*	20 %		
SDS*	0.01 %		
pH 8.3		pH 11	

* Used a variety of concentrations, more details in section 6.3.6.

6.3 Results and Discussion

6.3.1 MS methodology

Extraction method

A wide range of methods have been reported for protein extraction from different tissues, and skin is no exception [179-182]. Obtaining total protein from skin/ hide is difficult due to its structure and limited solubility, and it is common to use a combination of mechanical and chemical methods [180]. This experiment used glass beads and rotation to provide mechanical action followed by sequential extraction with two different buffer systems for optimal protein extraction. The two buffer systems were compared to see which was more effective.

The first method used a traditional lysis buffer recipe (Table 6.3) which contains urea/thiourea to denature the proteins, a reducing agent (DTT) to reduce disulfide bonds, the detergent CHAPs for solubilisation of poorly soluble proteins, and a protease inhibitor (cOmplete) to control undesirable proteolysis in a Tris buffer system, pH 7-9. The second method used a high salt (NaCl) buffer followed by a buffer containing a high concentration of urea. The NaCl buffer (1 M, Table 6.4) was used to maintain the ionic strength; it is also routinely used for extracting collagen a primary component of hide, and contained a reducing agent and a protease inhibitor in ammonium bicarbonate buffer (pH 8). The Urea buffer (Table 6.5) contained urea (8 M), a reducing agent (DTT) and protease inhibitor (cOmplete) in an ammonium bicarbonate buffer. The NaCl and Urea extractions were kept separate until analysis by MS. It should be noted that both these extraction methods are likely to extract only the soluble collagens and the amount of insoluble collagen and other matrix proteins remaining in the hide after these extractions is unknown. Nevertheless, the two different extraction methods showed different protein profiles both on the SDS-PAGE gel (Figure 6.3) and during the MS analysis (section 6.3.2).

SDS-PAGE Gel

After protein extraction the protein was re-solubilised and run on an SDS-PAGE gels (section 6.2.4 and 6.2.5). Several issues arose during this step that could impact the validity of the results. Firstly, re-solubilising the proteins after extraction proved difficult. Different techniques including the buffer used, heating and sonication were considered and/or tried, but most proved ineffective. This could lead to inconsistent and/or inaccurate results as the buffers used can affect the MS results [180]. Bradford assays were used to determine the concentration of the samples even although this method is known to be unreliable with collagen, a major component of the samples [183, 184] because other methods considered to more accurately measure collagen reacted unfavourably with the solubilisation buffer.

The SDS-PAGE gel (Figure 6.3) images show different protein profiles for the different extractions, layers of the hide and loose and tight samples. Different protein profiles were observed for the different extractions. The most noticeably different was the NaCl extraction, which contained many light bands throughout the gel that the others did not. The lysis and urea extraction protein profiles were similar although there were differences between the different layers. All three layers showed a similar band pattern at high molecular weight (over 150 kDa) that mimicked that of collagen. The grain and grain to corium junction samples, however, contained other bands indicating that they contained more non-collagenous proteins. While the gel images from tight, OSP (A) and loose, distal axilla (B) had fairly similar protein profiles there were some differences in the intensities and band patterns particularly between 75 and 37 kDa.

A

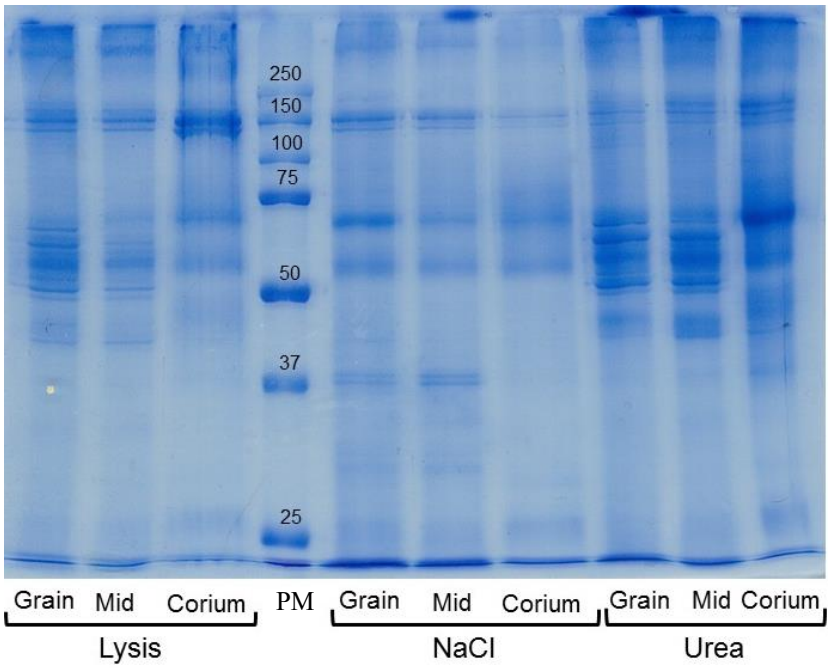

B

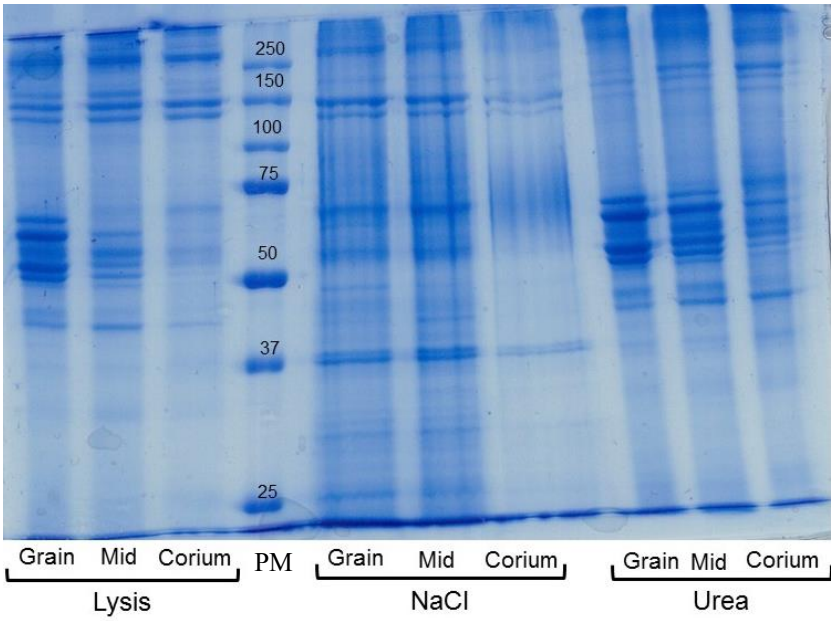

Figure 6.3 Examples of 12 % 1D SDS-PAGE gels (A) OSP and (B) distal axilla. Each lane contained approximately 2 µg/mL of protein. Mid refers to grain to corium junction. PM stands for protein marker, units kDa.

In-gel Digestion method

Sample preparation for MS can be carried out in two different ways: in gel or in solution. Both of these techniques have advantages and disadvantages. For example, the in-gel method

removes contaminants during electrophoresis and fractionates the sample, reducing the complexity of the sample which is also cleaner resulting in better spectra. However, its effectiveness can be limited by poor accessibility of the protease to the gel imbedded proteins and/or inefficient release of the peptides from the gel matrix as well as the poor migration of hydrophobic proteins on polyacrylamide gels [179]. It is also very time consuming [179, 185].

In-solution sample preparation introduces sample losses due to low re-solubilisation of aggregated proteins often resulting in a lower number of 'hits' [179, 185]. A compromise between protein solubilisation and protease activity contributes to less efficient proteolysis resulting in a smaller number of peptides. A major advantage is, however, the reduced time taken for sample preparation. This experiment used SDS PAGE separation of proteins followed by in-gel digestion and peptide extraction as the protocols for this method had previously been developed in house and had been shown to be effective at identifying a wide range of skin and/or hide proteins.

For each sample 3 technical replicates were prepared. The first batch of samples were cut into 13 pieces (T3) however the second two batches were only cut into 6 (T1 and T2), to save time and resources (Figure 6.2A and B). Protein ID's were obtained for each of the three technical replicates before more stringent parameters were set to determine how similar the replicates were. For each protein to be considered as significant, it had to be identified in 60 % of the samples. The differences in the technical replicates for the OSP samples extracted with lysis buffer are outlined below. 689 proteins were identified in all technical replicates. There was, however, a significant difference in the number of proteins identified between replicates. T1 and T2 had 764 and 733 protein IDs respectively whilst T3 had 888 protein IDs. This suggests that the size of the bands affected the MS analysis. Sample preparation and different chemical

reagents have been shown to affect the sensitivity of trypsin digestion [186, 187]. Thus, the reduced size of the bands in T3 (Figure 6.2B) may result in more efficient digestion, however more work would need to be done to support this conclusion.

MS analysis

After the samples were run through the MS (parameters listed in Appendix 9.C), the samples were analysed with Proteome Discoverer 2.2, using search parameters detailed in Appendix 9.D. The thousands of proteins initially identified were further filtered to obtain a more accurate list of IDs that were common to all samples, had a high confidence and had at least 2 unique peptides. Data for these samples were then further normalised to ensure the best representation of the results (details outlined in Appendix 9.E). T-tests were used to indicate significantly different responses between tight and loose and OSP and distal axilla samples.

6.3.2 Protein Identification: comparing lysis to NaCl/Urea extraction

The SDS-PAGE results from the two different extraction methods, lysis and NaCl/Urea, showed differences in the protein band pattern that was confirmed by the MS results. Figure 6.4 illustrates the differences in the number of proteins identified from the two methods. While 296 proteins were common to both extraction methods, 92 were unique to the lysis extraction and 335 were unique to the NaCl/Urea extraction. Although the NaCl/Urea extraction yielded a far greater number of protein IDs the fact that proteins were identified exclusively with the lysis extraction suggests that to get the greatest coverage, the two extractions are necessary.

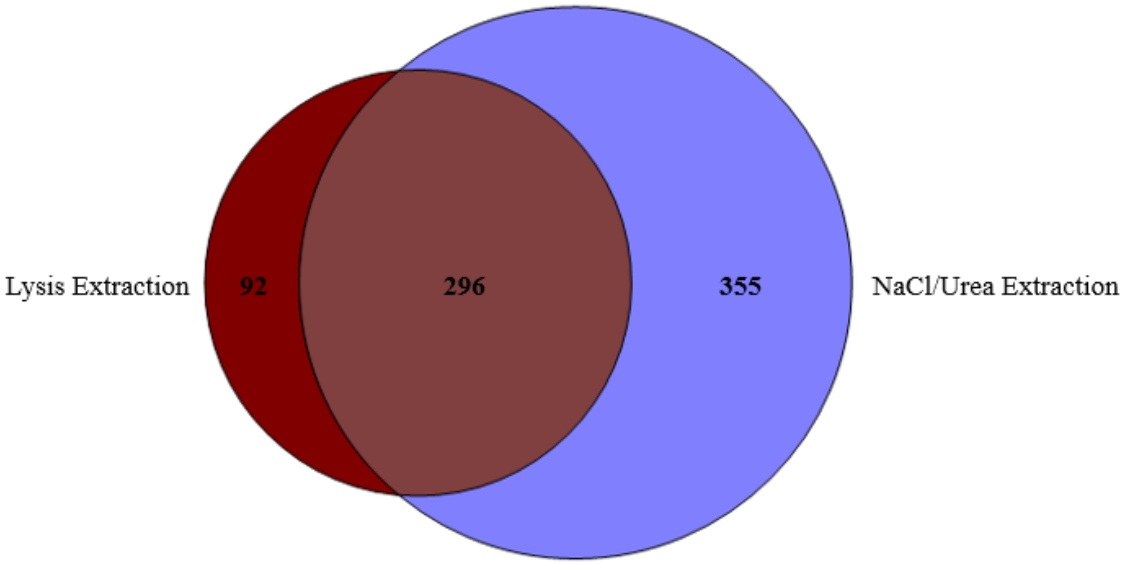

Figure 6.4 Differences in the number of proteins identified using two different extraction methods: lysis and NaCl/Urea.

The 50 most abundant proteins that were identified in the different layers of hide by the lysis and NaCl/Urea extraction, across all samples are listed in Appendix 9.F. They were organised according to protein type: collagen, other extracellular proteins, cellular proteins, serum proteins, uncharacterised proteins and keratins. This list appears very similar to the most abundant proteins found in human skin as reported by Mikesh *et al.* [188]. Although the majority of the most abundant proteins were commonly found in both extractions, there were noticeable differences especially in the collagens and other extracellular proteins. Proteins extracted using lysis buffer contained collagens type I, V, VI, VII and XII collagens, while those extracted with NaCl/Urea contained only collagens type I and VI. Proteoglycans that were found in high abundance in both extractions included asporin, fibromodulin and lumican. While asporin is closely related to the SLRPs decorin and biglycan, it is not a traditional proteoglycan due to it having a unique stretch of aspartic residues in its amino-terminal region, however during this study it will be categorized as a proteoglycan [189]. Decorin and mimecan were amongst the proteins found in high abundance in the lysis samples. Interestingly, Tenascin-X, a protein that regulates the structure and stability of elastic fibres and organises

collagen fibrils [190] was also found in the high abundance list, although, only in the corium samples extracted with NaCl/Urea. These results suggest that different buffers affect both the type and yield of proteins that are extracted, with some buffers being more effective at extracting different proteins than others.

This is further supported by the percentages of collagenous and non-collagenous proteins found using the two different extraction methods with collagenous proteins accounting for approximately 5 % of all proteins found in the lysis extract (~95 % non-collagenous proteins) compared to 2.7 % in the NaCl/urea extract (~ 97.3 % non-collagenous proteins). Prior to this it was expected that the NaCl/urea buffer would extract more collagen due to the presence of NaCl, which is a well-known agent for collagen extraction. Several differences in the components of the buffers may account for this. The lysis buffer pairs urea with thiourea, which aids in solubilising otherwise insoluble proteins [191]. Collagens, particularly fibrous collagen are known to be insoluble [192]. The lysis buffer also contains CHAPS which is a versatile zwitterionic detergent that aids in the solubilisation of proteins, particularly membrane proteins [193]. Typically, collagen extraction *via* NaCl is done at a low pH. It is possible that the higher pH of the ammonium bicarbonate buffer could reduce the effectiveness of the NaCl [192, 194]. Due to the differences in the types and abundance of the proteins extracted using the two different methods, both were used to extract proteins from the tight and loose samples providing very different results. Regardless of extraction method the percentage of collagen recovered in this study was very low compared to the value stated in the literature, 30 % wet weight, this is potentially due to insoluble collagen.

6.3.3 Protein Identification and quantitation of tight *vs* loose samples

The proteins identified in all samples were then analysed to identify any significant differences in protein concentrations between tight (under 4) or loose (over 4) hide samples. Four hides were investigated with both the OSP region and distal axilla region being sampled. 6 samples had looseness grades under 4 and 2 had looseness grades over 4. For all of these samples 3 technical replicates were tested.

Initially the ratio between non-collagenous proteins and collagenous proteins were investigated (Figure 6.5). Figure 6.5A shows that for the lysis extraction for all three layers, there is a greater ratio of non-collagenous proteins to collagenous proteins in loose samples compared to tight due to the reduced abundance of collagenous proteins and increased abundance of non-collagenous proteins. Figure 6.5B shows that only in the grain to corium junction and corium layer is there an increase in the ratio between non-collagenous protein and collagen in looser samples, for the NaCl/urea extract. There was no relationship between this ratio and looseness grade in the grain layer. All three layers of samples from loose hides had increases in the number of both collagenous and non-collagenous proteins identified, although these differences were only significant for the grain to corium junction and corium layer (p-values >0.05). The decrease in collagen in the grain to corium junction and corium layer in the lysis extract, supports the results obtained from the amino acid analysis while the increase in the NaCl/urea extraction does not. A possible reason for this difference is the extraction method. Prior to the amino acid analysis, the hides were hydrolysed, breaking down all of the collagen (both soluble and insoluble), visually observed by lack of cellular residues in the hydrolysate. Protein extraction for proteomics only encompasses the soluble proteins, and as stated in section 6.3.2, the lysis buffer appears to be more effective at extracting collagen than the NaCl/urea buffer which is more efficient at extracting non-collagenous proteins. However, it

is intuitive that samples from loose hides may be more amenable to extraction agents simply because of an increased ease of penetration of the various solubilisation agents in the lysis buffer compared to samples from tight skins.

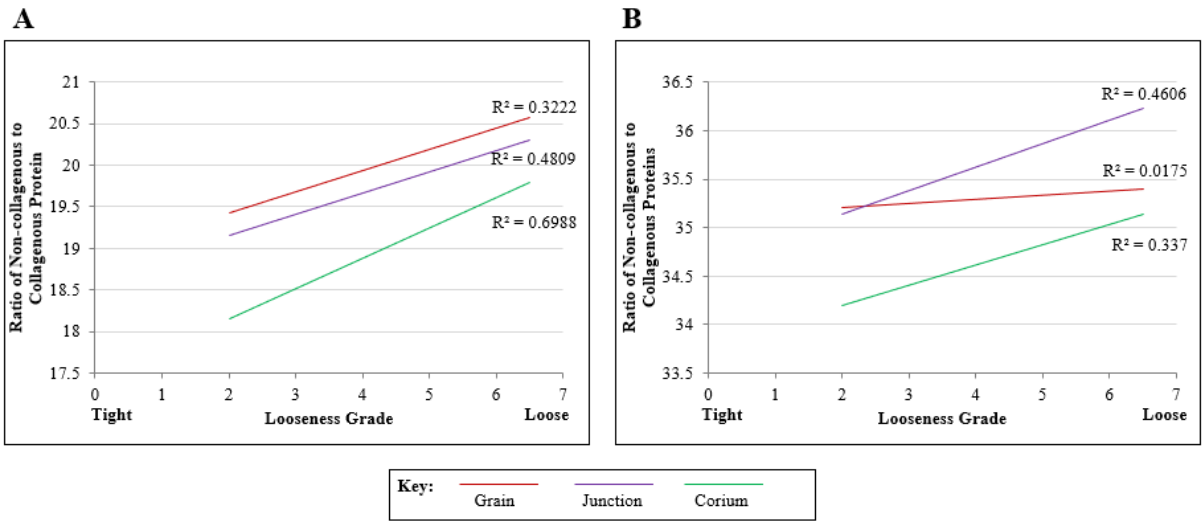

Figure 6.5 Relationship between ratio of non-collagenous to collagenous proteins and looseness grade in the (A) lysis extraction and (B) NaCl/Urea extraction. 6 replicates for tight and 2 for loose, average of three technical replicates.

The ratio of type III to type I collagens and fibrous to non-fibrous collagens were also investigated as previous studies have shown the type III to type I ratio increases with age [68], potentially contributing to wrinkle formation. In this study, however, no differences were found, suggesting that it does not have a similar role in contributing to loose leather. The ratio of fibrous to non-fibrous collagens was investigated as fibrous collagens form the main structural network of hide [33, 34]. Samples taken from loose hides and extracted using lysis buffer showed a decreased ratio of fibrous collagens to non-fibrous collagens (Figure 6.6), in all three layers of hide (R^2: 0.3963 grain, 0.7998 grain to corium junction and 0.5561 corium). Whilst the amount of non-fibrous collagen in all samples remained constant, a decrease in the amount of fibrous collagen in all loose samples was observed contributing to this decrease in ratio, although this was only significant in the corium layer (p-value: 0.003).

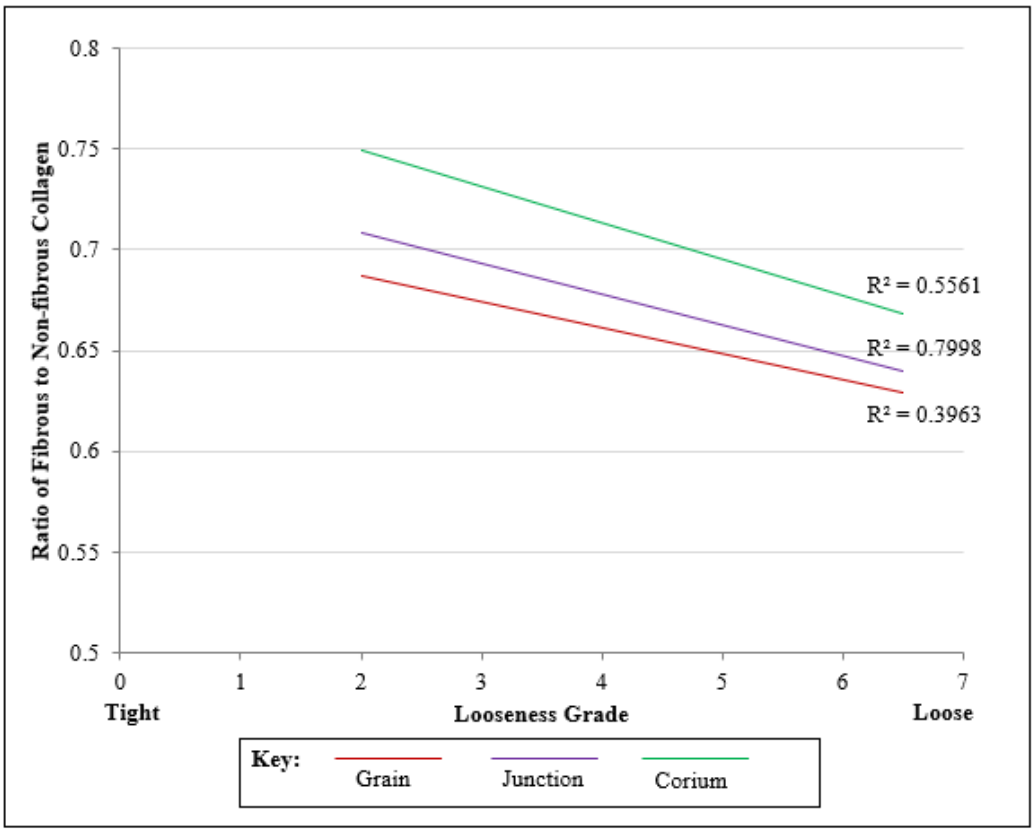

Figure 6.6 Relationship between the ratio of fibrous and non-fibrous collagens and looseness grade in the lysis extract found in all three layers of hide; grain, grain to corium ratio and corium. Each contain 6 replicates for tight and 2 for loose.

Individual proteins were then analysed to determine whether there were any significant differences between loose and tight samples. Although the small sample size potentially affects the validity of the results, a large number of proteins appeared to be significantly up or down regulated (p-values < 0.05). Figure 6.7 shows the volcano plots that were created using the proteomic data in the grain (1), grain to corium junction (2) and corium (3) layer of hide. The plots for all three layers of hide were similar, although the number of proteins is substantially greater in the NaCl/Urea extraction (B) compared to the lysis extraction (A). A far greater number of proteins were up-regulated in loose samples (meaning that they were present in the sample in greater concentration) than down-regulated. The proteins that were up and down regulated were then further investigated to see whether they could be contributing to the phenomenon of looseness.

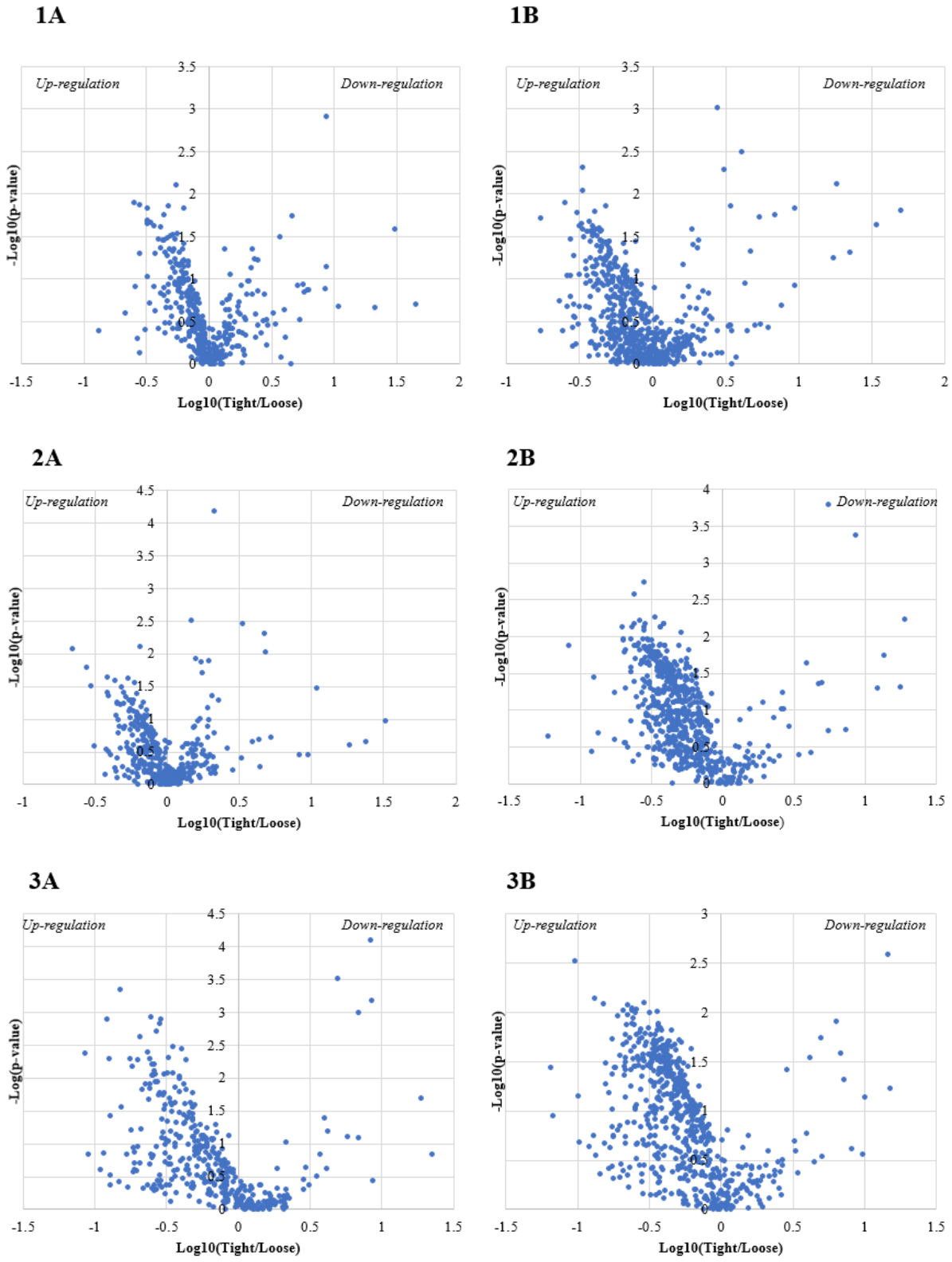

Figure 6.7 Volcano plots showing patterns of up and down regulation in the (1) grain, (2) grain-corium junction and (3) corium layers. Includes lysis extraction (A) and NaCl/Urea extraction (B).

Table 6.15 Differentially expressed collagens in tight and loose hides, with p-values below 0.05.

Protein	Accession No.	Layer of hide *Grain* *Junction* *Corium*	Extraction	Fold Change	P-value	Collagen Type
Down Regulated						
Collagen type I, alpha 1 CN8	0910139A	☑ ☑	Lysis	10.87 18.89	0.0333 0.0205	Fibril Forming
Collagen type I, alpha 1	AAI05185.1	☑ ☑	Lysis	4.77 8.56	0.0093 0.0007	
Collagen type I, alpha 2	AAI49096.1	☑ ☑	Lysis	4.73 8.35	0.0049 0.0001	
Isoform I of collagen type II, alpha 1	DAA29861.1	☑	Lysis	3.96	0.0396	
Precursor of collagen type III alpha 1	NP_001070299.1	☑	Lysis	6.84	0.0010	
Collagen type V, alpha 2	XP_024835542.1	☑ ☑	Lysis	3.65 4.91	0.0316 0.0003	
Up Regulated						
Collagen type III, alpha 1	P04258.1	☑	NaCl/Urea	0.51	0.0306	Fibril Forming
Collagen type VI, alpha 1	DAA32939.1	☑ ☑ ☑	NaCl/Urea	0.41 0.36 0.35	0.0306 0.0241 0.0283	Beaded filament-forming
Isoform X1 of collagen type VI, alpha 2	XP_005202110.1	☑	NaCl/Urea	0.51	0.0088	
Isoform X1 of collagen type VI, alpha 3	XP_024846030.1	☑ ☑	NaCl/Urea	0.76 0.61	0.0353 0.0328	
Collagen type VII, alpha 1	XP_002697097.2	☑	NaCl/Urea	0.30	0.0202	Anchoring
Collagen type XII, alpha 1	DAA26385.1	☑	NaCl/Urea	0.62	0.0231	FACIT
Isoform X1 of collagen type XIV, alpha 1	XP_024857663.1	☑	Lysis	0.27	0.0113	
Precursor of collagen type XV, alpha 1	NP_001178214.2	☑	NaCl/Urea	0.42	0.0272	Multiplexin
Isoform X1 of collagen type XVIII, alpha 1	XP_024830782.1	☑	NaCl/Urea	0.41	0.0354	

They included collagens, other extracellular proteins such as proteoglycans and glycoproteins, cellular proteins and keratins. Relative concentrations were considered significantly different if they had p-values below 0.05 and a fold change between tight and loose samples greater than 2. Keratins were excluded from this analysis as any differences are more likely to be caused by sampling issues than looseness.

Table 6.15 displays the different types of collagens that are up and down regulated in loose hides compared to tight. Only the down-regulated collagens meet the criteria for significance with p-values below 0.05 and fold changes greater than 2, the up-regulated collagens are included in the table, as although the fold change does not meet the criteria, the p-value does. The results identify at least 6 different types of collagens (I, III, V, VI, VII and XII) that are significantly different between loose and tight hides. However, collagens are often comprised of different alpha chains and the results indicate that only one of these is significantly different in some instances. It is unclear whether this is a flaw in the analysis or the result is real. Although significant in this analysis it raises reasonable doubt over whether these collagens actually contribute to looseness. In all of the sample's collagen type I, alpha 1 CN8 was identified as well as the full alpha 1 and alpha 2 chains. This appears to be a partial sequence (only 279 amino acids) of the type 1, alpha 1 collagen (1463 amino acids) and was first sequenced in 1983 by Glanville *et al.* [195]. It is likely an artefact of the trypsin digestion. Several other collagens: II, XIV, XV and XVIII also appear to be differentially regulated although only their isoforms or precursors were identified. Although collagen type XIV (FACIT collagen) and to a lesser degree types XV and XVIII (basement membrane collagens) have been found in skin [41, 196], it is unusual to see type II. This collagen is more frequently associated with cartilage and bone [35]. However, the same isoform of collagen II identified in this study has also been found in skin by Mikesh *et al.* [188].

The results indicate that more fibrous collagens are down regulated in loose samples and non-fibrous collagens are up regulated, which supports the previous finding regarding the ratio of fibrous to non-fibrous collagen. Fibrous collagen, particularly types I and III, provide structural support for the hide. This decrease could facilitate the removal of other molecules including non-collagenous proteins and GAGs during leather processing, resulting in a destabilised collagen network, thus causing loose leather. Previous studies have shown that the solubility of collagen changes throughout the animal's lifetime, decreasing as the animal ages [197], so it is entirely possible that reduced solubility is a factor in these results.

Other than collagens, 24 other proteins excluding keratins were down-regulated in loose hides (p-values < 0.05 and fold changes > 2, Appendix 9.G). The down-regulated proteins include cytoskeletal proteins, enzymes, proteins associated with proteoglycans and other miscellaneous proteins. Although there is no obvious link between these proteins and looseness, a few are involved in the organisation of the ECM such as the glial hyaluronate-binding protein and inter-alpha trypsin inhibitor heavy chain HI. Both of these proteins interact with HA, a non-sulfated GAG that has many roles in skin/hide including hydration and promotion of tissue integrity [94, 95]. Although HA has been linked to wrinkly skin both in humans and other animals, in this study it could not be quantitively analysed. Glial hyaluronate-binding protein is also thought to be a product of metalloproteinase digestion of the proteoglycan versican, which has been linked ageing [111, 198].

As well as a few different types of collagens 316 other non-collagenous proteins including proteoglycans, glycoproteins, cytoskeletal proteins, enzymes and proteins involved in cellular regulation were found to be up-regulated in loose samples. However, although all these proteins had p-values below 0.05, none had fold changes greater than 2. In fact, they all had fold changes

below 1. This brings up reasonable doubt over whether the differences found are due to looseness or caused through other factors such as biological variation or sampling issues. It is more likely that that they are due to the differences observed between fibrous collagens in loose samples resulting in increased efficiency of extraction. However, some proteins were identified that have been reported as being associated with wrinkle formation or ageing such as proteoglycans including asporin and biglycan [199] and glycoproteins including laminin, fibronectin and fibulin [74, 118]. All of these proteins are known to interact with either collagen and/or elastin fibres and to aid fibrillogenesis [74, 118, 199]. An increase in their concentration would therefore be expected to increase the concentration and organisation of collagen fibrils rather than decrease the concentration and organisation as observed in the amino acid analysis and confocal microscopy images of tight and loose samples. The weakness of this study is the small sample size and these preliminary results need to be confirmed by taking samples from a greater number of biological replicates, something that was outside the budget for this project.

Changes in these protein concentrations could contribute to looseness in one of two ways:

- The decrease in fibrous collagen in loose samples, supported by previous amino acid results, could result in a less organised collagen network. This is further supported by the decrease in collagen crosslinks found in loose samples. The change in collagen concentration and structure in the raw material could contribute to the change in collagen structure observed in finished leather [10, 12, 13].
- Non-collagenous proteins are typically removed during leather processing, and previous studies have shown that poor quality leather typically has a greater percentage of non-collagenous proteins [70, 200]. It is possible that the decrease in fibrous collagen observed in this study is accompanied by an increase in non-collagenous proteins that are not

removed during leather processing, resulting in loose leather. Although our results make this seem less likely.

To help support or negate these theories proteomics throughout leather processing in loose and tight samples could be carried out.

6.3.4 A comparison of the proteins identified in samples from the OSP *and* Distal Axilla

During the initial phase of this experiment 5 different regions of the hide were examined. Of these regions the OSP and distal axilla showed the most diverse differences in looseness grade, physical testing and microscopy. The results indicate that the distal axilla is more prone to looseness, interestingly produces a stronger leather and has a less organised and more open collagen network. Thus, the proteomes of these two areas were analysed for differences using four biological replicates, each with three technical replicates. Three main factors came to light when analysing the proteomic profiles of the OSP and distal axilla region.

In both the lysis and NaCl/Urea extraction, almost double the number of proteins were identified in the distal axilla compared to the OSP (Figure 6.8), supporting the fact it is easier to extract proteins from loose hides compared to tight hides. 439 proteins were identified in the lysis extraction from the OSP region in contrast to the 866 that were identified in the samples from the distal axilla. Of these 369 were common to both regions. In the NaCl/Urea extraction 660 proteins were identified in the OSP region whilst 1054 were identified in the distal axilla. Of these, 581 were common to both regions.

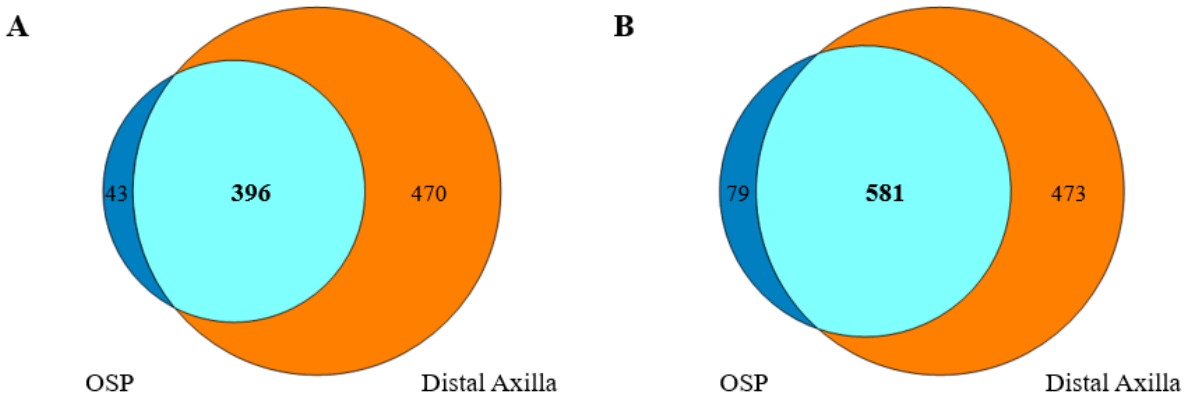

Figure 6.8 Number of proteins identified in the OSP and distal axilla in (A) lysis extraction and (B) NaCl/Urea extraction.

The ratio of non-collagenous to collagenous proteins and fibrous to non-fibrous collagens were investigated between the two regions. In both extractions the distal axilla had a significantly higher ratio (p-value >0.05) of non-collagenous protein and a significantly lower ratio (p-value >0.05) of fibrous collagen compared to collagenous and non-fibrous collagens respectively. This was the case for all three layers of hide; grain, grain to corium junction and corium as shown in Figure 6.9 and is comparable to the results obtained when examining looseness.

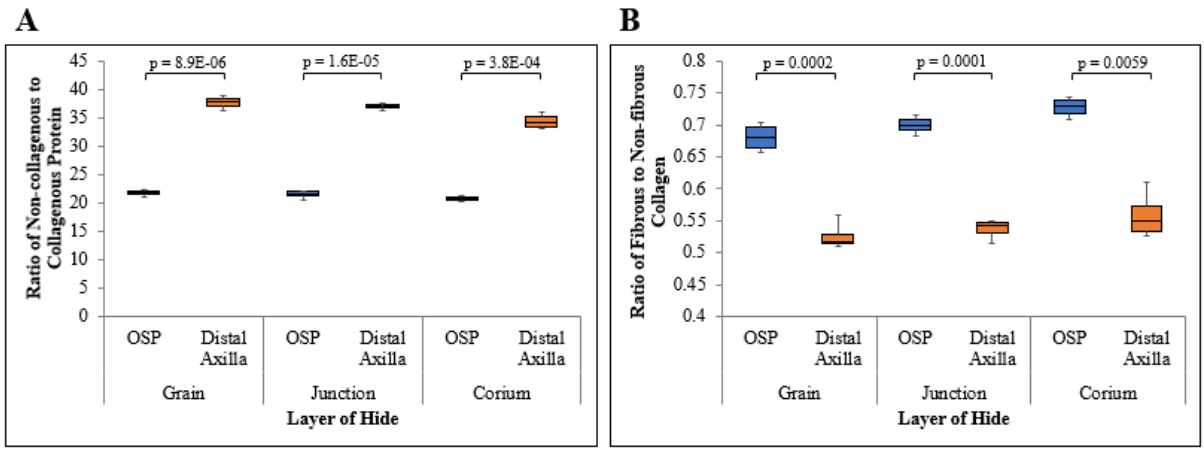

Figure 6.9 Ratio of non-collagenous to collagenous proteins between OSP and distal axilla regions (A) and ratio of fibrous to non-fibrous collagens between OSP and distal axilla region (B).

Proteins that were common between the OSP and distal axilla region were then statistically analysed. The volcano plots showed the same pattern as those between loose and tight hides, (Figure 6.10), with more proteins being up-regulated in the distal axilla than down-regulated. Between the two extraction methods over 500 different proteins were identified that were significantly up or down-regulated in distal axilla regions compared to OSP regions, (p-value >0.05). However only 10 proteins from the lysis extraction and 22 from the NaCl/urea extraction also had a fold change greater than 2. All of these proteins were down-regulated in the distal axilla. The full list is found in Appendix 9.H. These included proteins from the following categories; collagens, extracellular proteins, cellular proteins including cytoskeletal proteins, enzymes and other miscellaneous proteins. While type I collagen was down-regulated in the samples from the grain to corium junction layer extracted with lysis buffer, there were no significant changes in the relative amounts of other collagen types.

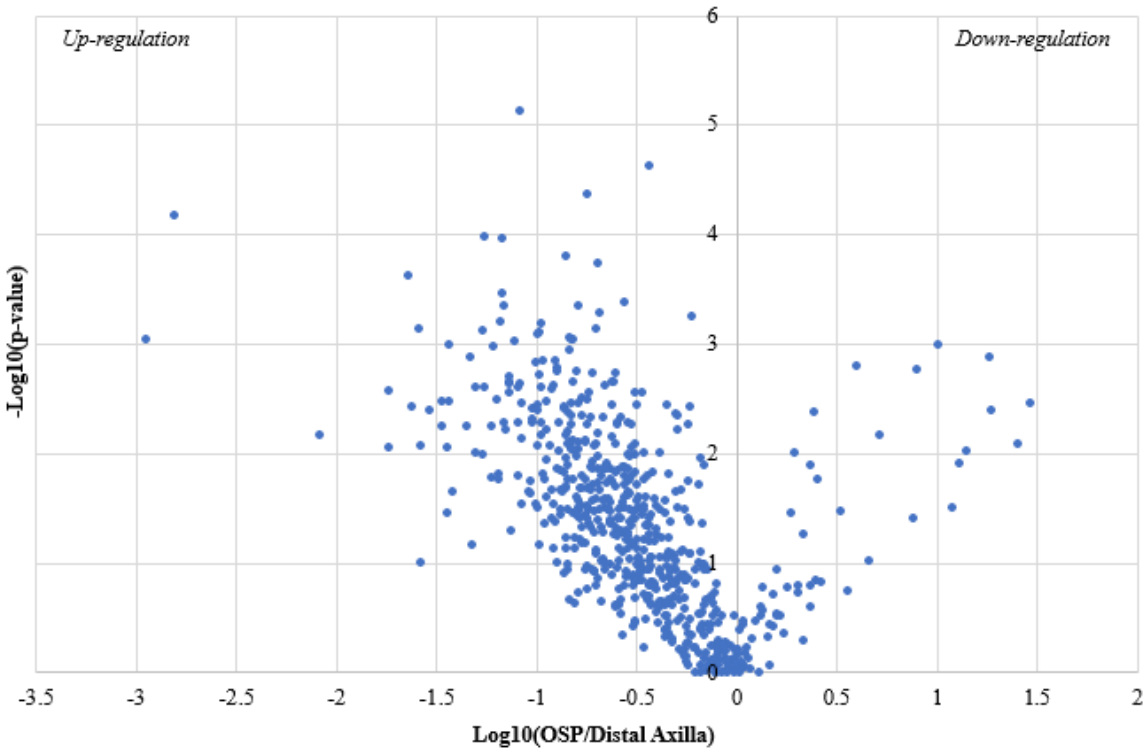

Figure 6.10 Example of a volcano plot showing regulation of proteins between the OSP and distal axilla (grain layer, NaCl/Urea extraction.

MS analysis of the OSP and distal axilla regions showed there was a greater variety of proteins in the distal axilla, most likely due to the more open, less organised collagen structure (as observed in the microscopy section) allowing better extraction of the proteins. The increased ratio of non-collagenous and decreased ratio of fibrous collagen observed helps support this claim and could explain why the distal axilla is more prone to looseness than the OSP. Whilst previous studies have shown differences in the proteins identified from different areas of skin/hide, they are less extreme. For example, Mikesh *et al.* [188] observed 155 proteins in the leg region and 174 in the breast region of human skin. Potentially the distal axilla (armpit) region is a superior area for proteomic studies due to ease of protein extraction in this area.

6.3.5 PTMs of collagen

PTMs are found on the majority of secreted proteins and directly alter their physiological properties [201]. They are enzymatically added both during and after synthesis and folding of the protein [201]. There are many different types of PTMs and they help regulate nearly all aspects of protein function. Advances in MS techniques enable these PTMs to be identified and quantified. During this experiment the bottom up MS approach was used which digests proteins of interest with site-specific proteases with the resulting peptides being analysed by MS. This technique is the most common and is the ideal technique for the generic screening of PTMs of proteins found in loose and tight samples. [201].

Collagen is a protein that is heavily modified, particularly the lysine and proline residues. Hydroxylation of the proline and lysine residues help stabilise the collagen molecule and enable covalent crosslinks to form [34, 52]. Meanwhile glycosylation of lysine residues (galactosyl and glucosylgalactosyl) in collagen has been linked to organisation of collagen fibres and stability. It is also likely to control the level of crosslinking and because of this, a brief

investigation into the glycosylation of the proteins extracted by lysis was carried out. The results indicate an increase in glycosylation of hydroxylysine in both loose and distal axilla samples (Figure 6.11 A and B respectively). The relative number of glycosylated hydroxylysines in collagens present in tight and loose samples particularly in the junction and corium layers were significantly different (p values of 0.02 and 0.01 respectively). The relative levels of glycosylated hydroxylysines were also significantly different between the grain and junction layers and between samples taken from the OSP and distal axilla (p-value 0.004 and 1.55E-06).

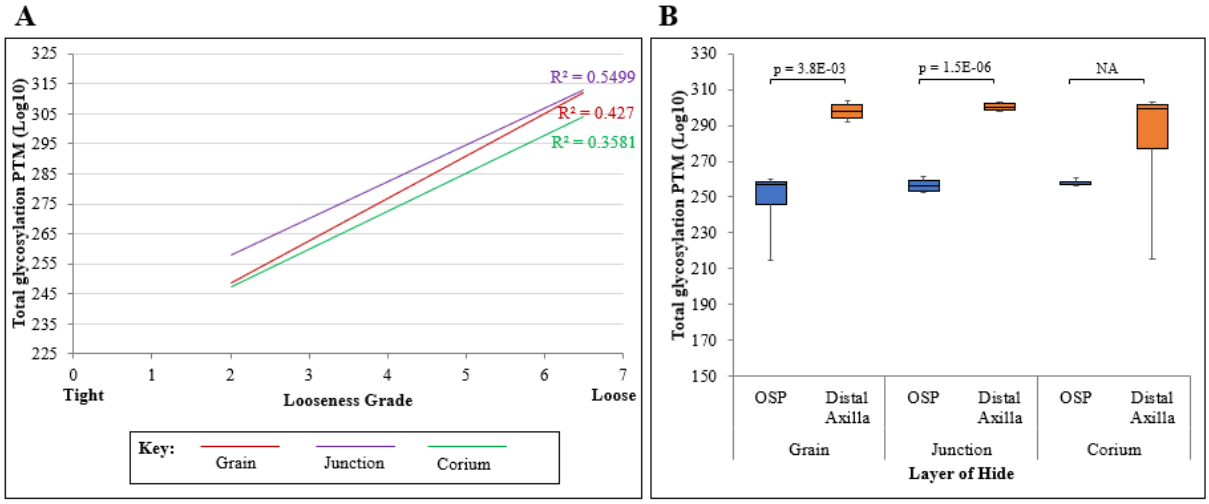

Figure 6.11 Total glycosylation PTM (log10) between (A) tight and loose samples, 6 replicates with 3 technical replicates for tight and 2 replicates with 3 technical replicates for loose. (B) OSP and distal axilla samples, 4 biological replicates with 3 technical replicates for OSP and distal axilla samples.

All samples showed glycosylation of various collagen I and VI peptides, however the distal axilla also showed glycosylation of a few collagen V and IV peptides. This does not mean that the other collagens or proteins do not have glycosylated PTMs, it just means that they were not identified using this methodology. When investigating the glycosylation between non-fibrous (IV and VI) and fibrous (I and V) collagens it was observed that there was a greater quantity of glycosylation in non-fibrous collagens, which supports results previously reported in the

literature [52]. It was also observed that loose samples and distal axilla samples had a lower ratio of glycosylation in fibrous collagens compared to non-fibrous collagens in all three layers of hide (p-value >0.05) (Figures 6.12A and B).

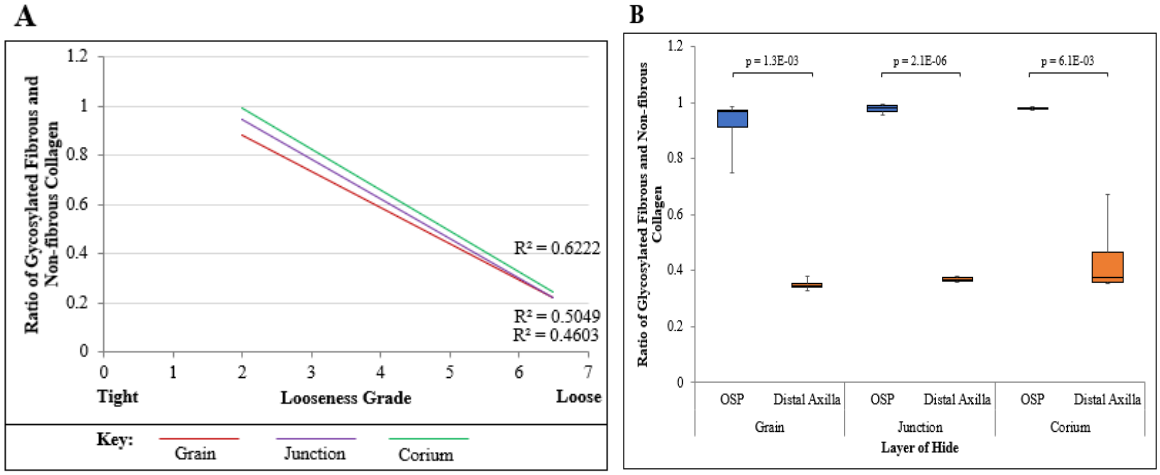

Figure 6.12 Ratio of glycosylation (PTM) in fibrous and non-fibrous collagen between (A) tight and loose samples, 6 replicates with 3 technical replicates for tight and 2 replicates with 3 technical replicates for loose. (B) OSP and distal axilla samples, 4 biological replicates with 3 technical replicates for OSP and distal axilla samples.

Glycosylation of collagen is thought to have many different biological functions including; control of collagen fibrillogenesis, crosslinking, remodelling, collagen-cell interaction and induction of vessel-like structures [52]. Glycosylation of lysine residues occurs prior to crosslinking. Thus, it is probable that the increase in glycosylated collagen observed in this study is responsible for the decrease in covalent crosslinks observed in chapter 5. Unfortunately, the enzymes responsible for both hydroxylation of collagen (lysyl oxidase) and glycosylation of collagen (glucosyltransferase) were not detected during this study.

The fact that no differences in the total carbohydrate content were observed between tight and loose samples or between samples taken from the OSP and distal axilla regions does not negate this result. The assay used to measure total carbohydrate does not discriminate between the origin of the saccharides measured and it is entirely possible that real differences will even out

to show no overall change. To further investigate the different molecules that make up the total carbohydrates in loose and tight hide would be beneficial. In particular non-enzymatic crosslinks (AGEs) which are thought to be influenced in part by glycation.

6.3.6 Western blots

Collagen I, III and V are all fibrous collagens. Previous results including microscopy and MS have indicated that a decrease in fibrous collagens could be a contributor to looseness. Western blots are a method utilised to validate these results. However, due to poor transfer of the standard collagens from the SDS-PAGE gel onto the membrane, no corroboration was made.

Dot blots were produced for all three collagens (Figure 6.13) showing that the antibodies purchased recognised the correct protein. The antibodies for collagens I and V (A and C) showed greater intensity when reacting with the correct standard than with collagen III (B). Thus, it was concluded that the protocol utilised for detection and visualisation was successful.

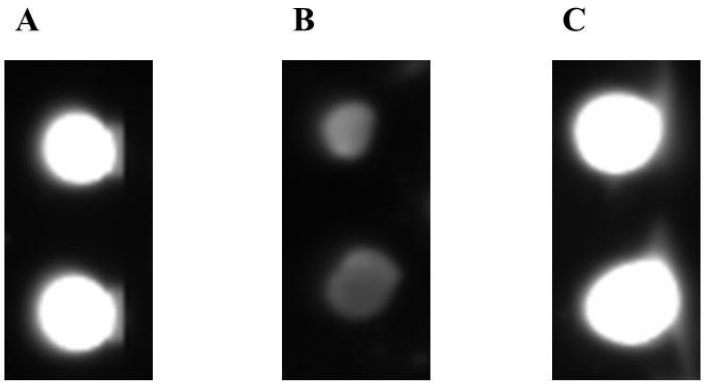

Figure 6.13 Dot blots showing responsiveness of antibodies to collagen standards; (A) collagen I, (B) collagen III and (C) collagen V.

Unfortunately, the bands on the gels did not transfer on to the membrane completely or consistently, with the majority remaining on the gel. Initially this was thought to be due to the high molecular weight of the collagens as such proteins are notoriously tricky to transfer. Standard transfer procedures obtained from sources such as Abcam, Millipore and Bio-Rad suggested altering the concentration of methanol and SDS in the transfer buffer. Methanol causes the gel to swell, thus lower concentrations are thought to aid in transfer and SDS is known to interfere with protein binding, though lower molecular weight proteins are more susceptible. The use of different transfer buffers, transfer times, transfer temperatures and type of membrane (nitrocellulose or PVDF) resulted in little or no improvement. It is unclear why transferring these bands was unsuccessful as other groups have shown success using similar protocols.

7. Conclusions and future research

7.1 Conclusions

Looseness is a defect found in 7 % of leather produced from cattle hide which lowers the quality of the finished product due to the appearance of surface wrinkles. Although looseness has been shown to be exacerbated by poor tanning practices, the fact that both loose and tight hides can be identified in the same tanning batch suggests that specific molecular components of the hides could also contribute to this defect. Various studies also indicate differences in the organisation of collagen fibres between tight and loose leather. Prior to this study, the molecular basis of looseness had not been investigated despite collagen, elastin and GAGs being frequently correlated with defects in skin including wrinkles associated with ageing.

This study used several cattle hides chosen at random and cut in half along the backbone. One half of each hide was processed to leather using the LASRA protocol while the other half was retained for analysis. The leather was then graded for looseness using the SATRA break scale. Five different regions on the hide were initially studied; the OSP, neck, belly, proximal and distal axilla. Two hides were identified that were looser than others, with three regions being higher than 4 on the SATRA break scale. However, it was apparent from these measurements that certain regions of hide were more prone to looseness than others. The average looseness grade of the OSP across all hides was 2.75 compared to the distal axilla which was 4.63.

The physical properties of loose and tight leather were further characterised using tear and tensile strength tests and corium to grain ratio as the strength of leather and the percentage of grain and corium have previously been linked to the molecular components that make up leather, particularly collagen. A very weak positive correlation was found between hide

strength and looseness with correlations of 0.2611 (tear) and 0.1059 (tensile). No correlation was found between the corium to grain ratio and looseness. However significant differences in strength based on the tear test and the corium to grain ratio were found between samples taken from the OSP and distal axilla regions of the hide (p values 0.0056 and 0.0100 respectively). The samples taken from the distal axilla were on average looser, stronger and had a greater percentage of corium. Thus, it is possible that the distal axilla region could provide a good model for investigative studies on the cause of looseness. Due to this the molecular components of the OSP and distal axilla were investigated in all four hides.

A diverse array of techniques were used to analyse the molecular components of loose and tight hides, and although these identified some potential differences, the small sample size hindered obtaining statistically significant results. Nevertheless, the results will be of interest to the leather industry and could provide the basis for further research into the identification of biomarkers for looseness which may lead to preventative breeding programs.

The structure (analysed by light and confocal microscopy), relative concentration (analysed by RPHPLC and gel LC-MS/MS) and composition (analysed by gel LC-MS/MS) of collagen in loose and tight hides were investigated. The microscopy results suggested that the corium of loose samples have collagen fibres with a lower angle of weave, which is especially significant between the OSP and distal axilla regions in both raw hide and finished leather (p-value 0.0268 and 0.0216). Loose samples also appeared to have a less organised collagen network in the corium with a greater amount of space between the collagen fibre bundles (R^2: 0.6048).

These findings were supported as the concentration of collagen in loose samples decreased (R^2: 0.7432), more gaps in the collagen network is likely to result in less collagen. Interestingly, no

significant difference was observed between the two areas tested, the OSP and the distal axilla. Breaking these differences down to the layers of the hide, the biggest decrease was observed in the grain to corium junction and the corium (R^2: 0.5104 and 0.8402 respectively), which is logical when it is these layers that contribute most to hide strength. However, this decrease in collagen content did not match up with our previous investigations into strength, with loose samples actually producing stronger leather. The finding that loose samples contained more non-collagenous protein and less fibrous collagen in all three layers also agrees with the structures seen in the microscopy study. This indicates that the gaps seen between the fibre bundles in samples prepared from loose hides are not voids, rather they are filled with either proteins other than collagen, polysaccharides or both. The fact that there are fewer fibre bundles also equates with the reduction in fibrous collagen. It is possible that this 'looser' structure allows better penetration of the chrome tanning agents and the other chemicals used to make leather. These agents act indiscriminately on any protein leading to the crosslinking of amino acid sidechains in close proximity to form a mesh of crosslinked proteins. Such a mesh throughout the structure would inevitably result in stronger leather. To investigate this possibility the chromium uptake could be analysed in loose and tight leather using HPLC.

All of these analyses rely on accuracy for the efficiency of extraction of the molecules being analysed, especially those that are intrinsically insoluble, which was why two different extraction methods were used. Results showed that the fibrous collagens, types I, II, III and V were all significantly down-regulated in loose samples with fold changes above 2 and p-values below 0.05. As extraction from samples taken from loose hides should intuitively be more efficient it is likely that this result is not due to inefficient extraction. Furthermore, the decrease in the relative concentrations of both total and fibrous collagens supports the decreased organisation and excess space between the collagen fibres observed by microscopy. As fibrous

collagen provides the structural support for hide, this decrease could however increase the efficiency of extraction of other proteins, resulting in the greater number of non-collagenous proteins found in both samples extracted from loose hides and from distal axilla.

Collagen crosslinks have been shown by others to correlate with both the strength and age of the material. In this study a slight decrease was observed in the 'total' enzymatic crosslinks, although no differences were observed between those isolated from the OSP and those isolated from the distal axilla. Also, no differences were observed when the number of individual crosslinks was correlated with looseness. The decrease in the 'total' number of enzymatic crosslinks found in loose samples is potentially a reflection of the decrease in collagen calculated from the hydroxyproline concentration. However, again it correlates with the decrease in collagen organisation observed by confocal microscopy. Although the exact biological function of glycosylation is unclear previous studies have suggested it aids in collagen organisation and stability. An overall increase in glycosylation of collagen HyLys was observed in both loose samples and the distal axilla region for all layers and was accompanied by a decrease in the ratio of glycosylated fibrous to non-fibrous collagen, as seen in the gel LC-MS/MS results. Interestingly, these regions actually have decreased collagen fibre organisation in this study, contradicting these findings. This is however consistent with a decrease in the number of crosslinks resulting in poorer organisation of the fibre bundles. HyLys is glycosylated in the Golgi before the protein is exported to the ECM and prevents the glycosylated residues from forming crosslinks. It is therefore possible that the level of glycosylation controls that of crosslinking and could be under genetic control and therefore phenotypic. To test such hypotheses would require a transcriptomic study of the enzymes involved in collagen glycosylation linked to a phenotypic study of cattle hides. Against this hypothesis is the finding that the concentrations of HyLys observed by amino acid analysis in

loose and tight samples remained unchanged. As glycosylated HyLys is unlikely to be detected in amino acid analyses, the concentration of HyLys should be lower in loose samples if the proportion of the glycosylated amino acid has increased. Nevertheless, differences in the collagen glycosylation patterns were observed using the more specific and accurate technique of gel LC-MS/MS, and targeting purified collagen bands rather than hide as a whole.

It was also observed that the relative levels of some proteoglycans, such as asporin and biglycan were upregulated in samples taken from loose samples as were the glycoproteins laminin, fibronectin and fibulin. Although the change was very small (below 2-fold) it is was significant, (p-value below 0.05), suggesting that this increase is more likely due to the increased efficiency of extraction from loose samples rather than an inherent increase in their concentrations. Because these proteins are associated with collagen and its organisation, this is a much more likely explanation especially when the microscopy results show that loose samples have less fibril organisation.

Elastin was investigated due to differences in the structure and concentration being found in both aged human skin and in the genetic disorder cutis laxa. Microscopy studies to locate elastin in hide sections stained with fuschin stain proved to be unsuccessful as was the Fastin^{TM} assay for quantitation of elastin in the hide samples. In the end, the concentration of the elastin crosslink desmosine was measured using the same technique as was used to isolate and measure the other crosslinks. This showed that elastin concentration does correlate with looseness with an R^2 of 0.671. The fact that there were also significant differences between the concentration of the elastin crosslink in the OSP and distal axilla region (p-value 0.0147), known to be 'looser' than the OSP validates the use of desmosine to quantitate elastin.

The above results suggest that loose hides have a decrease in the concentration of fibrillar collagen, contributing to the formation of excess space between the collagen fibres. A decrease in covalent collagen crosslinks was paired with an increase in glycosylation of HyLys residues, potentially affecting the organisation of the collagen fibres. The concentration of elastin in loose samples was also greater. These changes in the structure, concentration and composition of collagen and elastin molecules results in a more open, flexible network and is likely to affect the efficiency of extraction of non-collagenous material during leather processing.

This project provides the first glimpse into understanding the molecular cause of looseness in leather at the raw stage. Whilst it may not answer the question of what causes looseness it will hopefully provide a starting point for the next researcher to form a more targeted study. In the long term this will help the leather industry gain a better idea of how the molecular properties are shaping the quality of their leather and provide tools to improve it.

7.2 Directions for future research

1. The main flaw in this experiment was the low number of biological replicates, repeating these experiments with a greater sample size would help confirm whether the results of this study are true indicators of looseness or just due to biological variation. During this study no knowledge of the age, breed or sex of the animal was known. In future studies this may be advantageous as these factors need to be correlated with molecular differences.

2. Using more sensitive imaging techniques such as MALDI imaging, to study the collagen fibres and even how GAGs interact with the collagen fibres could give more information into the cause of looseness, especially in the grain layer.

3. A more comprehensive study on GAGs in the hides should be carried out as the initial results suggest the types and concentrations of some proteoglycans vary with looseness. GAGs play

an important role in fibrillogenesis, and the exact roles of the protein and carbohydrate domains has never been fully understood.

4. Several proteins were found to be up and down regulated in loose hides compared to tight hides. Validating these results with either western blots or ELISA would be the next step.

5. Glycosylation of hydroxylysine appeared to influence looseness and the formation of crosslinks. A larger transcriptomic study looking at the enzymes responsible for these PTMs may give some insight as to whether these processes are indeed interrelated.

6. Whilst this project has investigated differences in some of the molecular components of loose and tight raw hides, studying the molecular components throughout processing would also be useful to understand whether processing affects loose and tight hides differently as various processing stages are known to exacerbate looseness. Understanding the events at a molecular level would enable modifications to the process that may prevent excess wrinkling of the finished product.

8. References

1. Menon, G. K. (2015). Lipids and Skin Health. In A. Pappas (Ed.), (pp. 9-23). New York, USA: Springer International Publishing.
2. Chuong, C. M., Nickoloff, B. J., Elias, P. M., Goldsmith, L. A., Macher, E., Maderson, P. A., Sundberg, J. P., Tagami, H., Plonka, P. M., Thestrup-Pedersen, K., Schroder, B. A., Dotto, P., Chang, C. H., Williams, M. L., Feingold, K. R., King, L. E., Kligman, A. M., Rees, J. L., & Christophers, E. (2002). What is the 'true' function of skin? *Experimental Dermatology, 11*, 159-187.
3. Frantz, C., Stewart, K. M., & Weaver, V. M. (2010). The extracellular matrix at a glance. *Journal of Cell Science, 123*, 4195-4200.
4. Mouw, J. K., Ou, G., & Weaver, V. M. (2014). Extracellular matrix assembly: a multiscale deconstruction. *Nature Review, 15*, 771-785.
5. Tobin, D. J. (2006). Biochemistry of human skin - our brain on the outside. *The Royal Society of Chemistry, 35*, 52-67.
6. Mann, B. R., & McMillan, M. M. (2017). The Chemistry of the Leather Industry. *NZ Institute of Chemistry*, 1-17.
7. Covington, A. D., & Covington, T. (2009). *Tanning Chemistry: The Science of Leather*. Cambridge, UK: Royal Society of Chemistry.
8. Sharphouse, J. H. (1963). *The Leatherworker's Handbook*: Leather Producers' Association for England, Scotland and Wales.
9. Holmes, G. (2012). [Eliminating looseness in cattle hides proposed research program].
10. Wells, H. C., Holmes, G., & Haverkamp, R. G. (2015). Looseness in bovine leather: microstructural characterization *Journal of the Science of Food and Agriculture*.
11. Cooper, S. (2009). *Looseness in leather*. Paper presented at the Annual Leather and Shoe Research Association Conference, Wellington.
12. Wood, B. (2000). Looseness - Tanner's Dilemma. *Leather International, 64*.
13. Liu, C.-K., Laton, N. P., Lee, J., & Cooke, P. H. (2009). Microscopic observations of leather looseness and its effects on mechanical properties. *Journal of the American Leather Chemists Association, 104*, 230-236.
14. Rabinovich, D., & Lowenstein, J. H. (2001). Seeking soft leathers with a tight grain. *World Leather*, 27-32.
15. Passman, A., & Sumner, R. (1987). Effects of breed and age at slaughter on leather produced from export lambs reared on hill country. *New Zealand Journal of Experimental Agriculture, 15*(3), 309-316.
16. Passman, A., & Sumner, R. (1983). Effects of breed and level of feeding on leather production from 18-month-old wethers. *New Zealand Journal of Experimental Agriculture, 11*(1), 47-52.
17. van Stiphout, T. A. P. (2015). NMR Transverse relaxation analysis of leather looseness.
18. Wells, H. C., Holmes, G., & Haverkamp, R. G. (2016). Early detection of looseness in bovine hides using ultrasonic imaging. *Journal of the American Leather Chemists Association, 111*, 107-112.
19. Robinson, M., Visscher, M., LaRuffa, A. & Wickett, R. (2010). Natural moisturizing factors (NMF) in the stratum corneum (SC). 1. Effects of lipid extraction and soaking. . *Journal of Cosmetic Science, 61*, 13-22.
20. Pappas, A. (2009). Epidermal surface lipids. *Dermato-Endocrinolgy, 1*(2), 72-79.

21. Haines, B. M., & Barlow, J. R. (1975). The anatomy of leather. *Journal of Materials Science, 10*, 525-538.
22. O'Leary, D. N., & Attenburrow, G. E. (1996). Differences in strength between the grain and corium layers of leather. *Journal of Materials Science, 31*, 5677-5682.
23. Gustafsson, E., & Fassler, R. (2000). Insights into extracellular matrix functions from mutant mouse models. *Exp Cell Res, 261*(1), 52-68.
24. Naylor, E. C., Watson, R. E. B., & Sherratt, M. J. (2011). Molecular aspects of skin ageing. *Maturitas, 69*, 249-256.
25. Hamamy, H., Masri, A., & Ajlouni, K. (2005). Wrinkly skin syndrome. *Clinical and Experimental Dermatology: Clinical dermatology, 30*(5), 590-592.
26. Tian, X., Azpurua, J., Hine, C., Vaidya, A., Myakishev-Rempel, M., Ablaeva, J., Mao, Z., Nevo, E., Gorbunova, V., & Seluanov, A. (2013). High-molecular-mass hyaluronan mediates the cancer resistance of the naked mole rat. *Nature, 499*(7458), 346-349.
27. Olsson, M., Meadows, J. R., Truve, K., Pielberg, G. R., Puppo, F., Mauceli, E., Quilez, J., Tonomura, N., Zanna, G., & Docampo, M. J. (2011). A novel unstable duplication upstream of HAS2 predisposes to a breed-defining skin phenotype and a periodic fever syndrome in Chinese Shar-Pei dogs. *PLoS genetics, 7*(3), 1-11.
28. Waller, J. M., & Maibach, H. I. (2006). Age and skin structure and function, a quantitative approach (II): protein, glycosaminoglycan, water, and lipid content and structure. *Skin Research and Technology, 12*, 145-154.
29. Huang, C., Elmets, C. A., van Kampen, K. R., DeSilva, T. S., Barnes, S., Kim, H., & Tang, D. C. (2005). Prospective highlights of functional skin proteomics. *Mass Spectrometry Reviews, 24*, 647-660.
30. Fang, J., Wang, P., Huang, C., Chen, M., Wu, Y., & Pan, T. (2016). Skin ageing caused by intrinsic or extrinsic processes characterize with functional proteomics. *Proteomics, 16*, 2718-2731.
31. Randles, M. J., Humphries, M. J., & Lennon, R. (2017). Proteomic definitions of basement membrane composition in health and disease. *Matrix biology, 57-58*, 12-28.
32. Huang, C., Xu, H., Wang, C., & Elmets, C. A. (2005). Proteomic characterization of skin and epidermis in response to environmental agents. *Expert Review of Proteomics, 2*(5), 809-820.
33. Myllyharju, J., & Kivirikko, K. I. (2004). Collagens, modifying enzymes and their mutations in humans, flies and worms. *Trends in Genetics, 20*(1), 33-43.
34. Gelse, K., Poschl, E., & Aigner, T. (2003). Collagen - structure, function, and biosynthesis. *Advanced Drug Delivery Reviews, 55*, 1531-1546.
35. Ricard-Blum, S. (2011). The collagen family. *Cold Spring Harbor perspectives in biology, 3*(1), 1-19.
36. Maynes, R. (2012). *Structure and function of collagen types*: Elsevier.
37. Kefalides, N. A., Alper, R., & Clark, C. C. (1979). Biochemistry and metabolism of basement membranes. *International Review of Cytology, 61*, 167-228.
38. Stenn, K., Madri, J., & Roll, F. (1979). Migrating epidermis produces AB2 collagen and requires continual collagen synthesis for movement. *Nature, 227*, 229-232.
39. Keene, D. R., Ridgway, C. C., & Lozzo, R. V. (1998). Type VI microfilaments interact with a specific region of banded collagen fibrils in skin. *Journal of Histochemistry & Cytochemistry, 46*(2), 215-220.
40. Sakai, L. Y., Keene, D. R., Morris, N. P., & Burgeson, R. E. (1986). Type VII collagen is a major structural component of anchoring fibrils. *The Journal of cell biology, 103*(4), 1577-1586.

41. Agarwal, P., Zwolanek, D., Keene, D. R., Schulz, J.-N., Blumbach, K., Heinegard, D., Zaucke, F., Paulsson, M., Krieg, T., & Koch, M. (2012). Collagen XII and XIV-new partners of cartilage oligomeric matrix protein in the skin extracellular matrix suprastructure. *Journal of Biological Chemistry*, 22549-22559.
42. Grässel, S., Unsöld, C., Schäcke, H., Bruckner-Tuderman, L., & Bruckner, P. (1999). Collagen XVI is expressed by human dermal fibroblasts and keratinocytes and is associated with the microfibrillar apparatus in the upper papillary dermis. *Matrix biology, 18*(3), 309-317.
43. Eastoe, J. (1955). The amino acid composition of mammalian collagen and gelatin. *Biochemical Journal, 61*(4), 589-600.
44. Fratzl, P. (2008). *Collagen: structure and mechanics*. Boston, MA: Springer.
45. Ramachandran, G., Bansal, M., & Bhatnagar, R. (1973). A hypothesis on the role of hydroxyproline in stabilizing collagen structure. *Biochimica et Biophysica Acta (BBA)-Protein Structure, 322*(1), 166-171.
46. Krieg, T., & Aumailley, M. (2011). The extracellular matrix of the dermis: flexible structures with dynamic functions. *Exp Dermatol, 20*(8), 689-695.
47. Birk, D. E., Fitch, J. M., Babiarz, J. P., Doane, K. J., & Linsenmayer, T. F. (1990). Collagen fibrillogenesis in vitro: interaction of types I and V collagen regulates fibril diameter. *Journal of Cell Science, 95*, 649-657.
48. Kielty, C. M., & Grant, M. E. (2002). The collagen family: structure, assembly, and organization in the extracellular matrix. *Connective tissue and its heritable disorders: molecular, genetic, and medical aspects*, 159-221.
49. Prockop, D. J., & Kivirikko, K., I. (1995). Collagens: Molecular, biology, diseases and potentials for therapy. *Annual Review of Biochemistry, 64*, 403-434.
50. Prockop, D. J. K., K, I. . (1995). Collagens: Molecular, biology, diseases and potentials for therapy. *Annual Review of Biochemistry, 64*, 403-434.
51. Naffa, R. (2015). [Understanding the molecular basis of the strength differences in skins used in leather manufacture].
52. Yamauchi, M., & Sricholpech, M. (2012). Lysine post-translational modifications of collagen. *Essays In Biochemistry, 52*, 113-133.
53. Yamauchi, M., Woodley, D. T., & Mechanic, G. L. (1988). Aging and cross-linking of skin collagen. *Biochemical and Biophysical Research Communications, 152*(2), 898-903.
54. Reiser, K., McCormick, R. J., & Rucker, R. B. (1992). Enzymatic and nonenzymatic cross-linking of collagen and elastin. *The FASEB Journal, 6*(7), 2439-2449.
55. Avery, N. C., & Bailey, A. J. (2008). *Restraining Cross-Links Responsible for the Mechanical Properties of Collagen Fibers: Natural and Artificial*. Boston, MA: Fratzl P. (eds) Collagen. Springer.
56. Andriotis, O. G., Chang, S. W., Vanleene, M., H., H. P., Davies, D. E., Shefelbine, S. J., Buehler, M. J., & Thurner, P. J. (2015). Structure – mechanics relationships of collagen fibrils in the osteogenesis imperfecta mouse model. *Journal Royal Society Interface, 12*, 1-12.
57. Naffa, R., Holmes, G., Ahn, M., Harding, D., & Norris, G. (2016). Liquid chromatography-electrospray ionization mass spectrometry for the simultaneous quantitation of collagen and elastin crosslinks. *Journal of Chromatography A, 1478*, 60-67.
58. Hansen, P., Haraldsson, B. T., Aagaard, P., Kovanen, V., Avery, N. C., Qvortrup, K., Larsen, J. O., Krogsgaard, M., Kjaer, M., & Peter Magnusson, S. (2009). Lower strength of the human posterior patellar tendon seems unrelated to mature collagen cross-linking and fibril morphology. *Journal of applied physiology, 108*(1), 47-52.

59. Eyre, D. R., Paz, M. A., & Gallop, P. M. (1984). Cross-linking in collagen and elastin. *Annual Review of Biochemistry, 53*, 717-748.
60. Ricard-Blum, S., & Ville, G. (1989). Collagen cross-linking. *International Journal of Biochemistry, 21*(11), 1185-1189.
61. Naffa, R. (2017). *Understanding the molecular basis of strength differences in skins used in leather manufacture.* Massey University, Palmerston North, New Zealand.
62. Lavker, R. M., Zheng, P., & Dong, G. (1987). Aged skin: a study by light, transmission electron and scanning electron microscopy. *Journal of Investigative Dermatology, 88*, 44-51.
63. Rigal, J., Escoffier, C., Pharm, M., Querleux, B., Faivre, B., Agcohe, P., & Leveque, J. (1989). Assessment of ageing of the human skin by in vivo ultrasonic imaging. *Journal of Investigative Dermatology, 93*, 621-625.
64. Neerkan, S., Lucassen, G. W., Bisschop, M. A., Lenderink, E., & Nuijs, T. A. M. (2004). Characterization of age-related effects in human skin: a comparative study that applies confocal laser scanning microscopy and optical coherence tomography. *Journal of Biomedical Optics, 9*(2), 274-281.
65. Vasquez-Ortiz, F. A., Moron-Fuenmajor, O. E., & Gonzalez Mendez, N. F. (2004). Hydroxyproline measurement by HPLC: Improved method of total collagen determination in meat samples. *Journal of Liquid Chromatogaphy and Related Technologies, 27*(17), 2771-2780.
66. Shuster, S., Black, M., & McVitie, E. (1975). The influence of age and sex on skin thickness, skin collagen, and densitiy. *British Journal of Dermatology, 93*(6), 639-643.
67. Lovell, C. R., Smolenski, K. A., Duance, V. C., Light, N. D., Young, S., & Dyson, M. (1987). Type I and III collagen content and fibre distribution in normal human skin during aging. *British Journal of Dermatology, 117*, 419-428.
68. Gniadecka, M., Gniadecki, R., J., S., & Sondergaard, J. (1994). Ultrasound structure and digital image analysis of the subepidermal low echogenic band in aged human skin: diurnal changes and interindividual variability. *Journal of Investigative Dermatology, 102*, 362-365.
69. Buckley, M. (2016). Species Identification of Bovine, Ovine and Porcine Type 1 Collagen; Comparing Peptide Mass Fingerprinting and LC-Based Proteomics Methods. *International Journal of Molecular Sciences, 17*(445), 1-17.
70. Edmonds, R. L., Choudhury, S. D., Haverkamp, R. G., Britles, M., Allsop, T. F., & Norris, G. E. (2008). Using Proteomics, Immunohistology, and Atomic Force Microscopy to Characterize Surface Damage to Lambskins Observed after Enzymatic Dewooling. *Journal of Agricultural and Food Chemistry, 56*, 7934-7941.
71. Bailey, A. J., & Shimokomaki, M. S. (1971). Age Related Changes in the Reducible Cross-Links of Collagen. *FEBS LETTERS, 16*(2), 86-88.
72. Tanzer, M. L. (1973). Cross-Linking of Collagen. *Science, 180*, 561-566.
73. Sizeland, K. H., Edmonds, R. L., Basil-Jones, M. M., Kirby, N., Hawley, A., Mudie, S., & Haverkamp, R. G. (2015). Changes to collagen structure during leather processing. *Journal of Agricultural and Food Chemistry, 63*, 2499-2505.
74. Halper, J., & Kjaer, M. (2014). Basic Components of Connective Tissues and Extracellular Matrix: Elastin, Fibrillin, Fibulins, Fibrinogen, Fibronectin, Laminin, Tenascins and Thrombospondins. In J. Halper (Ed.), *Progress in Heritable Soft Connective Tissue Diseases* (pp. 31-47). Dordrecht: Springer Netherlands.
75. Tassabehji, M., Metcalfe, K., Hurst, J., Ashcroft, G. S., Kielty, C., Wilmot, C., Donnai, D., Read, A. P., & Jones, C. J. P. (1998). An elastin gene mutation producing

abnormal tropoelastin and abnormal elastic fibres in a patient with autosomal dominant cutis laxa. *Human molecular genetics, 7*(6), 1021-1028.
76. Uitto, J. (1979). Biochemistry of the Elastic Fibers in Normal Connective Tissues and its Alterations in Diseases. *Journal of Investigative Dermatology, 72*(1), 1-10.
77. Murakami, Y., Suzuki, R., Yanuma, H., He, J., Ma, S., Turino, G. M., Lin, Y. Y., & Usuki, T. (2014). Synthesis and LC-MS/MS analysis of desmosine-CH2, a potential internal standard for the degraded elastin biomarker desmosine. *Organic & Biomolecular Chemistry, 12*(48), 9887-9894.
78. Kiernan, J. A. (1990). *Histological and Histochemical methods: theory and practice* (2 ed.). Ontario, Canada: Pergamon Press.
79. Edmonds, R. (2008). *Proteolytic depilation of lambskins : a thesis presented in partial fulfilment of the requirements for the degree of Doctor of philosophy in Bioprocess Engineering at Massey University, Palmerston North, New Zealand.* (Doctor of Philosophy (Ph. D.) Doctoral), Massey University, Retrieved from http://hdl.handle.net/10179/892
80. Edmonds, R., & Cooper, S. (2011). *The importance of elastin distribution and morphology in ovine leather.* Paper presented at the XXXI IULTCS Congress, Valencia (Spain).
81. Percival, K., & Radi, Z. (2017). Comparison of five elastin histochemical stains to identify pulmonary samll vasculature. *Journal of Histotechnology, 40*(3), 73-78.
82. Honorio, A., Pinto, M. d. L., Goncalves, C., & Bairos, V. (2009). Elastin in the Avian Lungs. *The Open Chemical and Biomedical Methods Journal, 2*, 18-23.
83. Naum, Y., & Morgan, T. E. (1973). A Microassay for Elastin. *Analytical biochemistry, 53*, 392-396.
84. Humbert, P., Viennet, C., Legagneux, K., Grandmottet, F., Robin, S., Oddos, T., & Muret, P. (2012). In the shadow of the wrinkle: theories. *Journal of Cosmetic Dermatology, 11*, 72-78.
85. Michel, A. (2009). What's in it for you? - Elastin. *Leather*, 36-37.
86. Gandhi, N. S., & Mancera, R. L. (2008). The structure of glycosaminoglycans and their interactions with proteins. *Chemical biology & drug design, 72*(6), 455-482.
87. Raman, R., Sasisekharan, V., & Sasisekharan, R. (2005). Structural insights into biological roles of protein-glycosaminoglycan interactions. *Chemistry & biology, 12*(3), 267-277.
88. Comper, W. D., & Laurent, T. C. (1978). Physiolgoical Function of Connective Tissue Polysaccharides. *Physiological Reviews, 58*(1), 255-315.
89. Funderburgh, J. L. (2000). MINI REVIEW Keratan sulfate: structure, biosynthesis, and function. *Glycobiology, 10*(10), 951-958.
90. Gavriel, P., & Kagan, H. M. (1988). Inhibition by heparin of the oxidation of lysine in collagen by lysyl oxidase. *Biochemistry, 27*(8), 2811-2815.
91. Pins, G. D., Christiansen, D. L., Patel, R., & Silver, F. H. (1997). Self-assembly of collagen fibers. Influence of fibrillar alignment and decorin on mechanical properties. *Biophysical journal, 73*(4), 2164.
92. Rabenstein, D. L. (2002). Heparin and heparan sulfate: structure and function. *Natural product reports, 19*(3), 312-331.
93. Reed, C. C., & Iozzo, R. V. (2002). The role of decorin in collagen fibrillogenesis and skin homeostasis. *Glycoconjugate journal, 19*(4-5), 249-255.
94. Stern, R. (2003). Devising a pathway for hyaluronan catabolism: are we there yet? *Glycobiology, 13*(12), 105R-115R.

95. Triggs-Raine, B., & Natowicz, M. R. (2015). Biology of hyaluronan: Insights from genetic disorders of hyaluronan metabolism. *World Journal of Biological Chemistry, 6*(3), 110-120.
96. van Susante, J. L. C., Pieper, J., Buma, P., van Kuppevelt, T. H., van Beuningen, H., van der Kraan, P. M., Veerkamp, J. H., van den Berg, W. B., & Veth, R. P. H. (2001). Linkage of chondroitin-sulfate to type I collagen scaffolds stimulates the bioactivity of seeded chondrocytes in vitro. *Biomaterials, 22*(17), 2359-2369.
97. Berg, J. M., Tymoczko, J. L., & Stryer, L. (2012). *Biochemistry*. New York: W.H. Freeman and Company.
98. Trowbridge, J. M., & Gallo, R. L. (2002). Dermatan sulfate: new functions from an old glycosaminoglycan. *Glycobiology, 12*(9), 117R-125R.
99. Edmonds, R. (2008). *Proteolytic depilation of lambskins.* Massey University,
100. Tierney, C. M., Haugh, M. G., Liedl, J., Mulcahy, F., Hayes, B., & O'Brien, F. J. (2009). The effects of collagen concentration and crosslink density on the biological, structural and mechanical properties of collagen-GAG scaffolds for bone tissue engineering. *Journal of the mechanical behavior of biomedical materials, 2*(2), 202-209.
101. Frazier, S. B., Roodhouse, K. A., Hourcade, D. E., & Zhang, L. (2008). The quantification of glycosaminoglycans: a comparison of HPLC, carbazole, and alcian blue methods. *Open glycoscience, 1*, 31-39.
102. Homer, K. A., Denbow, L., & Beighton, D. (1993). Spectrophotometric method for the assay of glycosaminoglycans and glycosaminoglycan-depolymerizing enzymes. *Analytical biochemistry, 214*, 435-441.
103. Content-Audonneau, J. L., Jeanmaire, C., & Pauly, G. (1998). A histological study of human wrinkly strucutres; comparison between sun-exposed areas of the face, with or without wrinkles, and sun-protected areas. *British Journal of Dermatology, 140*, 1038-1047.
104. Werth, B. B., Bashir, M., Chang, L., & Werth, V. P. (2011). Ultraviolet irradiation induces the accumulation of chondroitin sulfate, but not other glycosaminoglycans, in human skin. *PLoS One, 6*(8), 1-11.
105. Schaefer, L., & Schaefer, R. M. (2009). Proteoglycans: from structural compounds to signaling molecules. *Cell and Tissue Research, 339*(1), 237-246.
106. Rees, S. G., Dent, C. M., & Caterson, B. (2009). Metabolism of proteoglycans in tendon. *Scandinavian Journal of Medicine & Science in Sports, 19*(4), 470-478.
107. Yoon, J. H., & Halper, J. (2005). Tendon proteoglycans: biochemistry and function. *Journal of Musculoskeletal and Neuronal Interactions, 5*(1), 22-34.
108. Kalamajski, S., & Oldberg, A. (2010). The role of small leucine-rich proteoglycans in collagen fibrillogenesis. *Matrix biology, 29*, 248-253.
109. Li, Y., Liu, Y., Xia, W., Lei, D., Voorhees, J. J., & Fisher, G. J. (2013). Age-dependent alterations of decorin glycosaminoglycans in human skin. *Scientific reports, 3*(2422), 1-8.
110. Chakravarti, S., Magnuson, T., Lass, J. H., Jepsen, K. J., LaMantia, C., & Carroll, H. (1998). Lumican regulates collagen fibril assembly: skin fragility and corneal opacity in the absence of lumican. *The Journal of cell biology, 141*(5), 1277-1286.
111. Carrino, D. A., Sorrell, J. M., & Caplan, A. I. (2000). Age-related Changes in the Proteoglycans of Human Skin. *Archives of Biochemistry and Biophysics, 373*(1), 91-101.
112. Madhan, B., Rao, J. R., & Nair, B. U. (2010). Studies on the removal of inter-fibrillary materials. I. Removal of protein, proteoglycan, glycosoaminoglycans from

conventional beamhouse process. *Journal of the American Leather Chemists Association, 105*(5), 145-149.
113. Saraswathy, N., & Ramalingam, P. (2011). 16 - Glycoproteomics. In N. Saraswathy & P. Ramalingam (Eds.), *Concepts and Techniques in Genomics and Proteomics* (pp. 213-218): Woodhead Publishing.
114. Stepper, J., Shastri, S., Loo, T. S., Preston, J. C., Novak, P., Man, P., Moore, C. H., Havlíček, V., Patchett, M. L., & Norris, G. E. (2011). Cysteine S-glycosylation, a new post-translational modification found in glycopeptide bacteriocins. *FEBS LETTERS, 585*(4), 645-650.
115. Argraves, W. S., Greene, L. M., Cooley, M. A., & Gallagher, W. M. (2003). Fibulins: physiological and disease perspectives. *EMBO reports, 4*(12), 1127-1131.
116. Kadoya, K., Sasaki, T., Kostka, G., Timpl, R., Matsuzaki, K., Kumagai, N., Sakai, L., Nishiyama, T., & Amano, S. (2005). Fibulin-5 deposition in human skin: decrease with ageing and ultraviolet B exposure and increase in solar elastosis. *British Journal of Dermatology, 153*(3), 607-612.
117. Pankov, R., & Yamada, K. M. (2002). Fibronectin at a glance. *Journal of Cell Science, 115*, 3861-3863.
118. Loeys, B., Maldergem, L. V., Mortier, G., Coucke, P., Gerniers, S., Naeyaert, J.-M., & Paepe, A. D. (2002). Homozygosity for a missense mutation in fibulin-5 (FBLN5) results in a severe form of cutis laxa. *Human molecular genetics, 11*(18), 2113-2118.
119. Kornak, U., Reynders, E., Dimopoulou, A., Van Reeuwijk, J., Fischer, B., Rajab, A., Budde, B., Nürnberg, P., Foulquier, F., & Dobyns, W. B. (2008). Impaired glycosylation and cutis laxa caused by mutations in the vesicular H+-ATPase subunit ATP6V0A2. *Nature genetics, 40*(1), 32.
120. Pelckmans, J. T., Fennen, J., & Christner, J. (2008). Advances in the degreasing of hides. *World Leather*, 31-33.
121. Nicolaides, N., Fu, H. C., & Rice, G. R. (1968). The skin surface lipids of man compared with those of eighteen species of animals. *Journal of Investigative Dermatology, 51*(2), 83-89.
122. Pappas, A. (2015). Skin Lipids: An Introduction and Their Importance. In A. Pappas (Ed.), *Lipids and Skin Health* (pp. 3-5). Cham: Springer International Publishing.
123. Drake, D. R., Brogden, K. A., Dawson, D. V., & Wertz, P. W. (2008). Thematic review series: skin lipids. Antimicrobial lipids at the skin surface. *Journal of lipid research, 49*(1), 4-11.
124. Feingold, K. R. (2007). Thematic review series: skin lipids. The role of epidermal lipids in cutaneous permeability barrier homeostasis. *Journal of lipid research, 48*(12), 2531-2546.
125. Smith, K., & Thiboutot, D. (2008). Thematic review series: skin lipids. Sebaceous gland lipids: friend or foe? *Journal of lipid research, 49*(2), 271-281.
126. Downing, D. T., & Lindholm, J. S. (1982). Skin surface lipids of the cow. *Comparative Biochemistry and Physiology, 73*(2), 327-330.
127. Greene, R. S., Downing, D. T., Pochi, P. E., & Strauss, J. S. (1970). Anatomical variation in the amount and composition of human skin surface lipid. *Journal of Investigative Dermatology, 54*(3), 240-247.
128. Ramasastry, P., Downing, D. T., Pochi, P. E., & Strauss, J. S. (1970). Chemical composition of human skin surface lipids from birth to puberty. *Journal of Investigative Dermatology, 54*(2), 139-144.
129. van-Stiphout, T. A. P., Pel, L., Galvosas, P., Prabakar, S., & Holmes, G. (2015). *NMR transverse relaxation analysis of leather looseness*. Technische Universiteit Eindhoven, Eindhoven.

130. Basil-Jones, M. M., Edmonds, R. L., Norris, G. E., & Haverkamp, R. G. (2012). Collagen fibril alignment and deformation during tensile strain of leather: a small-angle x-ray scattering study. *Journal of Agricultural and Food Chemistry, 60*, 1201-1208.
131. Mohanaradhakrishnan, V., Muthiah, P., & Hadhanyi, A. (1975). A few factors contributing to the mechanical strength of collagen fibres. *Arzneimittel-Forschung, 25*(5), 726-735.
132. Ornes, C. L., Roddy, W. T., & Mellon, E. F. (1960). Study of the effect of the elastic tissue of hide on the physical properties of leather. *Journal of the American Leather Chemists Association, 55*, 600-621.
133. Montes, G. S., & Junqueira, L. C. U. (1991). The use of the picrosirius polarization method for the study of the biopathology of collagen. *Memorias do Instituto Oswaldo Cruz, 86*, 1-11.
134. Junqueira, L. C. U., Bignolas, G., & Brentani, R. R. (1979). Picrosirius staining plus polarization microscopy, a specific method for collagen detection in tissue sections. *The Histochemical Journal, 11*(4), 447-455.
135. Antunes, A. P. M., Covington, A. D., Petford, N., Murray, T., & Wertheim, D. (2013). Three-dimensional visualization of dermal skin structure using confocal laser scanning microscopy. *Journal of Microscopy, 251*(1), 14-18.
136. Jor, J. W. Y., Nielsen, P. M. F., Nash, M. P., & Hunter, P. J. (2011). Modelling collagen fibre orientation in porcine skin based upon confocal laser scanning microscopy. *Skin Research and Technology, 17*, 149-159.
137. Vogel, B., Siebert, H., Hofmann, U., & Frantz, S. (2015). Determination of collagen content within picrosirius red stained paraffin-embedded tissue sections using fluorescence microscopy. *MethodsX, 2*, 124-134.
138. George, G. (1950). Aldehyde-fuchsin: a new stain for elastic tissue. *American Journal of Clinical Pathology, 20*(7), 665-666.
139. Ushiki, T. (2002). Collagen fibers, reticular fibers and elastic fibers. A comprehensive understanding from a morphological viewpoint. *Archives of histology and cytology, 65*(2), 109-126.
140. Bancroft, J. D., Gamble, M., & Jones, M. L. (2008). Connective Tissues and Stains. In J. D. Bancroft & M. Gamble (Eds.), *Theory and practice of histological techniques* (pp. 135-160): Elsevier Health Sciences.
141. Gurr, E. (1971). *Synthetic Dyes in Biology, Medicine and Industry*. New York: Academic Press.
142. Rasband, W. S. (2010). ImageJ. Retrieved from http://rsb.info.nih.gov/ij/
143. Bourke, P. (2002). Lens correction and distortion. Retrieved from http://local.wasp.uwa.edu.au/~pbourke/miscellaneous/lenscorrection/
144. Unser, M. (2011). Extended depth of field. Retrieved from http://bigwww.epfl.ch/demo/edf/index.html
145. Landini, G. (2010). How to correct background illumination in brightfield microscopy. Retrieved from http://imagejdocu.tudor.lu/doku.php?id=howto:working:how_to_correct_background_illumination_in_brightfield_microscopy
146. Thévenaz, P., & Unser, M. (2007). User-Friendly Semiautomated Assembly of Accurate Image Mosaics in Microscopy. *Microscopy Research and Technique, 70*(2), 135-146.
147. Sage, D. (1970). OrientationJ. Retrieved from http://bigwww.epfl.ch/demo/orientation/

148. Ruifrok, A. C., & Johnston, D. A. (2001). Quantification of histochemical staining by color deconvolution. *Analytical and Quantitative Cytology and Histology, 23*, 291-299.
149. Rasband, W., & Landini, G. (2004). Calculator Plus. Retrieved from http://rsbweb.nih.gov/ij/plugins/calculator-plus.html
150. Sizeland, K. H., Basil-Jones, M. M., Edmonds, R. L., Cooper, S. M., Kirby, N., Hawley, A., & Haverkamp, R. G. (2013). Collagen orientation and leather strength for selected mammals. *Journal of Agricultural and Food Chemistry, 61*, 887-892.
151. Pelchmans, J. T., Fennen, J., & Christner, J. (2008). Advances in the degreasing of hides. *World Leather*, 31-33.
152. Masuko, T., Minami, A., Iwasaki, N., Majima, T., Nishimura, S.-I., & Lee, Y. C. (2005). Carbohydrate analysis by a phenol–sulfuric acid method in microplate format. *Analytical biochemistry, 339*(1), 69-72.
153. Huynh, M. B., Morin, C., Carpentier, G., Garcia-Filipe, S., Talhas-Perret, S., Barbier-Chassefière, V., van Kuppevelt, T. H., Martelly, I., Albanese, P., & Papy-Garcia, D. (2012). Age-related changes in glycosaminoglycans from rat myocardium involve altered capacities to potentiate growth factors functions and heparan sulfate altered sulfation. *Journal of Biological Chemistry*, 1-22.
154. Homer, K. A., Denbow, L., & Beighton, D. (1993). Spectrophotometric method for the assay of glycosaminoglycans and glycosaminoglycan-depolymerizing enzymes. *Analytical biochemistry, 214*(2), 435-441.
155. Albalasmeh, A. A., Berhe, A. A., & Ghezzehei, T. A. (2013). A new method for rapid determination of carbohydrate and total carbon concentrations using UV spectrophotometry. *Carbohydrate polymers, 97*(2), 253-261.
156. Kubaski, F., Osago, H., Mason, R. W., Yamaguchi, S., Kobayashi, H., Tsuchiya, M., Orii, T., & Tomatsu, S. (2017). Glycosaminoglycans detection methods: applications of mass spectrometry. *Molecular genetics and metabolism, 120*(1-2), 67-77.
157. Anderson, S. M., & Elliot, R. J. (1991). A dye-binding assay for soluble elastin. *Biochemical Society Transactions, 19*(4), 388S.
158. Bischoff, R., & Schluter, H. (2012). Amino acids: Chemistry, functionality and selected non-enzymatic post-translational modifications. *Journal of Proteomics, 75*, 2275-2296.
159. Kliment, C. R., Englert, J. M., Crum, L. P., & Oury, T. D. (2011). A novel method for accurate collagen and biochemical assessment of pulmonary tissue utilizing one animal. *International journal of clinical and experimental pathology, 4*(4), 349.
160. Neuman, R. E., & Logan, M. A. (1950). The determination of hydroxyproline. *Journal of Biological Chemistry, 184*, 299-306.
161. Eyre, D. R., Weis, M. A., & Wu, J.-J. (2008). Advances in collagen cross-link analysis. *Methods, 45*(1), 65-74.
162. Last, J. A., Armstrong, L. G., & Reiser, K. M. (1990). Biosynthesis of collagen crosslinks. *International Journal of Biochemistry, 22*(6), 559-564.
163. Choudhury, S. D., & Norris, G. (2005). *Improved binary high performance liquid chromatography for amino acid analysis of collagens.* Paper presented at the Proceedings of The First International Conference on Sensing Technology, Palmerston North, New Zealand.
164. Nguyen, Q., Fanous, M. A., Kamm, L. H., Khalili, A. D., Schuepp, P. H., & Zarkadas, C. G. (1986). A comparison of the amino acid composition of two commercial porcine skins (rind). *Journal of Agricultural and Food Chemistry, 34*(3), 565-572.

165. Piez, K. A., & Gross, J. (1960). The amino acid composition of some fish collagens: The relation between composition and structure. *Journal of Biological Chemistry, 235*(4), 995-998.
166. Fountoulakis, M., & Lahm, H.-W. (1998). Hydrolysis and amino acid composition analysis of proteins. *Journal of Chromatography A, 826*(2), 109-134.
167. Cohen, S. A., & Michaud, D. P. (1993). Synthesis of a fluorescent derivatizing reagent, 6-aminoquinolyl-N-hydroxysuccinimidyl carbamate, and its application for the analysis of hydrolysate amino acids via high-performance liquid chromatography. *Analytical biochemistry, 211*(2), 279-287.
168. Naffa, R., Maidment, C., Holmes, G., & Norris, G. E. (2019). Insights into the molecular composition of the skins and hides used in leather manufacture. *The Journal of the American Leather Chemists Association, 114*, 29-37.
169. Wong, R., Geyer, S., Weninger, W., Guimberteau, J.-C., & Wong, J. K. (2016). The dynamic anatomy and patterning of skin. *Experimental Dermatology, 25*(2), 92-98.
170. Asghar, A., & Henrickson, R. L. (1982). *Advances in food research* (C. O. Chichester Ed. Vol. 28). New York: Academic Press.
171. Uzawa, K., Yeowell, H. N., Yamamoto, K., Mochida, Y., Tanzawa, H., & Yamauchi, M. (2003). Lysine hydroxylation of collagen in a fibroblast cell culture system. *Biochemical and Biophysical Research Communications, 305*(3), 484-487.
172. Piez, K. (1954). The separation of the diastereoisomers of isoleucine and hydroxylysine by ion exchange chromatography. *Journal of Biological Chemistry, 207*(1), 77-80.
173. Hamilton, P. B., & Anderson, R. A. (1955). Hydroxylysine: isolation from gelatin and resolution of its diastereoisomers by ion exchange chromatography. *Journal of Biological Chemistry, 213*(1), 249-258.
174. Nakornchai, S., Atsawasuwan, P., Kitamura, E., Surarit, R., & Yamauchi, M. (2004). Partial biochemical characterisation of collagen in carious dentin of human primary teeth. *Archives of oral biology, 49*(4), 267-273.
175. Naffa, R., Holmes, G., Zhang, W., Maidment, C., Shehadi, I., & Norris, G. (2019). Comparison of liquid chromatography with fluorescence detection to liquid chromatography-mass spectrometry for amino acid analysis with derivatisation by 6-aminoquinolyl-N-hydroxysuccinimidyl-carbamate: Applications for analysis of amino acids in skin. *Arabian Journal of Chemistry*, 1-12.
176. Keller, U., Prudova, A., Eckhard, U., Fingleton, B., & Overall, C. M. (2013). Systems-level analysis of proteolytic events in increased vascular permeability and complement activation in skin inflammation. *Science Signaling, 6*(258), 1-14.
177. Lundberg, K. C., Fritz, Y., Johnston, A., Foster, A. M., Baliwag, J., Gudjonsson, J. E., Schlatzert, D., Gokulrangan, G., McCormick, T. S., Chancet, M. R., & Wards, N. L. (2015). Proteomics of skin proteins in Psoriasis: From discovery and verification in a mouse model to confirmation in humans. *The American Society for Biochemistry and Molecular Biology, 14*(1), 109-119.
178. Vogel, C., & Marcotte, E. M. (2012). Insights into the regulation of protein abundance from proteomic and transcriptomic analyses. *Nature Reviews Genetics, 13*(4), 227.
179. Switzar, L., Giera, M., & Niessen, W. M. (2013). Protein digestion: an overview of the available techniques and recent developments. *Journal of proteome research, 12*(3), 1067-1077.
180. Zakharchenko, O., Greenwood, C., Alldridge, L., & Souchelnytskyi, S. (2011). Optimized protocol for protein extraction from the breast tissue that is compatible with two-dimensional gel electrophoresis. *Breast cancer: basic and clinical research, 5*, 38-42.

181. Jiang, X., Jiang, X., Feng, S., Tian, R., Ye, M., & Zou, H. (2007). Development of efficient protein extraction methods for shotgun proteome analysis of formalin-fixed tissues. *Journal of proteome research, 6*(3), 1038-1047.
182. Sheoran, I. S., Ross, A. R., Olson, D. J., & Sawhney, V. K. (2009). Compatibility of plant protein extraction methods with mass spectrometry for proteome analysis. *Plant Science, 176*(1), 99-104.
183. López, J., Imperial, S., Valderrama, R., & Navarro, S. (1993). An improved Bradford protein assay for collagen proteins. *Clinica chimica acta, 220*(1), 91-100.
184. Duhamel, R. C., Meezan, E., & Brendel, K. (1981). The addition of SDS to the Bradford dye-binding protein assay, a modification with increased sensitivity to collagen. *Journal of biochemical and biophysical methods, 5*(2), 67-74.
185. Barbour, J., Wiese, S., Meyer, H. E., & Wascheid, B. (2011). Mass Spectrometry. In J. v. Hagan (Ed.), *Proteomics Sample Preparation* (pp. 43-127). Weinheim, Germany: Wiley.
186. Kuzyk, M. A., Hardie, D. B., Yang, J., Smith, D. S., Jackson, A. M., Parker, C. E., & Borchers, C. H. (2010). A quantitative study of the effects of chaotropic agents, surfactants, and solvents on the digestion efficiency of human plasma proteins by trypsin. *Journal of proteome research, 9*(10), 5422-5437.
187. Burkhart, J. M., Schumbrutzki, C., Wortelkamp, S., Sickmann, A., & Zahedi, R. P. (2012). Systematic and quantitative comparison of digest efficiency and specificity reveals the impact of trypsin quality on MS-based proteomics. *Journal of Proteomics, 75*(4), 1454-1462.
188. Mikesh, L. M., Aramadhaka, L. R., Moskaluk, C., Zigrino, P., Mauch, C., & Fox, J. W. (2013). Proteomic anatomy of human skin. *Journal of Proteomics, 84*, 190-200.
189. Lorenzo, P., Aspberg, A., Önnerfjord, P., Bayliss, M. T., Neame, P. J., & Heinegård, D. (2001). Identification and characterization of asporin a novel member of the leucine-rich repeat protein family closely related to decorin and biglycan. *Journal of Biological Chemistry, 276*(15), 12201-12211.
190. Bornstein, P. (2009). Matricellular proteins: an overview. *Journal of cell communication and signaling, 3*(3-4), 163–165.
191. Rabilloud, T. (1998). Use of thiourea to increase the solubility of membrane proteins in two-dimensional electrophoresis. *ELECTROPHORESIS, 19*(5), 758-760.
192. Telis, V., Wolf, K., & Sobral, P. (2006). *Characterizations of collagen fibers for biodegradable films production.* Paper presented at the 13th World Congress of Food Science & Technology 2006.
193. Rodia, P. M., Bocco Gianello, M. D., Corregido, M. C., & Gennaro, A. M. (2014). Comparative study of the interaction of CHAPS and Triton X-100 with the erythrocyte membrane. *Biochimica et Biophysica Acta (BBA)-Protein Structure, 1838*(3), 859-866.
194. Woodlock, A. F., & Harrap, B. S. (1968). The effects of salts on the stability of the collagen helix under acidic conditions. *Australian Journal of Biological Sciences, 21*, 821-826.
195. Glanville, R. W., Breitkreutz, D., Meitinger, M., & Fietzek, P. P. (1983). Completion of the amino acid sequence of the α1 chain from type I calf skin collagen. Amino acid sequence of α1 (I) B8. *Biochemical Journal, 215*(1), 183-189.
196. Karppinen, S. M., Honkanen, H. K., Heljasvaara, R., Riihilä, P., Autio-Harmainen, H., Sormunen, R., Harjunen, V., Väisänen, M. R., Väisänen, T., & Hurskainen, T. (2016). Collagens XV and XVIII show different expression and localisation in cutaneous squamous cell carcinoma: type XV appears in tumor stroma, while XVIII

becomes upregulated in tumor cells and lost from microvessels. *Experimental Dermatology, 25*(5), 348-354.
197. Miyahara, T., Murai, A., Tanaka, T., Shiozawa, S., & Kameyama, M. (1982). Age-related Differences in Human Skin Collagen: Solubility in Solvent, Susceptibility to Pepsin Digestion, and the Spectrum of the Solubilized Polymeric Collagen Molecules1. *Journal of Gerontology, 37*(6), 651-655.
198. Perides, G., Asher, R., Lark, M., Lane, W., Robinson, R., & Bignami, A. (1995). Glial hyaluronate-binding protein: a product of metalloproteinase digestion of versican? *Biochemical Journal, 312*(2), 377-384.
199. Saville, C. R., Mallikarjun, V., Holmes, D. F., Emmerson, E., Derby, B., Swift, J., Sherratt, M. J., & Hardman, M. J. (2019). Distinct matrix composition and mechanics in aged and estrogen-deficient mouse skin. *bioRxiv*, 1-34.
200. Choudhury, S. D., Allsop, T., Passman, A., & Norris, G. (2006). Use of a proteomics approach to identify favourable conditions for production of good quality lambskin leather. *Analytical and bioanalytical chemistry, 384*(3), 723-735.
201. Lothrop, A. P., Torres, M. P., & Fuchs, S. M. (2013). Deciphering post-translational modification codes. *FEBS LETTERS, 587*(8), 1247-1257.

9. Appendices

9.A 3D confocal images at different locations on raw hide and finished leather

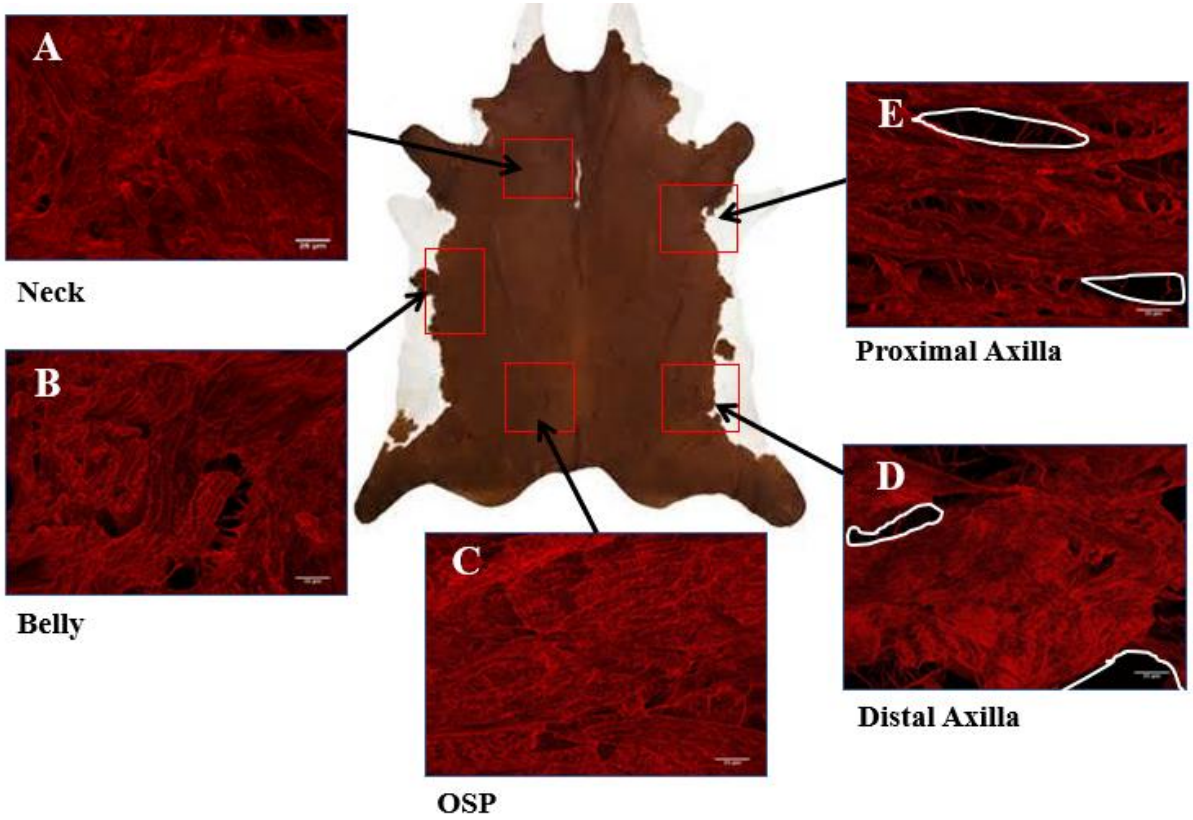

Figure 9.1 Organisation of collagen fibres in the corium layer throughout different regions of the raw hide: (A) Neck, (B) belly, (C) OSP, (D) distal axilla and (E) proximal axilla. In figure D and E white lines are drawn indicating the space between the fibre bundles. Scale bar 25 µm.

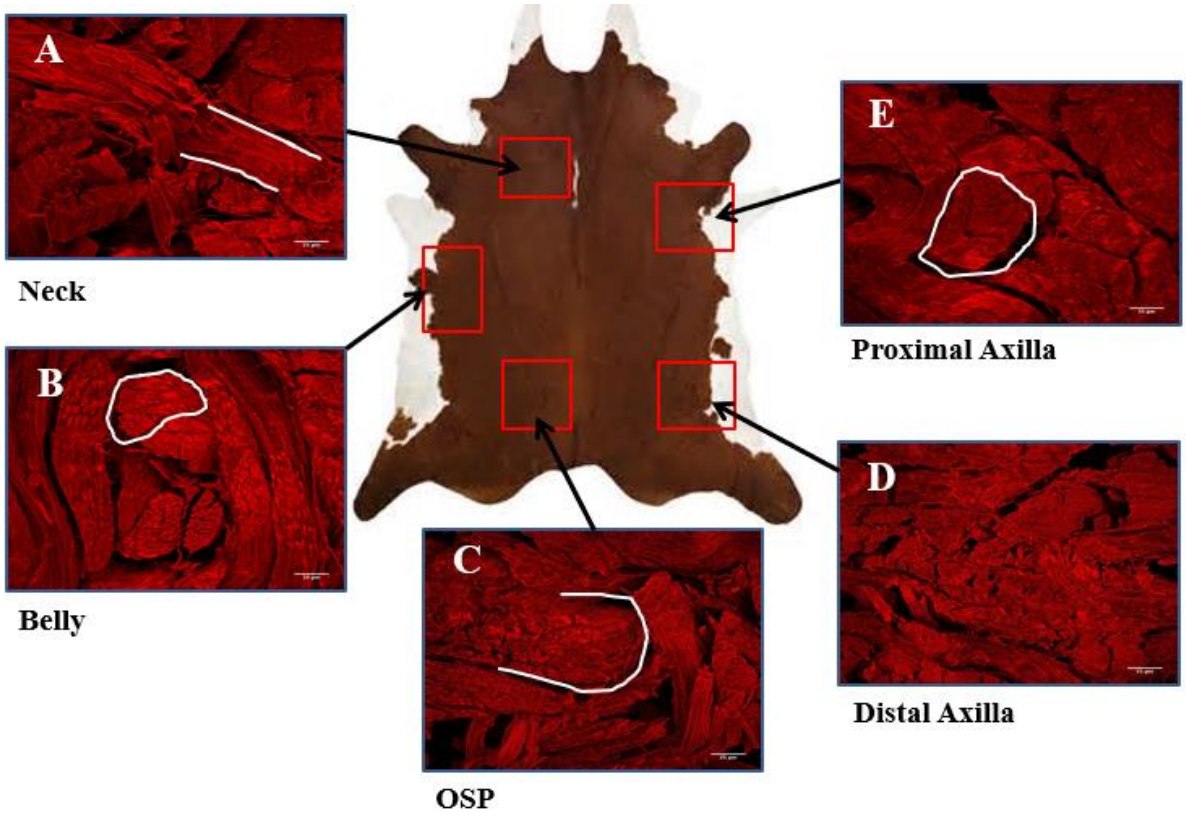

Figure 9.2 Organisation of collagen fibres in the corium layer throughout different regions of the finished leather: (A) Neck, (B) belly, (C) OSP, (D) distal axilla and (E) proximal axilla. White lines indicate collagen fibres grouped together to make collagen bundles. The size, orientation and organisation of the bundles varies not only between different locations on the hide but within the same locations as well. Scale bar 25 µm.

9.B Chromatographic and MS settings for detection of crosslinks

Table 9.1 Instrument configuration.

Instrument	Instrument settings
LC system	Dionex UltiMate™ LPG-3400RS Rapid Separation Quaternary Pump
Mass spectrometer	QExactive Focus
Ionization source	HESI
Analytical column	Cogent Diamond Hydride™, 2.2 µm particle size, 120 Å, 150 x 2.1 mm ID
Flow rate	0.4 mL/min
Column oven temperature	25°C
Buffers	A: 0.1% Formic acid/ MS H_2O B: 0.1% Formic/80% Acetonitrile/ MS H_2O
Gradient	20-60 %A in 10 minutes, then 60-90 %A in 5 min.

Table 9.2 Tune and Method parameter settings.

Parameter	Parameter settings
Capillary temperature	350°C
Sheath gas flow rate	30
Aux gas flow rate	4
Sweep gas flow rate	2
Source voltage [kV]	3.3 kV
S-Lens RF level	50
Aux gas heater temp	110
# Scan ranges	1
Max. injection times	Auto
Full MS mass range	100 - 600 [*m/z*]
AGC target	1e6
Resolution settings	70,000
No. of microscans	1
Spectrum Data	Profile

9.C Chromatographic and MS settings for proteomic analysis

Table 9.3 Instrument Configuration.

Instrument	Information
nanoLC system	Dionex UltiMate™ 3000 RSLCnano System
Mass spectrometer	Q Exactive Plus
Ionization source	Nano Flex
Trapping cartridge	PepMap100 C18, 5 µm particle size, 300 µm inner diameter, 5 mm length
Analytical column	PepMap C18, 2 µm particle size, 75 µm inner diameter, 50 cm length
Flow rates	Trap: 25 µL/min Analytical: 300 nL/min
Column oven temperature	50°C
Gradient	3-30% Acetonitrile in 0.1% formic acid over 55 minutes

Table 9.4 Method parameter settings.

Parameter	Settings
Capillary temperature	250°C
S-Lens RF level	50%
Source voltage [kV]	1.6
Max. injection times	Full MS 100 ms, MSn 150 ms (HCD)
Full MS mass range	375 - 1500 [*m/z*]
AGC target	Full MS 3e6, MS*n* (HCD) 5e5
Resolution settings	Full MS 70,000, MS*n* (HCD) 17,500
No. of microscans	Full MS 1
Isolation width [*m/z*]	1.4
Loop count (TopN)	10
MSX count	1
Collision energies	25, 30, 35
Charge Exclusion	Unassigned, 1, 6-8, >8
Peptide match	Preferred
Exclude isotopes	On
Dynamic Exclusion [s]	10
Detector for MS*n* spectra	Orbitrap

A

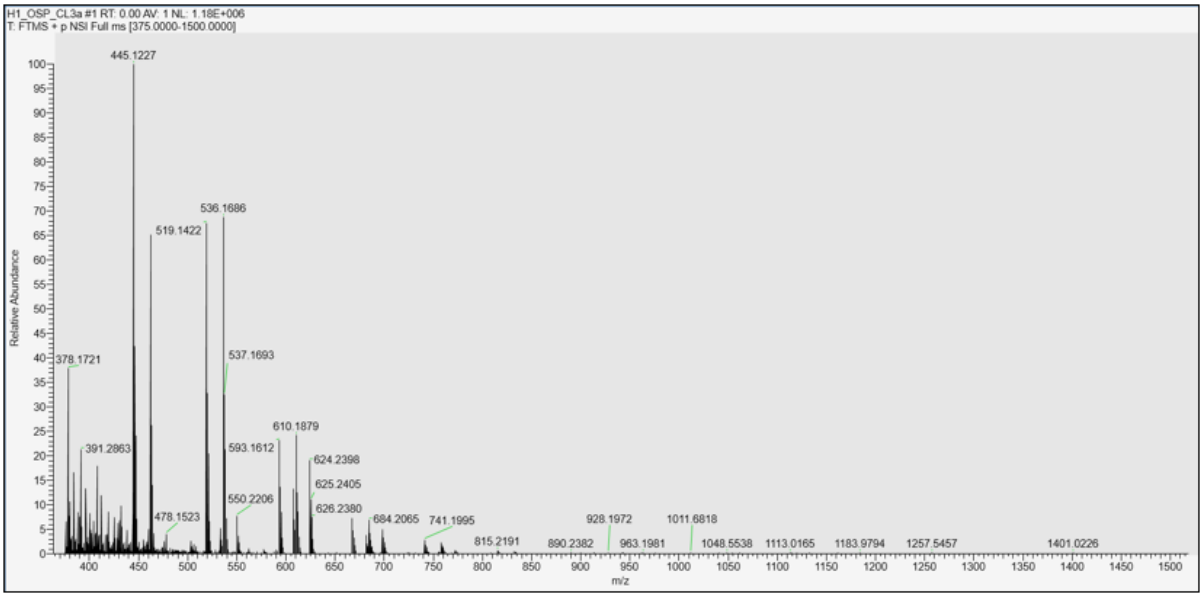

B

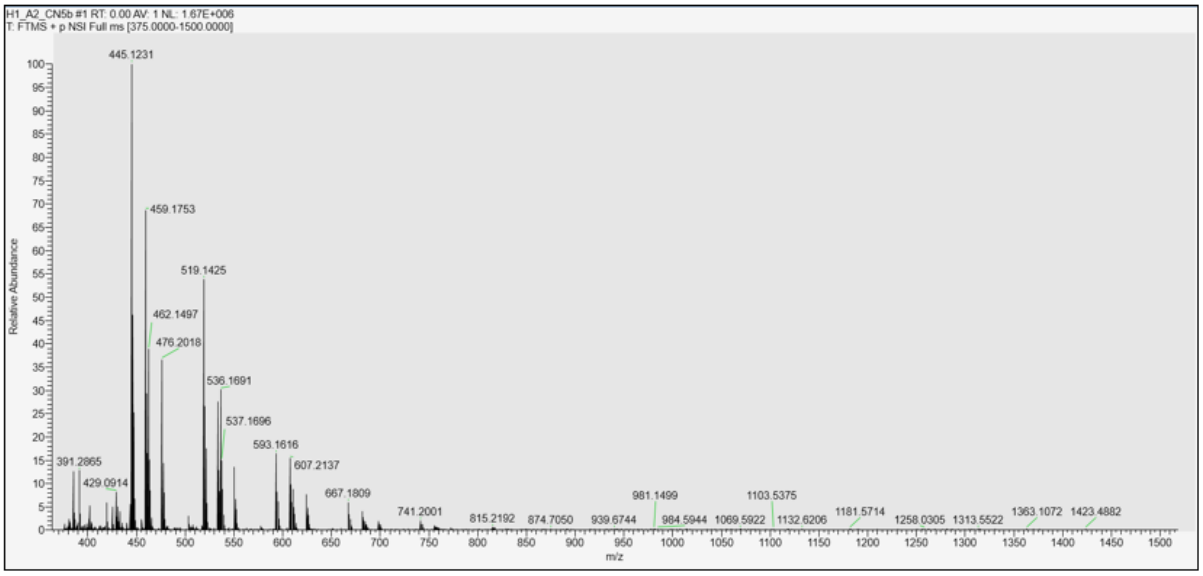

Figure 9.3 Example of a mass spectrum of peptides from samples extracted from (A) lysis buffer and (B) NaCl buffer.

9.D MS database search

Table 9.5 Search Engine

Search Parameter	Setting
Search engine	Proteome Discoverer v 2.2 SP1
Database	SwissProt on 21 Oct 2016
Taxonomy	Bovine
Enzyme	Trypsin
Max # of missed cleavages	2
Min peptide length	6
Precursor mass tolerance	10 ppm
Fragment mass tolerance	0.02 Da
# 13C	1
Peptide charge	2+, 3+, 4+
Protein mass	Unrestricted
Decoy database search	Enabled
Significance threshold	0.01%
Instrument type	Q-Exactive-General
Static modifications	Carbamidomethyl (C)
Variable modifications	Oxidation (M/K/P), N-terminal acetylation (N/G), Galactosyl (K), Glucosylgalactosyl (K), Hex (K)
Experimental mass values	Monoisotopic
False Discovery Rate (FDR)	Fixed to 1%

9.E Manual normalisation step for proteomic analysis

Abundances were normalised manually using the following steps:

a. Divide abundance by abundance count for each sample/protein (=abundance/abundance count).
b. Sum up each abundance (=sum(value1-valuex).
c. Work out which one is the maximum summed value (this will be used as a base). To make this easier can use equation (=max(value1-x).
d. Calculate factors for each sample (=maxed sum value/value of sample).

A mock example of how to normalise abundances is found in Table 9.6.

Significance was determined using T-tests to get p-values, p-values under 0.05 were considered significant:

a. Average technical replicates, keep biological replicates separate.
b. For each averaged biological replicate work out the log10 value (=log10(value)).
c. Use the T-test function in excel to determine the p-value: (=ttest(control;treated;2;1).
d. Sort the values based on the T-test values smallest to largest for easiest analysis of which samples are significant (below 0.05) or not (above 0.05).

Volcano plots were created manually in excel to observe differences in the pattern of up and down-regulated proteins:

a. Fold change of samples want to compare (=average(control)/average(treated)).
b. Log10value of fold change value (=log10(fold change)).
c. -log10value of p-values (=-log10(pvalue)).
d. Graph log10(fold change) vs -log10(pvalue) via scatter plot.

A mock example of how to calculate T-tests and create volcano plots is found in Table 9.7.

Table 9.6 Mock example of how to normalise abundances.

	Abundance				**Abundance Count**			
Accession	**Grain 1**	**Grain 2**	**Grain 3**	**Grain 4**	**Grain 1**	**Grain 2**	**Grain 3**	**Grain 4**
AAI05185.1	5.40E+09	3.59E+10	2.34E+09	2.37E+10	176	179	138	189
XP_024846030.1	1.10E+10	2.46E+10	1.04E+10	3.13E+10	239	216	227	230
AAI49096.1	3.48E+09	1.55E+10	2.22E+09	1.41E+10	148	152	106	156
XP_024852938.1	6.81E+09	6.27E+09	2.08E+09	6.83E+09	168	130	128	139
XP_002687292.2	2.12E+10	5.33E+10	4.18E+10	7.33E+10	96	95	103	98
DAA18432.1	3.97E+10	5.22E+10	4.02E+10	9.82E+10	89	90	86	89
NP_001193443.1	2.28E+09	4.26E+09	1.10E+09	3.89E+09	117	101	102	110
XP_005220820.1	3.09E+10	4.26E+10	4.54E+10	4.65E+10	90	79	88	81
AAI49078.1	1.26E+10	2.76E+10	2.61E+10	3.82E+10	72	72	75	73
NP_001179297.1	1.54E+09	1.92E+09	1.47E+09	3.09E+09	145	117	143	132
	Abundance/Count				**Normalised Abundance**			
Accession	Grain 1	Grain 2	Grain 3	Grain 4	Grain 1	Grain 2	Grain 3	Grain 4
AAI05185.1	3.06E+07	2.00E+08	1.69E+07	1.26E+08	1.36E+10	4.72E+10	4.28E+09	2.37E+10
XP_024846030.1	4.62E+07	1.14E+08	4.60E+07	1.36E+08	2.77E+10	3.23E+10	1.91E+10	3.13E+10
AAI49096.1	2.34E+07	1.02E+08	2.09E+07	9.01E+07	8.72E+09	2.03E+10	4.07E+09	1.41E+10
XP_024852938.1	4.06E+07	4.84E+07	1.63E+07	4.93E+07	1.71E+10	8.24E+09	3.80E+09	6.83E+09
XP_002687292.2	2.20E+08	5.63E+08	4.07E+08	7.45E+08	5.31E+10	7.00E+10	7.65E+10	7.33E+10
DAA18432.1	4.48E+08	5.81E+08	4.66E+08	1.10E+09	9.97E+10	6.86E+10	7.37E+10	9.82E+10
NP_001193443.1	1.94E+07	4.22E+07	1.08E+07	3.55E+07	5.72E+09	5.60E+09	2.02E+09	3.89E+09
XP_005220820.1	3.44E+08	5.42E+08	5.16E+08	5.71E+08	7.76E+10	5.60E+10	8.31E+10	4.65E+10
AAI49078.1	1.74E+08	3.84E+08	3.49E+08	5.26E+08	3.17E+10	3.63E+10	4.78E+10	3.82E+10
NP_001179297.1	1.06E+07	1.64E+07	1.03E+07	2.35E+07	3.87E+09	2.53E+09	2.70E+09	3.09E+09
Sum	1.36E+09	2.59E+09	1.86E+09	3.41E+09				
Factor	2.51	1.31	1.83	1.00				

Table 9.7 Mock example of how to calculate T-tests and volcano plots.

No.	OSP				Distal Axilla				P-value	Factor
	Grain 1	Grain 2	Grain 3	Grain 4	Grain 1	Grain 2	Grain 3	Grain 4	=ttest(Log10OSP; Log10Distal axilla;2;1)	=OSP/Distal axilla
1	4.64E+10	5.90E+10	1.02E+11	5.60E+10	1.43E+11	6.60E+10	1.09E+11	2.10E+11	0.1412	0.9743
2	4.61E+10	3.50E+10	4.77E+10	3.43E+10	2.42E+10	2.74E+10	1.89E+10	4.64E+10	0.2518	1.0157
3	4.43E+10	5.25E+10	3.77E+10	5.05E+10	3.75E+10	7.74E+10	3.42E+10	5.32E+10	0.7390	0.9982
4	3.36E+10	3.62E+10	3.37E+10	2.69E+10	3.27E+10	3.40E+10	2.69E+10	5.51E+10	0.6700	0.9959
5	3.01E+10	2.50E+10	1.65E+10	2.38E+10	2.82E+10	3.66E+10	2.32E+10	2.75E+10	0.1459	0.9916
6	2.97E+10	1.33E+10	7.76E+09	1.04E+10	3.88E+10	1.61E+10	3.70E+10	2.00E+10	0.1242	0.9722
7	2.65E+10	2.15E+10	1.41E+10	2.22E+10	2.71E+10	3.30E+10	2.20E+10	2.71E+10	0.0717	0.9886
8	2.53E+10	9.44E+10	9.85E+09	4.30E+10	7.19E+09	1.23E+11	4.33E+09	1.22E+10	0.1229	1.0328
9	2.38E+10	1.73E+10	1.29E+10	1.94E+10	5.65E+09	2.38E+09	5.50E+09	1.46E+10	0.0528	1.0508
10	2.16E+10	1.48E+10	1.55E+10	2.36E+10	8.44E+09	9.45E+09	8.81E+09	1.39E+10	0.0107	1.0270
No.	**Log10 OSP**				**Log10 Distal Axilla**				**Log(Factor)**	**-log(p-value)**
	Grain 1	**Grain 2**	**Grain 3**	**Grain 4**	**Grain 1**	**Grain 2**	**Grain 3**	**Grain 4**	=Log10(Factor)	=-Log10(p-value)
1	10.67	10.77	11.01	10.75	11.16	10.82	11.04	11.32	-0.0113	0.8502
2	10.66	10.54	10.68	10.53	10.38	10.44	10.28	10.67	0.0068	0.5990
3	10.65	10.72	10.58	10.70	10.57	10.89	10.53	10.73	-0.0008	0.1314
4	10.53	10.56	10.53	10.43	10.51	10.53	10.43	10.74	-0.0018	0.1740
5	10.48	10.40	10.22	10.38	10.45	10.56	10.37	10.44	-0.0036	0.8359
6	10.47	10.12	9.89	10.02	10.59	10.21	10.57	10.30	-0.0122	0.9060
7	10.42	10.33	10.15	10.35	10.43	10.52	10.34	10.43	-0.0050	1.1445
8	10.40	10.97	9.99	10.63	9.86	11.09	9.64	10.09	0.0140	0.9104
9	10.38	10.24	10.11	10.29	9.75	9.38	9.74	10.16	0.0215	1.2776
10	10.34	10.17	10.19	10.37	9.93	9.98	9.95	10.14	0.0116	1.9699

9.F 50 most abundant proteins identified using lysis and NaCl/Urea extraction methods

Table 9.8 50 most abundant proteins extracted *via* the lysis extraction buffer in the three different layers of hide; grain, grain to corium junction and corium.

		% Abundance		
Protein	**Accession no.**	*Grain*	*Junction*	*Corium*
Collagens				
Collagen type I, alpha 1	AAI05185.1	3.33	8.74	18.62
Collagen type I, alpha 2	AAI49096.1	1.58	4.39	9.62
Collagen type V, alpha 2	XP_024835542.1			0.16
Collagen type VI, alpha 1	DAA32939.1	2.20	3.62	4.00
Collagen VII, alpha 1	XP_002697097.2	0.23		
Collagen type XII, alpha 1	DAA26385.1		0.33	0.34
Precursor of collagen III, alpha 1	NP_001070299.1	0.20	0.52	0.71
Isoform 1 of collagen II, alpha 1	DAA29861.1			0.40
Isoform X1 of collagen VI alpha 2	XP_005202110.1	2.01	3.52	3.61
Isoform XI of collagen VI, alpha 3	XP_024846030.1	4.03	6.46	8.96
Isoform XI of collagen VI, alpha 5	XP_024852938.1	1.80	2.09	0.91
Other extracellular proteins				
Decorin A	1XCD	0.39	1.28	5.22
Lumican	Q05443.1	1.58	3.81	11.53
Isoform X1 of heparin cofactor 2	XP_005218256.1			0.16
Precursor of alpha-1-acid glycoprotein	CAH59718.2			0.26
Odorant-binding protein	XP_024844202.1		0.35	0.27
Isoform X1 of prolargin	XP_005216708.2	0.56	1.21	1.83
Precursor of asporin	DAA26584.1	0.14	0.34	0.55
Fibromodulin	P13605.2			0.29
Mimecan	AAI02527.1	0.56	1.75	5.79
Cellular proteins				
Actin, Cytoplasmic 1	3UB5	1.87	3.16	0.81
Annexin A2	4X9P	0.24	0.58	0.28
Desmoplakin	NP_001179297.1	0.46	0.39	
Alpha-tubulin	3EDL	0.19	0.37	
Isoform X1 of lamin	XP_005203678.1	0.31	0.42	0.21
Vimentin	NP_776394.2	0.47	0.77	0.46
Myosin-11	NP_001095597.1	0.18	0.45	
Gelsolin a	DAA26429.1	0.15	0.27	0.28
Isoform X2 of neuroblast differentiation-associated protein	XP_024843439.1	0.34	0.38	0.21
Isoform X7 of plectin	XP_024857680.1	0.31	0.37	0.24
Tubulin beta-4B chain	NP_001029835.1	0.14	0.38	
Elongation factor 1-alpha 1	DAA26396.1	0.38	0.49	0.61
Junction plakoglobin	AAI18115.1	0.17		
Epiplakin	XP_003586920.3	0.16		

Table 9.8 cont.

Protein	Accession no.	% Abundance		
		Grain	Junction	Corium
Enzymes				
Serpin A3-2	DAA17271.1			0.31
Isoform X1 of serpin A3-7	XP_005222191.1			0.16
Isoform 1 of kallikrein-related peptidase 5 preproprotein-like	DAA19722.1	0.24	0.38	0.36
Endo-1,5-alpha-l-arabinanase	4KCA			0.31
Serum proteins				
Alpha-2-macroglobulin	Q7SIH1.2			0.38
Transferrin	AAI22603.1	0.23	0.55	0.97
Complement C3	2B39	0.28	0.36	0.51
Fibrinogen beta chain	DAA20936.1		0.27	0.22
Immunoglobulin gamma heavy chain	AQT27060.1			0.38
Membrane-bound immunoglobulin gamma1 heavy chain constant region	ANN46376.1	0.19	0.37	0.72
Uncharacterized protein				
Hypothetical protein LOC789567	DAA21789.1		0.35	0.24
Keratins				
Keratin 6A	DAA29985.1	0.80	1.24	0.32
Keratin 10	AAI49078.1	8.25	2.16	1.33
Keratin 13	DAA18440.1	0.21	0.32	
Keratin 31	DAA18488.1	0.36	0.28	
Keratin 31	DAA18478.1	0.18		
Keratin 34	AAI18282.1	0.16		
Keratin 77-like	DAA29992.1	0.44		
Keratin 85	AAI19907.1	2.91	2.62	0.65
Keratin 86	DAA30000.1	2.92	2.30	0.66
Keratin, type I cytoskeletal 14	DAA18432.1	11.15	7.23	1.40
Keratin, type I cytoskeletal 17	A1L595.1	1.21	1.39	0.18
Keratin, type I cytoskeletal 25	DAA18454.1		0.26	
Isoform X1 of keratin, type I cuticular Ha3-I	XP_005220820.1		5.45	
Isoform X1 of keratin, type I cuticular Ha3-I	XP_005220820.1	6.45		0.89
Keratin, type II cuticular Hb3	AAI23472.1	7.68	5.06	0.71
Keratin, type II cytoskeletal 1	XP_002687292.2	12.92	2.53	2.08
Keratin, type II cytoskeletal 5	Q5XQN5.1	10.15	6.12	1.84
Keratin, type II cytoskeletal 7	Q29S21.1	0.26	0.38	0.24
Keratin, type II cytoskeletal 71	DAA29980.1	0.15	0.53	
Keratin, type II cytoskeletal 75	NP_001070385.1		0.29	
Isoform X1 of keratin, type II cytoskeletal 79	XP_024847298.1	0.44	0.25	
Keratin, type II cytoskeletal 2 epidermal	XP_024848194.1	1.06	0.39	0.30

Table 9.9 50 most abundant proteins extracted *via* the NaCl/Urea extraction buffer in the three different layers of hide; grain, grain to corium junction and corium.

		% Abundance		
Protein	**Accession no.**	*Grain*	*Junction*	*Corium*
Collagens				
Collagen type I, alpha 1	AAI05185.1	1.42	1.51	3.69
Collagen type I, alpha 2	AAI49096.1	0.39	0.36	0.50
Collagen type VI, alpha 1	DAA32939.1	0.92	1.85	3.18
Precursor of collagen, type III, alpha 1	NP_001070299.1			0.28
Isoform XI of collagen VI, alpha 2	XP_005202110.1	1.12	2.01	4.05
Isoform XI of collagen VI, alpha 3	XP_024846030.1	2.99	5.53	12.67
Isoform XI of collagen VI, alpha 5	XP_024852938.1	0.57	0.71	0.64
Other extracellular proteins				
Bovine Lipocalin Allergen Bos D 2	1BJ7			0.26
Fibromodulin	P13605.2			0.46
Isoform XI of periostin	XP_005213601.1	0.71	0.40	0.78
Isoform XI of prolargin	XP_005216708.2	1.49	2.02	3.42
Isoform XI of protein S100-A7	XP_024840625.1	0.29		
Lumican	Q05443.1	4.19	5.97	18.15
Membrane-bound immunoglobulin gamma1 heavy chain constant region	ANN46376.1	0.25	0.32	0.86
Odorant-binding protein	XP_024844202.1	0.30	0.37	0.44
Precursor of alpha-1-acid glycoprotein	CAH59718.2			0.25
Precursor of asporin precursor	DAA26584.1			0.80
Tenascin-X	CAA72671.1			0.28
Transforming growth factor-beta-induced protein ig-h3	P55906.2			0.33
Cellular proteins				
Actin, Cytoplasmic 1	3UB5	1.45	2.37	1.53
Annexin A1	NP_786978.2	0.33	0.31	
Annexin A2	4X9P	0.64	0.71	0.35
Desmoplakin	NP_001179297.1	0.33	0.38	
Elongation factor 1-alpha 1	DAA26396.1	0.46	0.94	0.77
Gelsolin a	DAA26429.1		0.27	0.31
Heat shock protein family B member 1	AOO19784.1	0.42	0.56	0.31
Histone cluster 2, H2aa3-like	DAA31727.1	0.63	0.69	
Histone H1.3	NP_001094536.1	0.59	0.40	
Histone H2B	AAI40623.1	0.45	0.52	
Isoform X1 of lamin	XP_005203678.1	1.07	1.18	0.47
Isoform X2 of neuroblast differentiation-associated protein	XP_024843439.1	0.92	0.79	0.46
Isoform X7 of plectin	XP_024857680.1	0.28	0.32	0.29
Isoform XI of filamin-A	XP_024843515.1	0.46	0.73	0.40
T-complex Protein 1 Subunit Beta	4B2T	3.11	2.88	3.30

Table 9.9 cont.

		% Abundance		
Protein	**Accession no.**	*Grain*	*Junction*	*Corium*
Cellular proteins cont.				
Vimentin	NP_776394.2	1.83	2.26	1.49
Enzymes				
Enolase 1, alpha	AAI03355.1			0.20
Hydroxyacylglutathione hydrolase, mitochondrial	NP_001030351.1	1.41	1.34	1.63
Isoforom X1 of serpin A3-7	XP_005222191.1			0.22
Precursor of protein disulfide-isomerase A3	AAI49343.1	0.25	0.26	0.26
Serpin A3-2	DAA17271.1			0.25
Serpin A3-5	XP_005222351.1			0.21
Tryptase alpha/beta 1	DAA17281.1	0.22		
Serum proteins				
Alpha-2-macroglobulin	Q7SIH1.2			0.40
Carbonmonoxy Liganded Bovine Hemoglobin, Ph 7.2	1G09	0.31	0.31	0.27
Complement C3	2B39			0.39
Serum albumin	AAN17824.1	3.00	3.38	12.03
Transferrin	AAI22603.1	0.43	0.52	1.16
Uncharacterized proteins				
Uncharacterized protein LOC516742	XP_015318508.1	0.28	0.31	
Keratins				
Keratin 6A	DAA29985.1	0.97	1.54	0.48
Keratin 10	AAI49078.1	4.99	2.16	0.93
Keratin 13	DAA18440.1	0.24	0.39	
Keratin 31	DAA18488.1	0.28	0.34	
Keratin 77-like	DAA29992.1	0.22		
Keratin 85	AAI19907.1	2.79	3.03	0.53
Keratin 86	DAA30000.1	3.61	3.70	0.44
Keratin, type I cytoskeletal 14	DAA18432.1	10.46	8.58	1.21
Keratin, type I cytoskeletal 17	A1L595.1	1.41	1.85	0.22
Keratin, type I cytoskeletal 25	DAA18454.1		0.27	
Isoform XI of keratin, type I cuticular Ha3-I isoform X1	XP_005220820.1	4.77	5.88	0.95
Keratin, type II cuticular Hb3	AAI23472.1	0.53	0.62	
Keratin, type II cytoskeletal 1	XP_002687292.2	9.86	2.87	1.30
Keratin, type II cytoskeletal 5	Q5XQN5.1	11.42	8.55	1.59
Keratin, type II cytoskeletal 7	Q29S21.1	0.24	0.30	0.23
Keratin, type II cytoskeletal 75	NP_001070385.1		0.30	
Keratin, type II cytoskeletal 71	DAA29980.1		0.49	
Isoform X1 of keratin, type II cytoskeletal 79	XP_024847298.1	0.68	0.50	
Keratin, type II cytoskeletal 2 epidermal	XP_024848194.1	0.31		

9.G Down-regulated proteins in loose samples (compared to tight)

Table 9.10 Down-regulated proteins in loose samples, p-values below 0.05 and fold change greater than 2.

Description	Accession	P-value	Factor	Extraction	Layer		
					Grain	*Junction*	*Corium*
Other Extracellular Proteins							
Glial hyaluronate-binding protein	AAB20399.1	0.0432	4.71	NaCl/Urea		☑	
		0.0123	6.33				☑
Isoform X1 of heparin cofactor 2	XP_005218256.1	0.0436	2.20	Lysis	☑		
Precursor of inter-alpha-trypsin inhibitor heavy chain H1	DAA16905.1	0.0465	4.65	NaCl/Urea	☑		
Cellular Proteins							
Actin, gamma-enteric smooth muscle	NP_001013610.1	0.0145	9.37	NaCl/Urea	☑		
Actin, Cytoplasmic 1	3UB5	0.0432	2.05	Lysis		☑	
Histone H2B type 1-K	DAA16155.1	0.0012	8.60	Lysis	☑		
Lymphocyte cytosolic protein 1 (L-plastin)	AAI03002.1	0.0051	3.06	NaCl/Urea	☑		
Moesin	NP_001039942.1	0.0345	2.07	NaCl/Urea	☑		
Myosin-11	NP_001095597.1	0.0258	6.82	NaCl/Urea			☑
Tubulin alpha-1C chain-like	XP_024838025.1	0.0156	50.01	NaCl/Urea	☑		
		0.0488	17.69			☑	
Tubulin beta-4B chain	NP_001029835.1	0.0075	18.04	NaCl/Urea	☑		
		0.0058	18.85			☑	
Isoform X13 of tropomyosin, alpha 1	XP_024853024.1	0.0004	8.58	NaCl/Urea		☑	
		0.0286	4.15				☑
Isoform X3 of tropomyosin, beta	XP_005210126.1	0.0176	6.81	NaCl/Urea	☑		
		0.0002	5.52			☑	

Table 9.10 cont.

Description	Accession	P-value	Factor	Extraction	Layer		
					Grain	*Junction*	*Corium*
Enzymes							
Bovine Mitochondrial F1-Atpase	2W6F	0.0227	34.01	NaCl/Urea	☑		
		0.0178	13.63			☑	
		0.0025	14.59				☑
Pyruvate Kinase 2	AAI02827.1	0.0135	3.39	NaCl/Urea	☑		
Precursor of protein-lysine 6-oxidase	DAA27688.1	0.0035	3.33	Lysis		☑	
Glutathione S-transferase Mu 2	AAI42537.1	0.0188	5.37	NaCl/Urea	☑		
		0.0377	2.87				☑
Serpin A3-4	ABM55497.1	0.0425	4.97	NaCl/Urea		☑	
Isoform X2 of serpin B6	XP_015315506.2	0.0484	22.43	NaCl/Urea	☑		
Transforming protein RhoA	P61585.1	0.0010	2.75	NaCl/Urea	☑		
Serum proteins							
Albumin	754920A	0.0494	12.27	NaCl/Urea		☑	
		0.0480	7.15				☑
Bovine Fab E03 Light Chain	5IJV	0.0230	3.87	NaCl/Urea		☑	
		0.0183	4.92				☑
Immunoglobulin J chain	AAB03643.1	0.0179	4.63	Lysis	☑		
Precursor of antithrombin-III	DAA21124.1	0.0031	4.08	NaCl/Urea	☑		

9.H Down-regulated proteins in the distal axilla (compared to OSP)

Table 9.11 Down-regulated proteins in distal axilla region, p-values below 0.05 and fold change greater than 2.

Description	Accession	P-value	Factor	Extraction	Layer		
					Grain	*Junction*	*Corium*
Collagens							
Collagen type 1, alpha1 CN8	0910139A	0.0017	6.70	Lysis		☑	
		0.0372	5.87				☑
Collagen, type I, alpha 1	AAI05185.1	0.0014	3.13	Lysis		☑	
Collagen, type I, alpha 2	AAI49096.1	0.0065	3.19	Lysis		☑	
Other extracellular proteins							
Glial hyaluronate-binding protein	AAB20399.1	0.0064	6.11	NaCl/Urea		☑	
Protein HP-25	ACV32359.1	0.0238	4.49	Lysis			☑
Cellular proteins							
Annexin I	AAB25084.1	0.0479	18.25	Lysis			☑
		0.0260	7.34	NaCl/Urea			☑
Actin, Cytoplasmic 1	3UB5	0.0090	2.63	Lysis		☑	
Actin, gamma-enteric smooth muscle	NP_001013610.1	0.0010	10.11	NaCl/Urea	☑		
Isoform X1 of heat shock protein, beta-6	XP_005219035.2	0.0334	2.54	NaCl/Urea			☑
Histone H2B type 1-K	DAA16155.1	0.0186	3.88	Lysis		☑	
Moesin	NP_001039942.1	0.0171	2.50	NaCl/Urea	☑		
Myosin-11	NP_001095597.1	0.0120	12.91	NaCl/Urea	☑		
		0.0063	14.75			☑	
		0.0011	9.45				☑
Isoform X1 of periostin	XP_005213601.1	0.0066	5.14	NaCl/Urea	☑		
		0.0021	4.35			☑	
		0.0030	26.09				☑

Table 9.11 cont.

Description	Accession	P-value	Factor	Extraction	Layer		
					Grain	*Junction*	*Corium*
Cellular proteins cont.							
Isoform X13 of tropomyosin, alpha 1	XP_024853024.1	0.0092	13.95	NaCl/Urea	☑		
		0.0023	4.80				☑
Isoform X3 of tropomyosin, beta	XP_005210126.1	0.0017	7.82	NaCl/Urea	☑		
Tubulin, alpha-1C chain-like	XP_024838025.1	0.0082	25.04	NaCl/Urea	☑		
		0.0035	26.92			☑	
		0.0208	16.73				☑
Tubulin, beta-4B	NP_001029835.1	0.0013	18.34	NaCl/Urea	☑		
		0.0023	14.41			☑	
		0.0040	10.89				☑
Tubulin, alpha 4a	AAI18200.1	0.0125	4.29	NaCl/Urea			☑
Enzymes							
Bovine Mitochondrial F1-Atpase	2W6F	0.0034	28.94	NaCl/Urea	☑		
		0.0151	10.64			☑	
		0.0049	11.40				☑
Gamma-interferon-inducible lysosomal thiol reductase	AAI49407.1	0.0166	3.43	NaCl/Urea		☑	
Glutathione S-transferase Mu 2	AAI42537.1	0.0004	2.61	NaCl/Urea		☑	
		0.0034	3.73				☑
Pyruvate Kinase 2	AAI02827.1	0.0331	3.29	NaCl/Urea	☑		
		0.0037	2.59			☑	
Precursor of protein-lysine 6-oxidase	DAA27688.1	0.0376	2.78	Lysis		☑	
		0.0264	8.72				☑
Serpin A3-4	ABM55497.1	0.0378	7.63	NaCl/Urea	☑		
		0.0295	5.92			☑	

Table 9.11 cont.

Description	Accession	P-value	Factor	Extraction	Layer		
					Grain	*Junction*	*Corium*
Enzymes cont.							
Isoform X2 of serpin B6	XP_015315506.2	0.0040	18.58	NaCl/Urea	☑		
		0.0071	12.05			☑	
Serum proteins							
Albumin	754920A	0.0313	11.83	NaCl/Urea	☑		
		0.0195	12.99			☑	
		0.0397	4.87				☑
A Chain A, Bovine Fab E03 Light Chain	5IJV	0.0058	6.13	NaCl/Urea			☑
Immunoglobulin lambda light chain variable region	AAC48554.1	0.0042	2.44	NaCl/Urea	☑		
Immunoglobulin lambda light chain variable region	AAC48557.1	0.0217	2.44	Lysis		☑	
Precursor of antithrombin-III	DAA21124.1	0.0016	3.92	NaCl/Urea	☑		
Uncharacterized proteins							
Hypothetical protein LOC511239	AAI12509.1	0.0255	3.22	Lysis			☑